CEH-28 and ZAG-1 function in regulating differentiation of the C. elegans M4 pharyngeal neuron

By

Kalpana Ramakrishnan

B.Tech., SASTRA University, 2007

M.S., Illinois Institute of Technology, 2011

THESIS

Submitted as a partial fulfillment for the requirements
for the degree of Doctor of Philosophy in Biological Sciences
in the Graduate College of the
University of Illinois at Chicago, 2014

Thesis Committee:

Dr. Brian Kay (Committee Chair)

Dr. Peter Okkema (Thesis Advisor)

Dr. Teresa Orenic

Dr. Janet Richmond

Dr. Yang Dai (Department of Bioengineering)

ACKNOWLEDGEMENTS

First, I want to immensely thank my thesis advisor Peter Okkema for his continuous support, encouragement and inspiration. Pete is a dedicated mentor and an inspiring teacher who devotes a lot of time, attention and interest towards research. His support and guidance was critical in helping me finish this dissertation.

I want to thank my thesis committee members: Brian Kay, Janet Richmond, Teresa Orenic, and Yang Dai for their advice, suggestions and critical comments with my thesis.

I also want to thank Dr. Aixa Alfonso, and members from her laboratory for regularly attending our lab meetings and providing ideas and suggestions for research. I also extend my thanks to Dr. Harald Hutter and the *C. elegans* worm community for providing us with strains and plasmids required for this project.

I want to thank the past and present members of the Okkkema lab: Ray Miller, Tanya Crum, Tom Ronan, Lynn Clary, Angenee Milton, Paul Huber, Alena Kozlova and Michelle Lotfi for being great friends and excellent colleagues and most importantly, providing a great work environment.

I want to thank my family: my parents, for constantly motivating me and showering me with unconditional love, enthusiasm and support. I want to specially thank my husband for his love, patience and positive energy without which I couldn't have completed this dissertation

KR

TABLE OF CONTENTS

CHAPTER **PAGE NUMBER**

TABLE OF CONTENTS (continued)

TABLE OF CONTENTS (continued)

TABLE OF CONTENTS (continued)

LIST OF TABLES

LIST OF FIGURES

LIST OF FIGURES (continued)

LIST OF ABBREVIATIONS

ACh	Acetylcholine
bp	base pairs
cm	centimeter
cDNA	complimentary DNA
cuEx	Extrachromsomal array generated in Okkema Lab
cuIs	Integrated transgenic strain generated in Okkema Lab
DIC	Differential Interference Contrast
DNA	Deoxyribonucleic acid
gfp/GFP	green fluorescent protein
F1	First generation progeny in a genetic cross
F2	Second generation progeny in a genetic cross
F3	Third generation progeny in a genetic cross
F4	Fourth generation progeny in a genetic cross
L1-L4	Larval development stages in *C. elegans*
M	Molar
mg	milligram
ml	milliliter
mM	millimolar
mRNA	messenger RNA
ng	nanogram
OP50	*E. coli* strain
orf	open reading frame
NA22	*E. coli* strain
NEP	Nystatin Enriched Peptone (growth media)
NGM	Nematode growth medium
PCR	Polymerase chain reaction
PO	Oligo nucleotides designed in Okkema Lab
pOK	Plasmid generated in Okkema Lab
RNA	Ribonucleic Acid
RNAi	RNA mediated interference
rpm	revolutions per minute
°C	Degree Celsius

SUMMARY

The nervous system is a neural network through which neurons communicate with each other and with other cell types by transmitting and receiving information. Nervous system function requires proper function of individual neurons that form the neural network. Motor neurons are an important class of neurons which stimulate muscle contractions by release of appropriate neurotransmitters. Many excellent studies have investigated the role of transcription factors in specification of motor neurons, however terminal differentiation mechanisms that determine morphology, connectivity, neuronal signaling and gene expression in neurons are only beginning to be understood. To understand mechanisms that regulate terminal differentiation of individual motor neurons, we studied the *C. elegans* M4 pharyngeal motor neuron, which regulates muscle contractions that facilitate feeding, and extensively characterized the roles of two transcription factors CEH-28 and ZAG-1 in M4. We find that CEH-28 regulates a neuroendocrine signaling function of the M4 neuron by activating expression of the family gene *dbl-1* gene, which encodes a TGF-β ligand, *egl-17* gene which encodes the FGF family ligand and the FMRF family gene, *flp-5*. ZAG-1 functions in M4 and activates isthmus muscle contractions required for normal feeding. Furthermore, ZAG-1 acts as an upstream regulator of *ceh-28* and its downstream targets in M4 and regulates additional aspects of M4 differentiation.

Taken together, my work identifies a new gene regulatory network in the M4 neuron, which regulates signaling and differentiation functions and also provides insights regarding how multifunctionality of motor neurons is regulated.

CEH-28 is an NK-2 family homeodomain transcription factor which functions exclusively in the M4 neuron to regulate M4 synapse morphology and assembly. We find that a *dbl-1::gfp* transcriptional fusion was not expressed specifically in the M4 neuron in *ceh-28(cu11)* mutants. We further characterized the *dbl-1* promoter and identified an M4 specific enhancer which is

directly activated by CEH-28. We find that the TGF-β ligand DBL-1, signals from M4 to the nearby gland cells which are innervated by M4. In the absence of DBL-1 signaling from M4, g1 gland cells exhibit abnormal gland cell morphology that includes thickened processes and abnormal swellings in *dbl-1* mutants and *ceh-28* mutants. Similar gland cell defects were found in mutants of *daf-4* and *sma-6* which encode the Type I and Type II receptors of the TGF-β signaling pathway. Expression of *dbl-1* in M4 partially restored the gland cell defects in *dbl-1* and *ceh-28* mutants. Based on these results, we identified a novel neuroendocrine function for M4 and an additional role of *dbl-1* in the *C. elegans* pharynx.

In addition to *dbl-1*, we also identified *egl-17, flp-5, flp-2* and *zag-1* as additional downstream transcriptional targets of CEH-28 based on an extensive literature search for M4 expressed genes. We find that *flp-5* and *zag-1* contain CEH-28 binding sites in their promoters suggesting that they might be directly regulated by CEH-28.

We further characterized the role of the Zinc finger homeodomain transcription factor ZAG-1, in the M4 neuron and showed that it activates M4 isthmus peristalsis. *zag-1(hd16)* null mutants completely lack isthmus peristalsis. They have neuronal signaling defects, and the M4 cell is unable to respond to stimulation by serotonin to produce isthmus peristalsis. However, the isthmus muscles can be stimulated in *zag-1* mutants to produce isthmus peristalsis, even in the absence of M4 signaling. Consistent with its established role as a regulator of motor neuron differentiation, we find that ZAG-1 acts as a broad regulator of M4 differentiation by activating expression of *ceh-28* and its downstream targets. However expression of *unc-17*, which specifies cholinergic fate, and *flp-21*, which regulates M4 hypoxia response function, are normal in *ceh-28* mutants, suggesting that ZAG-1 is not the only major regulator of M4 differentiation

In conclusion, my study identifies a complex hierarchical gene regulatory network in the M4 neuron regulated by CEH-28 and ZAG-1 and provides insights regarding how such an

apparently simple motor neuron in the pharynx regulates diverse functions such as feeding, neuroendocrine signaling and hypoxia response in the entire animal.

1 INTRODUCTION

1.1 Background

The nervous system is a network of neurons consisting of diverse cell types which communicate with each other to form a fully functional nervous system. The formation of fully functional individual neurons is essential for the normal function of the entire nervous system

Motor neurons are an important class of neurons within the nervous system that contact muscles through synapses and stimulate muscle contractions by releasing appropriate sets of neurotransmitters. Failure of motor neuron function and signaling has been implicated in neurodegenerative diseases, such as Amyotrophic lateral sclerosis (Wijesekera and Leigh, 2009), Huntington disease (Walker, 2007) and neuromuscular disease, such as myasthenia gravis (Conti-Fine et al., 2006). While a number of excellent studies have highlighted the mechanisms that specify motor neuron fates, the terminal differentiation programs that affect motor neuron differentiation and signaling are still being extensively researched (Jacob et al., 2001; Thor and Thomas, 2002; Dalla Torre di Sanguinetto et al., 2008) due to their importance in the pathogenesis of the above mentioned diseases.

Investigating the mechanisms governing the differentiation and function of individual motor neurons will provide valuable insights regarding how motor neurons function and signal in the nervous system. Analyzing mechanisms that control differentiation and function of individual neurons in many animal models is a challenging task given the complexity of the nervous system and the lack of viable mutants that affect neuronal function.

The focus of this study is to understand mechanisms that regulate terminal motor neuron differentiation and signaling at the single neuron level using *C. elegans* pharynx as a model system.

1.2 ***C. elegans* is an excellent model for studying neuronal function**

C. elegans is a free living soil nematode which is transparent and microscopic. *C. elegans* hermaphrodites are self-fertilizing, have a short growth cycle and produce more than 300 progeny in a short time span of 3-5 days. Due to its advantages, it was introduced as a model system to perform genetics research by Sydney Brenner (Brenner, 1974). It is an ideal system for studying neuronal function, since it has a simple and well characterized nervous system consisting of 302 neurons (White et al., 1986a). Since the worm is transparent, neuronal activity can be visualized *in vivo* using fluorescent proteins and controlled using optogenetic approaches (Schafer, 2006; Boulin et al., 2006). Since most of the known mutants affecting nervous system function are viable, we can readily analyze loss of function mutants that affect neuronal function. Due to ease of performing genetic crosses, it is also possible to examine the function of several genes and proteins in different genetic backgrounds. Since many of the *C. elegans* proteins have orthologs in humans, it has been used as a successful disease model to study multiple neuronal diseases including Alzheimer disease, Parkinson's disease and Huntington disease (Kaletta and Hengartner, 2006). In the *C. elegans* Alzheimer's disease model, studies by Link showed that transgenic worms expressing the human β amyloid A peptide contained amyloid deposits (Link, 1995). In a model for understanding Parkinson's disease, overexpression of the wild-type or mutant forms of the human α synuclein protein resulted in loss of dopaminergic neurons in *C. elegans* (Lakso et al., 2003). Additionally *C. elegans* is also a valuable tool for performing neurobiological studies to understand the molecular basis of pain and neuronal regeneration (Yanik et al., 2004; El Bejjani and Hammarlund, 2012)

1.3 Overview of the *C. elegans* nervous system

C. elegans is an ideal system for studying neuronal function since it has a well characterized nervous system consisting of 302 neurons (White et al., 1986a).

Neurons are formed during the proliferating embryonic stages as well as the first and second and larval stages of development (Sulston and Horvitz, 1977; Sulston et al., 1983). The 302 neurons in the adult hermaphrodite can be classified into 118 classes based on morphology, connectivity and function (White et al., 1986a). This precise and detailed classification of neuronal cell types is possible because electron micrographic reconstructions have elucidated the complete neural circuit and the synaptic connectivity within the worm (White et al., 1983; Albertson and Thomson, 1976), which consists of approximately 5000 synapses and 2000 neuromuscular junctions. The neurons can be classified based on function as sensory neurons, which receive sensory input, motor neurons, which form synapses and stimulate muscles, interneurons which both receive input as well as stimulate other neurons and polymodal neurons, which can perform more than one of the above functions. They are also classified based on types of neurotransmitter they release. Some of the common neurotransmitters types include: Acetylcholine (ACh), Serotonin (5HT), Dopamine (DA), Tyramine (TA), Octapamine (OA), Glutamate (Glu), Gamma-amino butyric acid (GABA) (Lewis et al., 1980; McIntire et al., 1993; Sulston et al., 1975).

Motor neurons are found frequently in the *C .elegans* nervous system and primarily regulate locomotion that includes sinusoidal movement, swimming and thrashing in liquid media. Among the 302 neurons, a total of 113 neurons are classified as motor neurons. 75 motor neurons innervate the body wall muscle and are further classified into 8 different types: cholinergic (secrete ACh) and stimulatory (VA, VB, DB, DA, AS), D-type motor neurons (VD, DD) which are GABAergic and inhibitory and the VC motor neurons which stimulate vulval

muscles. The VA,VB,VC and VD neurons innervate the ventral vulval muscles and the DA, DB and DD neurons innervate the dorsal vulval muscles (White et al., 1986a).

1.3.1 **Overview of the pharyngeal nervous system**

The pharyngeal nervous system consists of 20 neurons and is almost independent of the extra-pharyngeal nervous system. Only the RIP interneurons in the extra pharyngeal nervous system connect the two nervous systems together (Sulston and Horvitz, 1977; Sulston et al., 1983; White et al., 1986a). The 20 neurons in the pharynx can be further classified into 14 subtypes, 6 of which are bilateral pairs of neurons and 8 are single neurons. There are 5 types of motor neurons: M1, M2, M3, M4 and M5, 6 types of interneurons I1-I6 and 4 types of other neurons MI, NSM, MC L/R (Albertson and Thomson, 1976). Most of the pharyngeal neurons can be ablated without affecting viability or feeding behavior in the worm (Avery and Horvitz, 1989). While the function of most of the pharyngeal neurons is unknown, the MC neurons function as pacemakers of pumping and initiate pharyngeal muscle action potentials (Avery and Thomas, 1997a). Laser ablation of MC neurons decreases the rate of pharyngeal pumping (Raizen et al., 1995). The MC neurons release ACh to post synaptically stimulate the nicotinic receptors encoded by *eat-2* and *eat*-18, which function in the pharyngeal muscle (McKay et al., 2004). The pharyngeal NSMs (Neurosecretory motor neurons) are located sub-ventrally in the pharyngeal metacorpus and extend three processes along the pharynx. The NSMs are believed to have neurohumoral function and sense bacteria in the lumen through their processes and communicate this information to the rest of the worm's body (Albertson and Thomson, 1976). While laser ablation of the serotonergic NSMs does not affect pharyngeal pumping or peristalsis (Avery and Thomas, 1997a; Avery et al., 1993), recent laser ablation studies of the NSMs have demonstrated that they are required for an 'enhanced slowing response', a behavior that allows starved animals to stay close to the presence of food (Sawin et al., 2000).

1.4 **Anatomy of the pharynx**

The pharynx is a neuromuscular feeding organ which contracts rhythmically and facilities feeding. The detailed anatomy of the pharynx was described by Donna Albertson (Albertson and Thomson, 1976). It is a bilobed organ surrounded by a basement membrane. The buccal cavity connects the mouth to the anterior pharynx (Figure 1), while the pharyngeal intestinal valve connects the posterior pharynx to the intestine and terminal bulb (Figure 1).

The pharynx consists of a total of 80 cells, which can be classified as muscles (37 nuclei), neurons (20 nuclei), gland cells (5 nuclei), epithelial cells (9 nuclei), and marginal cells (9 nuclei) (Figure 2) and these cells are derived from the Aba and MS blastomeres (Sulston et al., 1983).

The muscles in the pharynx are grouped into eight types pm1-pm8 and are arranged radially around the pharyngeal lumen (Albertson and Thomson, 1976). The pharyngeal muscles are not separated by a hypodermal layer and they directly contact the cuticle. Most of the pharyngeal muscles are made up of three syncytial cells arranged in a threefold symmetric arrangement thus giving the pharynx a threefold rotational symmetry (Figure 3). The pm1 is the anterior most muscle is a single cell with six nuclei which extend processes anteriorly towards the outer edges of the marginal cells. The pm2 muscle has 2 nuclei which project processes anteriorly. The pm5 muscles are located in the isthmus. There are three 3 pm5 muscles which each contain two nuclei and they are innervated by the M4, M2 and M3 neurons.

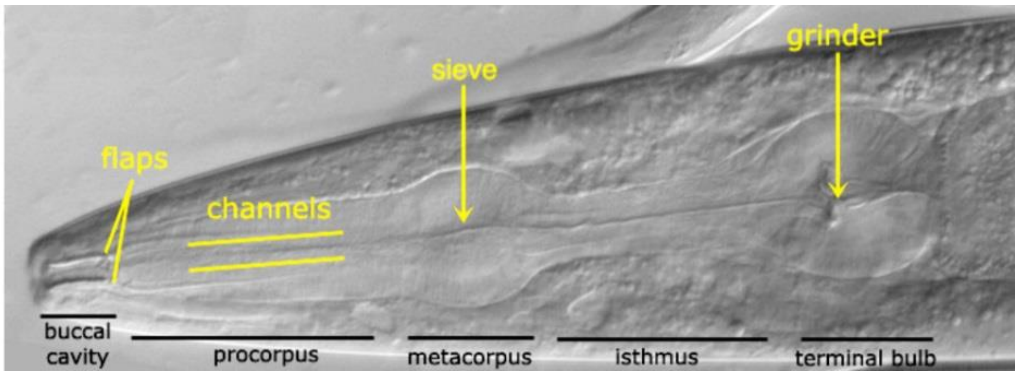

Figure 1 Morphology of the *C. elegans* pharynx

DIC image of the pharynx of *C. elegans* adapted from WormAtlas (http://www.wormatlas.org/) highlighting the anatomical regions of the pharynx. Anterior is to the left. The different morphological regions of the pharynx consisting of the buccal cavity, procorpus, metacorpus, isthmus and terminal bulb are labelled in black lines. The yellow lines and arrows represent the specialized cuticular structures in the pharynx which are important for feeding.

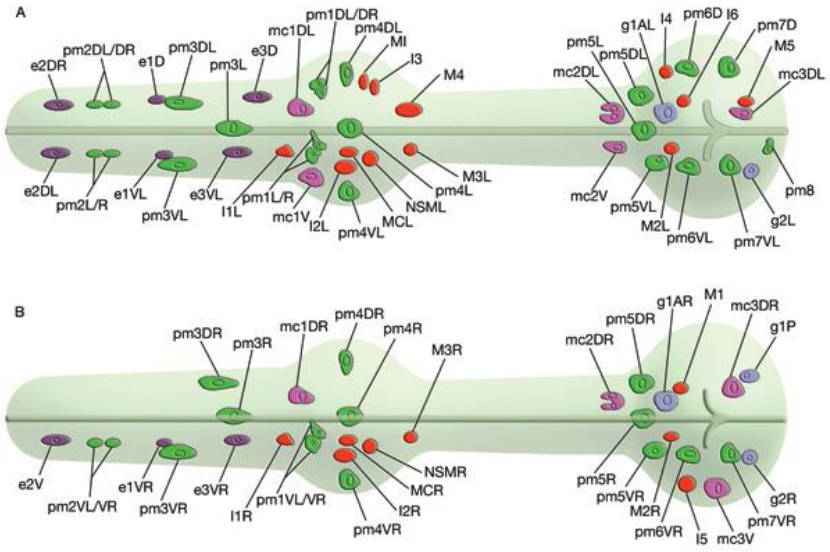

Figure 2 ***C. elegans*** **pharyngeal nuclei**

Diagram adapted from WormAtlas (http://www.wormatlas.org/) showing the positions of the various cell types in the *C. elegans* pharynx. Neurons (red), pharyngeal muscle (green), gland cells (lavender) marginal cells (fuschia) and epithelial cells (purple). (A). Indicates the various cell types located on the right side of midline. (B) Indicates the various cell types cells located on left side of the midline.

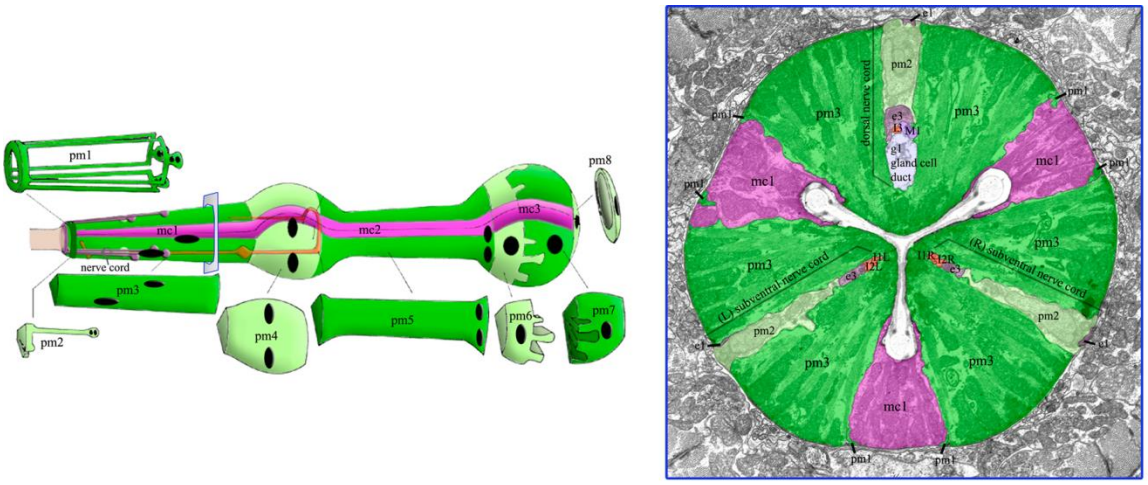

Figure 3 Anatomy of pharyngeal muscles

Schematic adapted from WormBook (http://www.wormbook.org/) depicting the location of pharyngeal muscles pm1-pm8 (left) shown in green. The Muscle nuclei are shown in black. The mariginal cells are denoted (mc1-mc3) are shown in pink. A micrograph of a TEM cross section mid-way through the procopus of the pharynx (right) showing the tri radiate arrangement of the muscles and depicts the 3 fold rotational symmetry of the pharynx

The pm6 - pm8 muscles are located in the terminal bulb. The pm1-pm4 muscles function in taking up bacteria, the pm5 isthmus muscles regulate contractions which transport the food through the isthmus. The pm6-pm8 muscles regulate terminal bulb contractions that result in grinder movement, which breaks up the bacteria on which the animal feeds.

The pharyngeal glands are single cells and their cell bodies are located in the posterior bulb. They extend processes of different lengths that fuse with the pharyngeal lumen (Figure 4A). There are a total of five gland cells which are classified into two types: the g1 gland cells (3 cells – 2 g1A cells and 1 g1P cell) and the g2 gland cells (2 cells) (Figure 4B). The g1 cells extend three processes that contact the pharyngeal lumen. The g1P cell extends the longest dorsal process which is about 125 µm in length. These processes terminate at the anterior end of the pharynx (Figure 4A). The g2 gland cells extend shorter processes which are less than 10 µm in length and connect to the lumen of the posterior bulb (Raharjo et al., 2011). The glands function by releasing secretions which help to loosen and break open the cuticle lining of the pharyngeal lumen during molting, and lack of proper gland cell differentiation results in molting defects (Fernandez et al., 2004). Recently, a novel role for the g1 gland cells in axonal guidance of the M1 pharyngeal motor neuron has been demonstrated (Refai et al., 2013). The g1 gland cells are in close proximity to the M1 cell body and they provide axonal guidance cues for the proper development of the proximal trajectory of the M1 axon. Laser ablation of the g2 gland cells results in axonal guidance defects in the distal process of the M1 neuron. The g2 gland cell functions in regulation of worm feeding. Loss of g2 gland cells results in larval arrest and a stuffed pharynx phenotype due to bacteria being stuck in the anterior pharynx. The g2 gland cells secrete mucin-like proteins which lubricate the pharynx and help in efficient passage of food through the pharyngeal lumen (Smit et al., 2008).

.

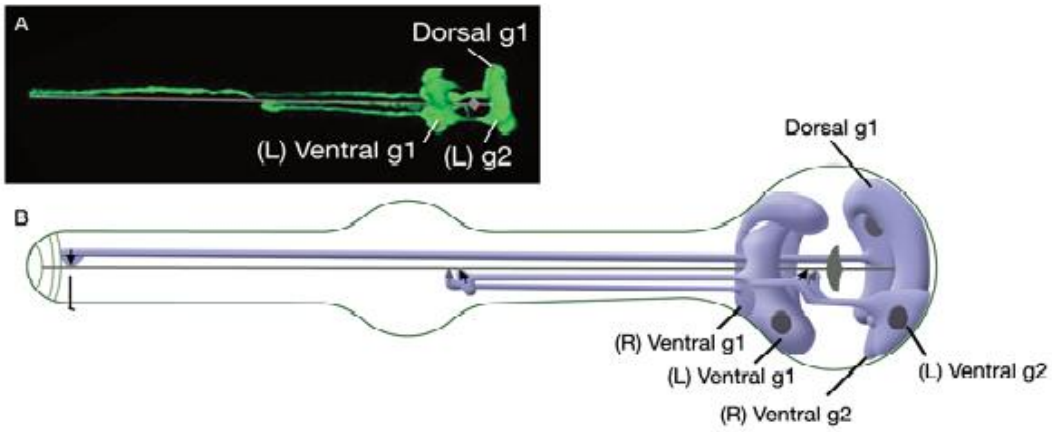

Figure 4 Gland cell morphology

Figure adapted from WormAtlas (http://www.wormatlas.org/). (A). GFP image of an animal expressing the gland cell reporter *B0280.7::gfp* in the two g2 gland cells and 1 dorsal g1 gland cell. (B). Schematic depicting the presence of 5 gland cells (3 g1 and 2 g2 gland cells) and the extent of their processes in the pharynx. Lines indicate the positions where they connect to the pharyngeal lumen.

1.4.1 **Function of the pharynx in regulation of feeding behavior**

The pharynx is a neuromuscular feeding organ which functions during feeding. Pumping and peristalsis are the two main pharyngeal muscle contractions that facilitate feeding in the worm. During a pump, the muscles in the anterior pharynx and terminal bulb contract simultaneously to ingest bacteria and concentrate it in the anterior pharynx (Avery and Horvitz, 1989). The pharyngeal muscle contractions during pumping pull the lumen open to suck in liquid and bacteria (Figure 5B). A simultaneous relaxation following the contraction expels the bacteria and retains the liquid. The rate of pumping is regulated by the MC neuron, which initiates pharyngeal muscle contractions. The MC neuron is stimulated by the presence of either food (Avery and Horvitz, 1989; Raizen et al., 1995) or serotonin (Avery and Thomas, 1997a; Hobson et al., 2006). Following a pump, a peristaltic a wave like contraction of the isthmus muscles transports food through the isthmus into the posterior pharynx (Figure 5C) (Avery and Horvitz, 1989). Isthmus peristalsis is a relatively infrequent event following every 4^{th}-40^{th} pump and activation of isthmus peristalsis depends on the M4 pharyngeal neuron (Avery and Horvitz, 1987).

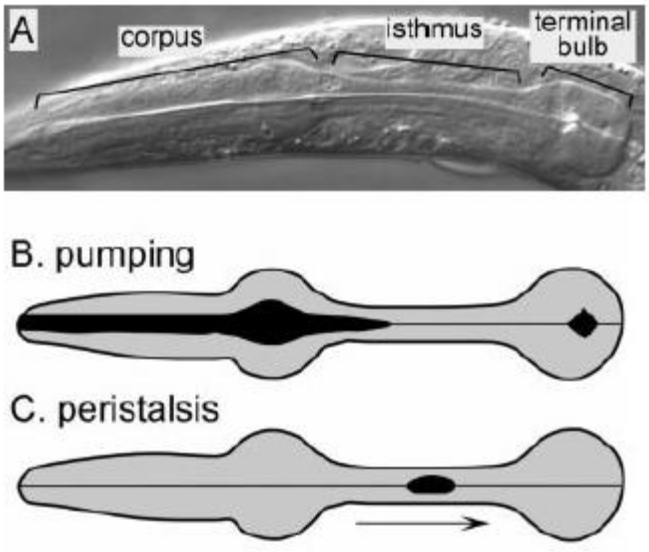

Figure 5 Pharyngeal muscle contractions during pumping and peristalsis

Schematic adapted from Ray et al showing the muscle contractions that occur during pumping and peristalsis. (A). DIC image of the pharynx and its morphological features consisting of the corpus, isthmus and the terminal bulb. (B). The muscle contractions during A pump that allow the intake of food are shown. (C). Isthmus peristalsis transports food from the anterior isthmus into the posterior pharynx (Ray et al., 2008).

1.5 Modulators of feeding behavior

1.5.1 Roles of muscarinic acetylcholine receptors

Muscarinic acetylcholine receptors (mAChR) are G-protein coupled receptors that regulate the activity of neurons and muscles within the nervous system. They act post-synaptically in the muscles, and their roles in mammalian smooth muscle contraction, heart muscle contraction, neuronal plasticity and the regulation of food intake are well understood (Bartus et al., 1982; Wess et al., 2003). In the G-protein signaling pathway, heterotrimeric G protein subunits α, β, and γ signal though guanine nucleotide exchange and hydrolysis. Gα-GDP associates with Gβγ and also with the G-protein coupled receptors which are seven-pass transmembrane proteins. When a ligand activates the receptors, it stimulates exchange of GDP for GTP on the αsubunit; Gα-GTP dissociates from Gβγ, and both subunits can activate downstream signaling pathways. Hydrolysis of GTP restores the Gα-GDP form, which then reassociates with Gβγ and the receptor to terminate signaling. Guanine nucleotide exchange factors (GEF) proteins, which promote formation of Gα-GTP act as positive regulators of G protein pathways while, Regulators of G-protein Signaling (RGS), which promote GTP hydrolysis, act as negative regulators.

The *C. elegans* genome encodes 21 Gα subunits, 2 Gβ, 2γ subunits and three muscarinic AcetylCholine receptor subunits, *gar-1, gar-2* and *gar-3*. *gar-3* is the only receptor which is expressed in the pharyngeal muscle (Steger and Avery, 2004), and it can be stimulated by the muscarinic AcetylCholine receptor agonist, arecoline. Expression of *C. elegans* GAR-3 in heterologous systems can activate Phospholipase C (PLC) and Protein kinase C (PKC) (Lee et al., 2001; Min et al., 2000). Treating wild-type animals with arecoline produces enhanced peristaltic contraction suggesting that arecoline most likely hyperstimulates the GAR-3 receptor on the isthmus muscles to elicit this enhanced muscle contraction (Ray et al., 2008).

1.5.2 **Effect of Serotonin on feeding behavior**

Serotonin is a neurotransmitter which has well established roles in increasing pharyngeal pumping, inhibition of locomotion, motor defecation program, stimulation of egg laying (Horvitz et al., 1982; Niacaris and Avery, 2003; Sawin et al., 2000; Weinshenker et al., 1995; Segalat et al., 1995; Waggoner et al., 1998). Serotonin activates pumping and peristalsis in the pharynx by activating separate pathways that signal through the SER-7 receptor (Song and Avery, 2012). The increase in pumping is achieved through the SER-7 in the MC neurons, which activate cholinergic transmission to the pharyngeal muscles through the Gsα signaling pathway components. Regulation of peristalsis requires activation of SER-7 in the M4 neuron and presumably components of G (12) α components, which signal to the pharyngeal isthmus muscles to trigger peristalsis.

1.6 **Anatomy of the M4 pharyngeal motor neuron**

M4 is a cholinergic motor neuron that expresses the vesicular acetylcholine transporter UNC-17 (Avery and Thomas, 1997a) and is located dorsally in the pharynx. The M4 cell body sends out two processes which travel circumferentially around the nerve ring and run posteriorly on the sub ventral axis to the terminal bulb (Figure 6). At the terminal bulb, the processes turn dorsally and run anteriorly for a short distance on the isthmus. The M4 processes make synapses in the posterior region of the isthmus where they presumably release acetyl choline to stimulate isthmus muscles. M4 contains a large number of dense core vesicles (Albertson and Thomson, 1976) which presumably package neuropeptides. M4 expresses neuropeptide genes such as *flp-2, flp-5* and *flp-21* (Kim and Li, 2004).

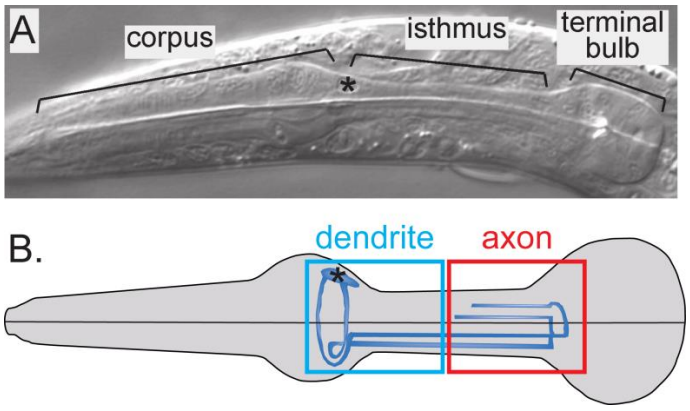

Figure 6 Morphology of the M4 neuron

Schematic adapted from Ray et al showing the morphology of the M4 neuron. (A) DIC image showing the morphological features of the pharynx. (B) Schematic showing the morphology of the M4 neuron. The M4 cell body denoted by asterisk is located dorsally in the pharynx. It extends two processes which travel circumferentially around the nerve ring and run subventrally. They turn dorsally at the terminal bulb and extend anteriorly for a short length on the isthmus (Albertson and Thomson, 1976; Ray et al., 2008). The M4 cell has axonal and dendritic characteristics. The posterior M4 processes forms synapses with the isthmus muscles and have axonal characteristics, while the anterior M4 processes receive information and have dendritic characteristics.

The primary function of the M4 neuron is to activate isthmus peristalsis. Laser ablation of M4 eliminates isthmus peristalsis and results in a stuffed pharynx phenotype due to which bacteria cannot be transported through the pharynx. As a result the worms arrest as larvae due to cessation of feeding (Avery and Horvitz, 1989). M4 also has additional functions in regulating locomotion during hypoxia (Pocock and Hobert, 2010) and regulates neuroendocrine signaling of DBL-1 from M4 (Ramakrishnan et al., 2014).

1.7 **Function of CEH-28 in M4**

CEH-28 is an NK-2 family homeodomain transcription factor. It is one of the four NK-2 family genes in the worm. The others include *ceh-22, ceh-24* and *ceh-27* (Harfe and Fire, 1998; Okkema et al., 1997).

CEH-28 is exclusively expressed in M4 starting from mid embryogenesis where it regulates M4 synapse assembly and morphology (Ray et al., 2008). *ceh-28(cu11)* mutants have M4 abnormal and mispositioned M4 synapses (Figure 7) due to which they hyperstimulate isthmus muscles resulting in feeding defects. Due to inefficient feeding, *ceh-28* mutants have a stuffed pharynx, and they exhibit frequent and prolonged peristalsis. Modulation of muscarinic receptor activity can either phenocopy or suppress feeding defects in *ceh-28* mutants, suggesting that these phenotypes are most likely mediated by the GAR-3 muscarinic receptor.

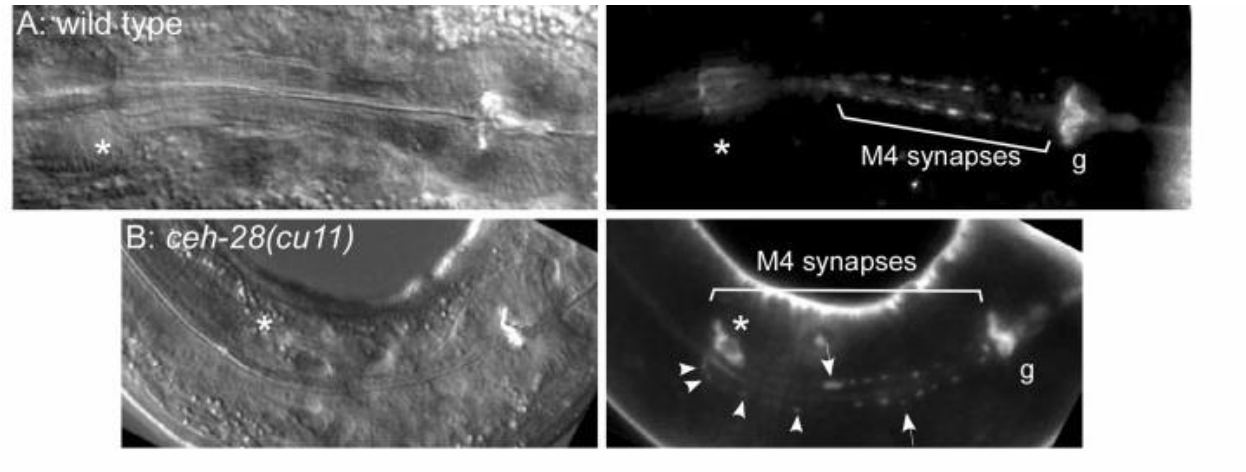

Figure 7 M4 synapse defects in *ceh-28(cu11)* mutants

Figure adapted from Ray et al. (A). DIC image of a wild - type animal in which only a part of the pharynx is in focus. The location of the M4 cell body is indicated by an asterisk. (Left) GFP image of the same animal in which the M4 synapses are visualized using a SNB-1::GFP. The synapses are present only in the posterior half of the isthmus. (B) DIC image of a *ceh-28(cu11*) mutant. (Left) The M4 synapses in the *ceh-28* mutant are visualized using the SNB-1::GFP and ectopic synapses (arrowheads) are present more anteriorly and these synapses are irregularly spaced and irregular in size (Ray et al., 2008).

1.8 Overview of TGF-β signaling

Transforming growth factor β proteins are a family of cytokines that regulate many important biological processes such as cell proliferation and differentiation, apoptosis, cell migration, bone and cartilage formation, embryogenesis and maintenance of cell fates in vertebrates and invertebrates (Patterson and Padgett, 2000; Dennler et al., 2002; Massague, 1998; Wu and Hill, 2009; Derynck and Akhurst, 2007). TGF-beta signaling also has critical roles in regulating cancer metastasis (Padua and Massague, 2009).

The TGF-β signaling pathway is activated when the ligand binds the Type II receptor which encodes a serine threonine kinase on the cell surface thus forming a tetrameric complex. The ligand bound Type II receptor, promotes phosphorylation of the kinase domain of the Type I receptor thus activating it. The activated Type I receptor then further propagates the signal through phosphorylation of receptor Smad proteins (R-Smads). The phosphorylated R-Smad proteins then bind a Co-Smad. This complex translocates to the nucleus to bind target gene promoters and regulates transcription (Massague, 1998). In the non-canonical TGF-β signaling mechanisms, the activated tetramer consisting of the ligand and the Type I and Type II receptor directly activate other signaling pathways without the requirements of R-Smads and Co-Smads (Zhang, 2009).

1.8.1 TGF-β signaling in *C. elegans*

The *C. elegans* genome contains 5 genes namely: *dbl-1, daf-7, unc-129, tig-2* and *tig-3* which encode ligands for the TGF-β signaling pathway. *daf-6* and *sma-1* encode Type I receptors, *daf-4* encodes the Type II receptor, *sma-2, sma-3, daf-8* and *daf-14* encode R-Smads while *sma-4* and *daf-3* encode Co-Smads (Gumienny and Savage-Dunn, 2013).

1.8.2 **Sma/Mab TGF-β pathway**

The Sma/ Mab signaling pathway regulates the TGF-β family ligand DBL-1 (Morita et al., 1999; Suzuki et al., 1999), which regulates body size, male tail patterning and aversive olfactory learning and innate immunity (Gumienny and Savage-Dunn, 2013; Zugasti and Ewbank, 2009) (Figure 8).

In the *dbl-1* pathway, the DBL-1 ligand binds the tetrameric complex consisting of the type II receptor, DAF-4 (Estevez et al., 1993), and the type I receptor ,SMA-6 (Krishna et al., 1999) to activate the signal transduction pathway. The activated receptors can initiate signal transduction through the canonical TGF-β signaling pathway or the non-canonical TGF-β signaling pathway.

In the canonical pathway, the activated tetramer consisting of the ligand and Type I and Type II receptors, binds the signal tranducer R-Smads SMA-2 and SMA-3 and the Co-Smad SMA-4. This complex translocates into the nucleus to bind target gene promoters and activate gene transcription.

In the non-canonical TGF-β signaling mechanism, the activated DBL-1 ligand bound to the Type I and Type II receptors can directly activate downstream potential signaling pathways such as MAPK, Rho-like GTPase signaling pathways, and phosphatidylinositol-3-kinase/AKT pathways independently of Smad proteins (Zhang, 2009).

In other systems, Smad independent TGF-β signaling can promote epithelial to mesenchymal transitions. Activated TGF-β phosphorylates Type I and Type II receptors. The phosphorylated receptors then recruit Grb2/Sos and the Ras, Rho and Raf pathways ultimately leading to activation of Erk. Erk is an important regulator of epithelial to mesenchymal transition (EMT). Although EMT is a part of normal development during embryogenesis, activation of

EMT in later development stages promotes tumors. During EMT, the cells lose epithelial properties, such as cell polarity, cell adhesion and gain invasive and cancerous properties (Lee et al., 2006; Thiery, 2003). Another example of non-canonical TGF-β signaling is its ability to activate Jun N-terminal Kinase (JNK) without the requirement of Smad3 or Smad4 proteins (Engel et al., 1999; Hocevar et al., 1999).

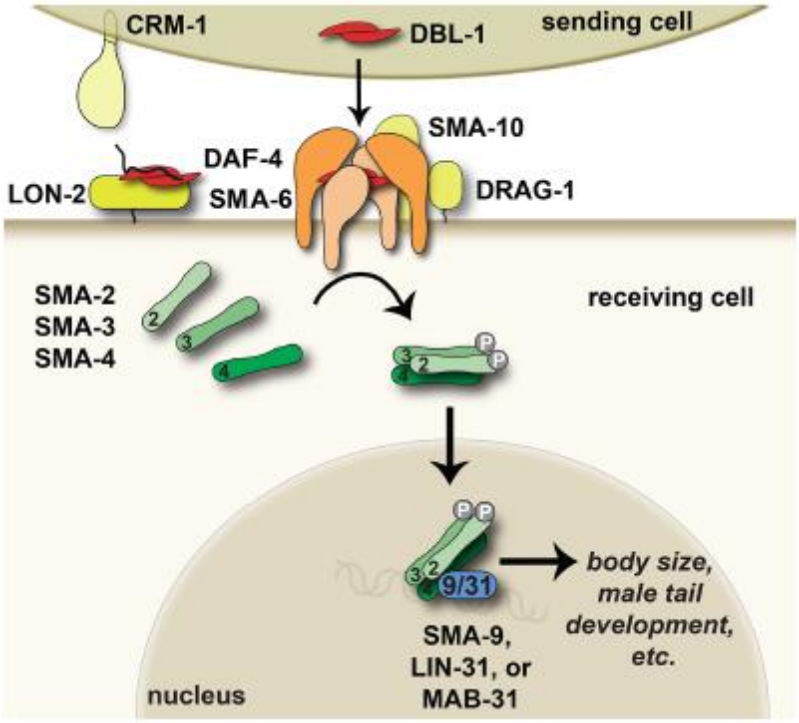

Figure 8 Sma/Mab TGF-β pathway

Figure adapted from wormbook (http://www.wormbook.org) showing the Sma/Mab pathway in *C. elegans*. The DBl-1 signal (red) activates the heterotrimeric receptor consisting of 2 subunits of the Type I receptor, SMA-6 (light orange) and 2 subunits of Type II receptor, DAF-4 (darker orange). CRM-1, LON-2, DRAG are extracellular regulators of this pathway. CRM promotes DBL-1 signaling by functioning in the extracellular space, while DRAG-1 and SMA-10 act on the membrane of the cell receiving the DBL-1 signal. LON-2 (yellow) inhibits this pathway. The Smads, SMA-2, SMA-3 and SMA-4(green) act as signal transducers in this pathway. Several transcription factors such as SMA-9/LIN-31/MAB-1 (shown in blue) act in conjunction with the Smads to regulate signal transduction pathways which regulate body size, male tail development (Gumienny and Savage-Dunn, 2013).

1.8.3 **Dauer pathway in *C. elegans***

The dauer larva is an alternative developmental stage of *C. elegans* larva in response to harsh environmental conditions such as heat or starvation (Cassada and Russell, 1975; Golden and Riddle, 1984). The decision to enter the L2 dauer larva (L2d) stage is made during the L1 stage and in the absence of food. If food is provided, L2 d exit this stage and resume normal growth.

In the continued absence of food, L2d animals, enter an alternative L3 dauer stage in which their body is significantly remodeled. If provided with food, the dauer animals then resume a normal L4 stage of development. The dauer pathway components include the ligand DAF-7, type II receptor, DAF-4 and the Type I receptor, DAF-14. DAF-8 and DAF-14 function as R-Smads in this pathway, while DAF-3 functions as a Co-Smad (Figure 9). The TGF-β pathway and the dauer pathway share a common Type II receptor DAF-4. However the ligands and the R-Smads for both pathways are different.

1.9 **Neuropeptides regulate neuronal function**

Neuropeptides are short peptide fragments which can modulate synaptic and neuronal activity. Unlike neurotransmitters, mature neuropeptides are processed by posttranslational modifications of a precursor neuropeptide and are stored in dense core vesicles. Neuropeptides have important neuromodulatory roles. The role of brain neuropeptides in the regulation of pain sensation and pituitary function has been previously characterized (Krieger, 1983). Neuropeptides have additional roles in regulating neurological disorders such as epilepsy, anxiety and post-traumatic stress disorders.

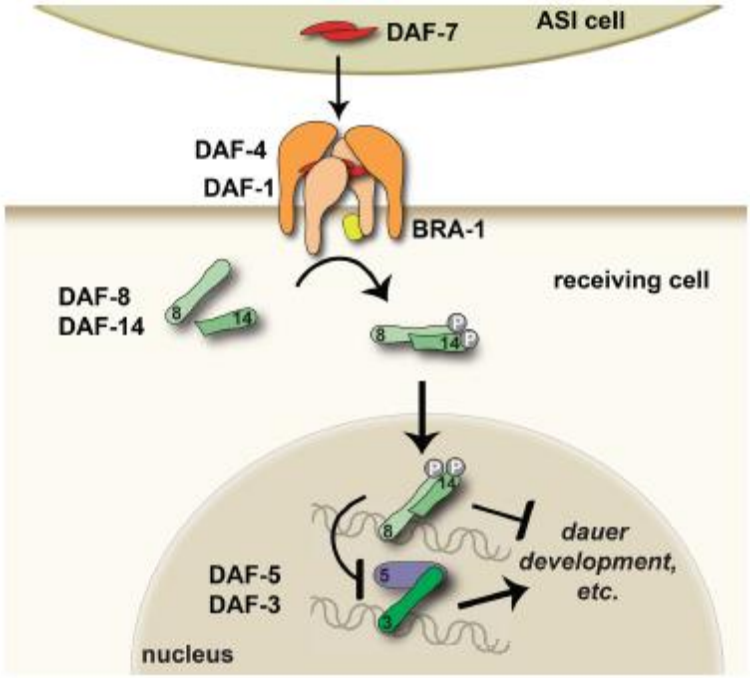

Figure 9 Dauer pathway in *C. elegans*

Schematic adapted from wormbook (http://www.wormbook.org) showing the dauer pathway. The Dauer pathway is activated when the DAF-7 ligand (red) binds and activates the heterotrimeric receptor complex containing 2 subunits of the Type I receptor, DAF-I and 2 subunits of the Type II receptor, DAF-4. The R-Smads, DAF-8 and DAF-14 (light green), act as signal transducers of the DAF-7 signal. The activated Smads can inhibit the function of the Co Smad, DAF-3 (dark green) and DAF-5 (indigo) and inhibit dauer development (Gumienny and Savage-Dunn, 2013).

Mice carrying a deletion for the Galanin neuropeptide or the Galanin receptor GALR are highly susceptible to epileptic seizures (Fetissov et al., 2003; Lerner et al., 2008). Additionally, the hippocampus of GALR KO mice also display altered expression of other neuropeptides such as Enkephalin, Dynorphin and Neuropeptide Y (NPY). Studies in several animal models have shown that the NPY neuropeptide also has additional physiological roles in the regulation of anxiety disorders such as depression and post-traumatic stress disorders (Wu et al., 2011).

1.9.1 **Neuropeptide genes in *C. elegans***

The *C. elegans* genome encodes about 113 neuropeptide genes. These peptides can be classified as insulin like peptides (Pierce et al., 2001), FMRF like peptides (FLP) and other non-insulin and non FMRF related neuropeptides. 70 genes encode FMRF-related peptides (Li, 2005; Li, Kim, et al., 1999; Li, Nelson, et al., 1999). The neuropeptide precursors are packaged in dense core vesicles. The mature neuropeptides are generated by cleavage of the precursor at the C terminus using proprotein convertases (PC). The precursors are further processed by carboxypeptidase E enzyme to generate the mature neuropeptides. The *C. elegans* genes, *kpc-1*, *egl-3/kpc-2, aex-5/kpc-3* and *bli-4/kpc-4* encode PCs, (Thacker and Rose, 2000),and *egl-21* encodes the carboxypeptidase enzyme (Jacob and Kaplan, 2003).

The expression patterns of 24 *flp* genes, *flp-1-flp-24* have been previously characterized using promoter gfp fusions (Kim and Li, 2004) ,and these genes are expressed predominantly in neurons. The *flp-2*, *flp-5* and *flp-21* genes are expressed in the M4 neuron. The functions of most of the *flp* genes in *C. elegans* are unknown;however, loss of *flp-1* function results in multiple behavioral defects, such as uncoordinated motion and insensitivity to osmolarity (Nelson et al., 1998). Recently a function for FLP-21 in the regulation of locomotion during hypoxia was described (Pocock and Hobert, 2010). Under hypoxic conditions, FLP-21 secreted from M4 produces an enhanced locomotory response.

1.10 **ZEB family transcription factors are highly conserved proteins**

C. elegans ZAG-1 (Zinc finger defective in Axonal Guidance) is a conserved protein, which has several orthologs in other species that include Zfh1 in *Drosophila* (Fortini et al., 1991), δEF1 in chick and mouse (Funahashi et al., 1993) , Zfhx1 in sea urchins (Yaguchi et al., 2012), ZEB and AREB6 (Watanabe et al., 1993) proteins in humans (Wacker et al., 2003). Together, these proteins are referred to as the ZEB family proteins. These proteins have an array of two or more C2H2 Zinc fingers and a centrally located homeodomain. They have other domains such as the Smad binding domain (SBD), the CtBP Interacting Domain (CID), and these domains have repressor activity (Figure 10). While *Drosophila* and *C. elegans* have only one homolog, namely ZAG-1 and Zfh1 respectively (Clark and Chiu, 2003; Fortini et al., 1991), the vertebrate proteins have two homologs ZEB1/ δEF1 and ZEB2/SIP1 (Smad Interacting Protein) (Verschueren et al., 1999). ZEB2/SIP1 also contains a cluster of Zinc Fingers at the N and C terminus and these Zinc Finger clusters at the two termini share a high degree of sequence identity with ZEB1/ δEF1 (Figure 10).

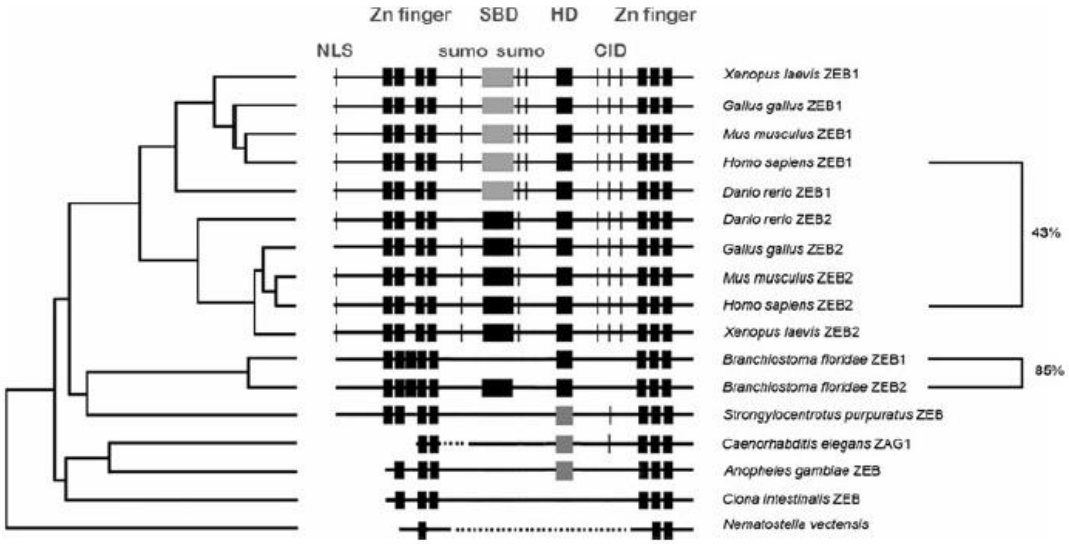

Figure 10 Structure of ZEB proteins

Schematic adapted from Gheldof et al showing the evolutionary phylogenetic analysis of ZEB proteins from vertebrates and invertebrates. All the vertebrates have 2 homologs of the ZEB proteins. These proteins contain a cluster of Zinc fingers at the N and C terminal ends, a centrally located homeodomain (HD) and a nuclear localization signal (NLS). Other domains include the Smad binding domain (SBD) and CtBP interaction domain (CID). These proteins can confer repressor activity through the SBD and CID. Many vertebrate homologs of the ZEB proteins contain SUMO binding sites suggesting that they can be post-translationally modified by SUMO (Vandewalle et al., 2005). The homeodomains of *S.purpuratus*, *C . elegans, A. gambiae* are shown in grey since they are less similar to the vertebrate ZEB proteins (Gheldof et al., 2012).

The ZEB proteins are expressed mainly in neurons and muscle tissues. *Drosophila Zfh1* is expressed in the motor neurons, muscles and many mesoderm derived tissues (Lai et al., 1991; Broihier et al., 1998). Mouse δEF1 is expressed in neural crest derived tissues such as the notochord and skeletal muscle (Higashi et al., 1997). In sea-urchins, the zfhx1 gene is expressed in the serotonergic precursor cells (Yaguchi et al., 2012). *C. elegans* ZAG-1 is expressed in the pharyngeal muscles, anal depressor muscle, the M4 neuron and many motor neurons in the ventral cord (Wacker et al., 2003; Clark and Chiu, 2003).

1.10.1 **Dual roles of ZEB proteins in transcriptional regulation**

1.10.1.1 **Mechanisms of transcriptional repression by ZEB proteins**

ZEB proteins can act as transcriptional repressors as well as activators depending on the cellular context (Figure 11). The ZEB family proteins can act as repressors of transcription by binding with CtBP (C-terminal binding protein) which is a transcriptional co-repressor (Postigo and Dean, 1999; Zhang et al., 2002). CtBP recognizes a PLDS sequences on the C-terminus of ZEB proteins. To further explore the mechanism of CtBP based repression, Shi et al, purified the CtBP complex from Hela cells expressing epitope tagged human CtBP (Shi et al., 2003). They demonstrated that the CtBP associated proteins included ZEB-1 and other histone modifying enzymes, such as histone deacetylases HDAC1 and HDAC2 and histone methyltransferases, which confer transcriptional repression. Another group of co-repressor proteins called CoREST (Ballas et al., 2001; You et al., 2001), was also isolated along with the CtBP complex. Thus ZEB proteins can repress gene transcription by recruiting co-repressor type proteins such as the CtBP and CoREST and chromatin modifying enzymes.

Another mode of transcriptional repression by ZEB proteins involves competing against activators. The ZEB proteins repress transcription of immunoglobulin, α 7 integrin and p73 genes by competing against activators and the alpha 7 integrin by competing against activators (Genetta et al., 1994; Fontemaggi et al., 2001; Pipaon et al., 2005; Jethanandani and Kramer,

2005). Drosophila Zfh1 can repress expression of *mef2* during muscle development (Postigo and Dean, 1999).

1.10.1.2 **Mechanisms of transcriptional activation by ZEB proteins**

ZEB proteins can also activate gene transcription in certain cases. Drosophila Zfh1 activates the expression of FMRF-a in neurons (Vogler and Urban, 2008). The human AREB6 homolog of ZEB proteins can activate and increase transcription of the of the rat Na,K-ATPase a1 subunit gene in a cell-specific manner (Watanabe et al., 1993). ZEB proteins can also transcriptionally activate the Vitamin D Receptor (VDR). Lazarova et al showed that the ZEB proteins bind the two E box promoters on the VDR promoter in vitro using gel shift assays. Using luciferase assays, the authors show that the ZEB proteins upregulated the transcription of the VDR promoter by 5.5 fold in colon carcinoma cells. The VDR promoter containing single and double E box site mutations show decreased levels of transcriptional activation compared to the wild-type VDR promoter (Lazarova et al., 2001). ZEB proteins can activate TGF-β signaling by activating the transcription of Smads (Postigo, 2003). Ikeda et.al demonstrated that the ZEB protein, AREB6, can activate transcription of a heterologous Hsp70 promoter by binding DNA through its C- terminal end in in vitro assays (Ikeda and Kawakami, 1995). Dillner et al showed that the ovalbumin gene can be activated by both chick δEF1 and human ZEB1. Using gel shift mobility assays, they identified two δEF1 binding sites which are needed for induction of the ovalbumin gene. The ability of δEF1 to activate transcription of ovalbumin was lost when the C terminal acidic residues were deleted from the δEF1 protein. They also showed that the acidic domain of δEF1 was capable of activating transcription of a heterologous promoter (Dillner and Sanders, 2004). Taken together, these studies show that ZEB proteins can have multiple transcriptional regulation mechanisms through which they regulate their target genes.

1.10.1.3 **ZEB proteins undergo post-translational modifications**

Post-translational modifications that occur in the ZEB protein could explain why ZEB proteins can have dual roles as activators and repressors of transcription. Although the significance of phosphorylation on ZEB transcription is still not understood, hyperphosphosphorylated and hypophosphorylated ZEB proteins are expressed in different cell lines (Costantino et al., 2002). The ZEB proteins can act as activators or repressors based on the differential recruitment of cofactors that bind the ZEB proteins (Postigo et al., 2003) (Figure 8). In the ZEB protein regulation of TGF-β signaling pathway, ZEB1 activates Smad mediated transcription, while the interactions of ZEB2 with the Smad proteins represses their activity. ZEB1 transcriptional activation is associated with the interaction of p300 and p/CAF which encode acetyltransferases (Bannister and Kouzarides, 1996; Ogryzko et al., 1996) that activate transcription (Figure 11). Binding of p300 to ZEB1 acetylates several residues following the CtBP interaction domain and this displaces the CtBP repressor from the ZEB1 locus. Additionally both ZEB1 and ZEB2 can be sumolyated, and this modification could potentially affect repressor activity (Figure 10). The SUMOylation of ZEB2 by the polycomb protein, Pc2, displaces CtBP binding and relieves the repression of E-cadherin by ZEB (Long et al., 2005).

1.10.2 **ZEB proteins are regulators of neuronal differentiation**

C. elegans ZAG-1 functions as a major regulator of motor neuron differentiation (Clark and Chiu, 2003; Wacker et al., 2003). ZAG-1 is required for axonal pathfinding of several types of motor neurons. In the absence of ZAG-1, several motor neurons have premature or defective axons which lack proper commissures. The expression of several motor neuron markers, such as *glr-1::gfp*, *unc-4::gfp* and *unc-47::gfp* is misregulated in a *zag-1(rh315)* hypomorph indicating that ZAG-1 is required for motor neuron differentiation. ZAG-1 has been described as a repressor which negatively regulates its own expression and genes required for GABA synthesis (Clark and Chiu, 2003; Wacker et al., 2003).

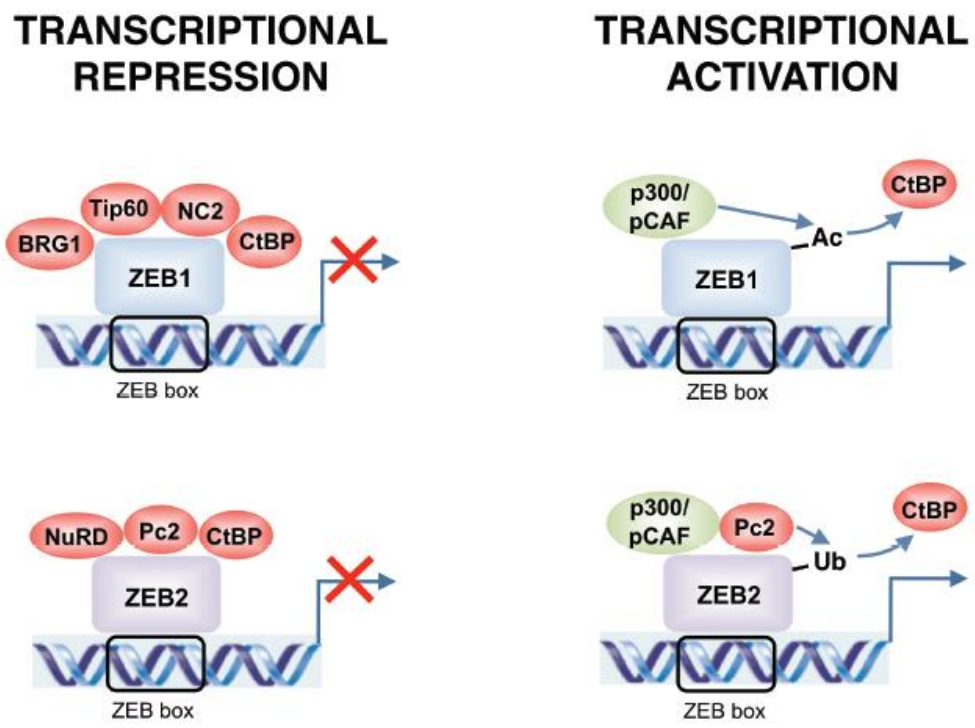

Figure 11 Dual modes of transcriptional regulation by ZEB proteins

Figure adapted from Sanchez Tillo et al showing that ZEB proteins can act as transcriptional repressors or activators based on the type of cofactors they bind and the target tissue they regulate. Binding of ZEB by CtBP recruits co-repressors BRG1,Tip60, and Nc2 which can repress transcription. ZEB2 has been shown to bind proteins from the Polycomb group such as Pc2 and the nuclear remodeling complex NuRD which confer gene repression. ZEB proteins can activate gene transcription through p300/pCAF. p300/pCAF binding to ZEB acetylates lysine residues in the CID and displaces CtBP from binding. This results in transcriptional activation of target genes (Sanchez-Tillo et al., 2011).

1.10.3 **ZEB proteins are regulators of neuronal differentiation**

C. elegans ZAG-1 functions as a major regulator of motor neuron differentiation (Clark and Chiu, 2003; Wacker et al., 2003). ZAG-1 is required for axonal pathfinding of several types of motor neurons. In the absence of ZAG-1, several motor neurons have premature or defective axons which lack proper commissures. The expression of several motor neuron markers, such as *glr-1::gfp*, *unc-4::gfp* and *unc-47::gfp* is misregulated in a *zag-1(rh315)* hypomorph indicating that ZAG-1 is required for motor neuron differentiation. ZAG-1 has been described as a repressor which negatively regulates its own expression and genes required for GABA synthesis (Clark and Chiu, 2003; Wacker et al., 2003). *zag-1* null mutants arrest shortly after feeding as L1 larvae since they lack peristalses necessary for normal feeding and hence, develop a stuffed pharynx phenotype. *zag-1* mutants do not display any muscle development defects unlike the vertebrate or fly homologs. ZAG-1 can also function as a transcriptional switch and regulate neuronal cell fates in sensory neurons (Smith et al., 2013).

The sea urchin ZEB homolog, Zfhx1 is required for differentiation of serotonergic neurons (Yaguchi et al., 2012). The zfhx1/Z81 protein is expressed in the gastrula stage in the precursor cells of the neuroectoderm. When translation of zfh1 was knocked down by morpholinos, the embryos failed to express the serotonergic marker, tryptophan synthase *(tph-1::gfp)* and the synaptotagmin B marker in the animal plate ,indicating that zfhx1 is required specifically for the proper differentiation of serotonergic neurons.

1.10.4 **Role of ZEB proteins in tumor progression**

ZEB1 and ZEB2 proteins are important regulators of tumor progression and they regulate epithelial to mesenchymal transition (EMT) by repressing E-Cadherin (Comijn et al., 2001; Eger et al., 2005; Liu et al., 2008). E-cadherin is present at adherens junctions, interacts with cytoskeletal proteins and Catenins and is a critical regulator of epithelial cell polarity.

During EMT, repression of cadherin results in loss of epithelial cell polarity and the acquisition of a stem like fate. As a result, cells which are increasingly resistant to apoptosis and acquire all the properties of invasive tumor cells are generated resulting in cancer metastasis (Mani et al., 2008; Singh and Settleman, 2010). Overexpression of ZEB1/ZEB2 results in an EMT in the epithelial cells. Along with E-cadherin, other epithelial cell polarity markers in gap junctions, desmosomes and tight junctions are also repressed (Vandewalle et al., 2005; Aigner et al., 2007). Many downstream signaling cascades such as the TGF-β pathways, NFκB and HIF-1 (Shirakihara et al., 2007; Chua et al., 2007) are activated in these tumors as a result of ZEB1/ZEB2 repression of E-cadherin. Since ZEB-1 is an inhibitor of E-cadherin, it is not expressed in normal epithelial tissues. Overexpression of ZEB-1 occurs in invading cancers of the lung, pancreas, gallbladder and breast.

1.10.4.1 **ZEB proteins promote replicative cell senescence**

Replicative cell senescence is a tumor suppressor mechanism that prevents uncontrolled cell division. Tumor cells overcome this inhibitory mechanism and divide indefinitely. ZEB1 functions in tumor cells by repressing expression of the cell cycle inhibitory proteins p15INK4b and p21CDKN1, which have potent tumor suppressor function (Krimpenfort et al., 2007) and thus allows cells to divide indefinitely.

1.10.5 **ZEB proteins are regulators of development and disease**

δEF1/ZEB1 expression is detected in the lateral plate mesoderm at E8.5 in mice. At E9.5, expression is detectable in the neural crest and branchial arches. ZEB-1 knockout mice have severe respiratory defects and contain severe craniofocal abnormalities, cleft palate, dysplasia of septum, skeletal defects that include malformed ribs, limbs and defects in intervertebral discs (Takagi et al., 1998). They also have severe T cell deficiency of the thymus. These phenotypes indicate that δEF1/ZEB-1 has a major role in regulating development in

mice. ZEB2 mutant mice exhibit neural tube closure defects, improper ectoderm development, severe growth defects and die by E13.5 (Van de Putte et al., 2003).

1.10.5.1 **Mutations in ZEB proteins cause Mowat Wilson Syndrome**

Mowat Wilson Syndrome (MWS) is a congenital disorder which results in facial abnormalities, mental retardation, genital abnormalities, congenital heart disease and Hirschsprung disease (HSCR) (Mowat et al., 1998). The correlation between MWS and ZEB proteins was first established by two independent groups who analyzed patients with MWS and found de novo chromosomal translocations which resulted in deletion or mutation of the of the ZEB2/SIP1 gene locus (Cacheux et al., 2001; Wakamatsu et al., 2001). Following this observation, several groups have identified mutations in ZEB2 as a major cause of MWS (Zweier et al., 2002; Wilson et al., 2003; Dastot-Le Moal et al., 2007). Dastot et al, reviewed several reported cases of MWS to identify the nature of mutations that occurred at the ZFHX1B gene. In a total of 160 individuals the mutations present in the patients were classified as gene deletions, missense mutations, insertions and deletions and complex mutations. Small insertions and deletions in the ZFHX1B coding sequence accounted for almost 60% of the cases reported. Exon 8 of the ZFHX1B gene in particular was prone to have a higher frequency of small insertion and deletion mutations. All the small insertions and deletion mutations result in a frame shift that causes premature truncation of the protein. Nonsense mutations in exon 8 account for 40% of the reported cases (Dastot-Le Moal et al., 2007).

2 MATERIALS AND METHODS

2.1 The *C. elegans* strains, plasmids and oligonucleotides used in this study are listed in Appendices E – G

2.2 General methods

2.2.1 Handling of Nematodes

C. elegans strains used in this study were grown under standard conditions (Lewis and Fleming, 1995) on NGM plates seeded with the OP50 strain of *E. coli* or on NEP plates seeded with NA22 bacteria. To store and maintain worm stocks on a long term basis, worm strains were frozen down and stored in liquid nitrogen. To freeze down worms, each strain was grown on five 6 cm diameter NGM plates to obtain freshly starved worms. The worms from each plate were then washed off in 1.5-2 ml of a 1:1 mixture of M9 buffer (20 mM KH_2PO_4, 40 mM Na_2HPO_4, 30mM NaCl, 1 mM $MgSO_4$) and freezing buffer (100 mM Nacl, 50 mM KH_2PO_4, 30% glycerol, 140 mM NaOH, 0.6 mM $MgSO_4$) and aliquoted into Nunc cryovial tubes which were stored at -80°C. The frozen strains were validated the next day by thawing out one vial of frozen worms on three or four 6 cm NGM plate seeded with OP50 bacteria, using a plastic Pasteur pipette. The following day, the plates were screened for the presence of viable worms or transgenic rollers whenever necessary. The remaining vials were transferred to liquid nitrogen tanks.

2.2.2 **Performing Germline transformations in *C. elegans***

Germline transformations were performed using standard techniques (Mello and Fire, 1991) using pRF4 that contains dominant the *rol-6* allele as a transformation marker by micro injection.

2.2.2.1 **Microparticle bombardment protocol**

Microparticle bombardment was performed using methods described previously (Merritt and Seydoux, 2010) using a Biolistic particle delivery system (Bio-Rad 165-2257) and the Hepta adapter (Bio-Rad 165-2225), 1 µm gold beads (Bio-Rad 165-2263), Microcarriers (Bio-Rad 165-2335), rupture discs (1550 psi) (Bio-Rad 165-2333), Hepta stopping screen (Bio-Rad 165-2226). On the day of the bombardment, the hepta adapter, forceps, stopping screens, microcarriers, and another empty glass petri dish were autoclaved using the Dry20 cycle to ensure the bombardment apparatus was sterile. To autoclave the microcarriers, they were transferred into a glass petri dish using forceps. The area near the bombardment chamber was also wiped with 70% ethanol to ensure additional sterile conditions.

The gold bead stock was prepared by weighing 35 mg of 1 µm gold beads into a siliconized eppendorf tube. The beads were soaked in 1 ml of 70% ethanol and vortexed for 5 minutes and soaked for 15 minutes. The beads were pelleted by centrifugation at 1500 rpm and the supernatant was removed. The beads were washed with 1 ml of sterile water 3 times and then pelleted, following which the supernatant was removed. The beads were resuspended in 1 ml of sterile 50% glycerol. This bead stock was stored at 4°C and this was sufficient to perform 5 bombardments.

To prepare the DNA for 1 bombardment, 100 µl of gold beads were aliquoted from the bead stock solution. Vortexed gold beads were resuspended in the gold bead solution prior to aliqoting as the gold beads tend to pellet at the bottom. 100 µl of gold bead suspension was

mixed with 10 µg of the desired plasmid DNA (35-50 µl) of a mini prep reaction along with 100 µl of 2.5 M $CaCl_2$ and 40 µl of 0.1 M Spermidine, soaked for 2 min after which the reaction was centrifuged at 1500 rpm to pellet the DNA and gold and the supernatant was removed. The pellet was washed once with 280 µl of sterile 70% ethanol, twice with 280 µl of 100% ethanol by flicking the tube to resuspend the pellet, and centrifuged at 1500 rpm after which the supernatant was removed. The pellet was then resuspended in 70 µl of 100% ethanol by flicking the tube. This is the DNA prep that is used for the bombardment. The DNA was vortexed at medium speed for 3-5 secs to ensure the DNA and gold beads are in suspension immediately prior to bombardment.

The sterile microcarriers were removed from their support paper casing and 7 of these were placed on an autoclaved glass petri dish using sterile forceps. 10 µl of the DNA prep was pipetted on to the center of the 7 microcarriers and allowed to air dry for 2-3 minutes to remove the ethanol. The microcarriers were transferred into the microcarrier holder using the forceps and the stopping screen was assembled using methods described in the Bio-rad manual. A rupture disc soaked in isopropanol was placed in the retainer of the hepta adaptor and tightened to the top of the bombardment chamber. To ensure it fits firmly, the special Bio-Rad tool was used to ensure it was completely tightened. The microcarrier holder was placed on the first rung in the bombardment chamber directly beneath the hepta adaptor and aligned such that each of the adaptor pins was directly pointing down at the microcarriers containing the DNA using methods described in the manual. The gene gun apparatus was turned on by activating the vacuum pump and the helium tank. The pressure in the helium tank was set to 1750 psi. The open petri plate containing the worms was taped to a sample holder in the second rung of the bombardment chamber using a rolled piece of adhesive tape or double sticky tape. The chamber was closed and the vaccum was pulled to 27 In of Hg. The fire button was pressed until the rupture disc ruptured. The vacuum in the chamber was released by pressing and

holding the Vent button and then the chamber was opened to remove the plate. The gene gun apparatus and the vacuum pump were turned off and the helium tank valve was closed after ensuring there was no pressure left in the line.

The worms were recovered by incubating at room temperature for 1 hour and then resuspended in 15ml of M9. 1ml of bombarded worms was plated on to a fresh 10 cm NEP plate.

The plates were incubated at 25°C for 2-2.5 weeks following which transformants were identified by screening for non Uncs that contain the *unc-119* rescue cassette and the gene of interest. The Transformants were verified by PCR genotyping appropriate genotyping assays.

It is possible to get revertants at a rate of up to 20% -25% and this varies based on the type of the transgene and the size of the construct. Revertants can sometimes be identified by isolating plates which have a lot of non-Uncs that resemble a near 100% transformation efficiency. Thus it is important to verify if the potential nonUnc worms are transformants which contain the transgene of interest using appropriate genotyping assays.

Extrachromosomal arrays which contain the transgene of interest and also segregate varying amounts of Uncs (5%-25%) can also be generated as a result of microparticle bombardment.

2.2.3 **Microscopy**

Worms were visualized using a Zeiss Axioskop capable of capturing differential interference contrast and fluorescence microscopy images. Images were acquired using an Axiocam MRm camera and processed using Axiovison software and processed in Adobe Photoshop. Movie recordings of pumping and peristalsis in wild-type and *zag-1* mutants were performed using methods described in detail in section 2.8.2.3.

2.3 Methods for manipulating nucleic acids

2.3.1 Isolation of Plasmid DNA

Single colonies were grown in 2-3 ml of 2xTY growth media containing the appropriate antibiotic and DNA was isolated using commercially available mini prep kits (Qiagen and Promega) using the manufacturer's protocol.

2.3.2 Restriction endonuclease digestion and DNA gel electrophoresis

DNA fragments were digested with restriction enzymes supplied by commercial manufacturers (New England Biolabs, Fermentas). Typically restriction digestion reactions were performed in a 30 µl reaction consisting of 4-5 µl (300-500 ng) of the DNA to be digested and incubated with 0.5 Units of the desired restriction enzymes in the recommended buffers using specific conditions recommended by the manufacturer's manual.

Digested products were visualized on 0.8-1.2% agarose gels based on size using 1X TAE buffer (40 mM Tris base, 30 mM acetic acid, 5mM sodium acetate, 1 mM EDTA) containing 0.3 µg /ml Ethidium Bromide (Et Br) and molecular weights of the digested product were determined by comparison to DNA ladders. DNA ladders were generated by digesting Lambda DNA (New England Biolabs) with HindIII and KpnI to determine molecular weights of DNA fragments greater than 1000bp. DNA ladders from commercial manufacturers (Invitrogen 100bp ladder, 1kb ladder, Gene ruler Fermentas) were also used to identify molecular weights of DNA fragments smaller than 1 kb. The agarose gel electrophoresis apparatus used consisted of Thermo EC, Maxicell Primo EC340 electrophoretic gel boxes that were connected to a Thermo EC 105 power supply. The agarose gel was analyzed on the alpha imager using UV light and the images were saved as TIFF files.

2.3.3 DNA purification using agarose gel electrophoresis

PCR products or plasmids were often gel purified following a restriction digest to improve the efficiency of the cloning process by eliminating undigested plasmid DNA which often causes background colonies during transformation. To perform gel purification, the DNA to be gel purified was run on a low melt agarose gel in 1X TAE buffer containing 0.3 µg/ml Et Br and the products were visualized using the UV trans-illuminator. The desired bands were excised and transferred into a 1.5 ml microfuge tube. The DNA was extracted from the gel slice using the QIAquick Gel Extraction Kit (Qiagen, Catalog # 28704) using the manufacturer's instructions.

2.3.4 Quantification of nucleic acids

Quantification of DNA and RNA was performed using the Nanodrop (ND-1000) according to manufacturer's instruction. To calibrate the instrument, distilled water was used as a blank solution, since all the nucleic acids were dissolved in nuclease free water or distilled water.

2.3.5 Design and preparation of primers

Primers were designed using Mac Vector software to include restriction sites or homologous sequences based on the experimental requirements and purchased from Integrated DNA technologies or Sigma-Aldrich. The primer samples were dissolved in 100 µl of distilled water and stored long term at -20°C. Working stocks were prepared by diluting the master stock to arrive at the desired concentrations.

2.3.6 DNA ligations

Ligations were performed using purified fragments of insert and vector DNA or using digested plasmid DNA. Ligation reactions were set up in 10 µl reactions containing 1:5 or 1:3 molar ratios of insert to vector to promote ligation of insert and vector along with 1 µl of T4 DNA

ligase and 2 µl of 5X ligase buffer. The vector was dephosphorylated using Alkaline Phosphatase to prevent re-ligation of the empty vector. Ligation reactions were carried out 16° C overnight or for 1 hour at the bench at room temperature and transformed into DH5 alpha *E. coli.*

2.3.7 **DNA Transformations**

DNA was transformed into competent cells by the heat shock method of transformation. Plasmid DNA or the ligation mixture containing the recombinant DNA was incubated with 100 µl competent cells which were prepared using standard protocols or commercially purchased and incubated on ice for 30 minutes. Cells were subjected to heat shock at 42°C for 30 seconds and returned to ice immediately and incubated for 2 min. Following the heat shock, the cells were recovered by adding 100 µl of 2xTY media to the cells and incubated by shaking at 220 rpm at 37°C for 1 hour. The recovered cells were spread on plates containing the appropriate antibiotic selection markers. The plates were incubated at 37°C overnight and scanned for the presence of single colonies in the plate.

2.3.8 **Sequencing DNA**

Plasmids were sequenced at the DNA services facility at the University of Illinois at Chicago using custom designed sequencing primers or standard sequencing primers available at the sequencing facility.

2.4 **Analysis of *dbl-1* promoter and the M4 enhancer**

2.4.1 **PCR Genotyping to identify *ceh-28(cu11)* homozygotes**

Single worm PCR was performed by picking 1-5 worms from each genotype onto a PCR tube containing 2.5 µl of 1X worm lysis buffer (50mM KCl, 10 mM Tris pH 8.3, 2.5 mM $MgCl_2$, 0.45% Triton X-100, 0.45% Tween 20,0.1% gelatin) and 120 µg/µl Proteinase K. The PCR

tubes containing worms were incubated at 60°C for 1 hour followed by 95°C for 15 minutes. PCR was performed using this lysed worm DNA as a template. The genotyping assay for identifying *ceh-28(cu11)* homozygotes was performed with primers PO640, P0641 and PO642 using methods and conditions described previously (Ray et al., 2008). The PCR program used was 94° C- 2 min, 94 °C -30 secs, 55° C – 45 secs, 72°C – 1 min, goto step 2, goto step -39 times, 72°C – 5 min, 12° C –Forever. Under these conditions, a *ceh-28(cu11)* homozygote will amplify a 516 bp that can be visualized on a 1% agarose gel.

2.4.2 **Generating 5' deletion constructs of the *dbl-1* promoter**

The *dbl-1* promoter deletion constructs were generated by restriction digestion of pOK205.01 containing the full length *dbl-1* promoter along with the respective restriction enzymes and re-circularization of the digested plasmid DNA.

A 30 µl reaction containing 3 µl pOK205.01 (500ng) was incubated with 0.5 units of Sph I and 3 µl of NEB buffer for 1.5 hours at 37°C. The digested product was PCR purified and ligated in a 10 µl ligation reaction containing 5 µl of digested DNA, 0.5 µl of T4 DNA ligase and 2µl 5X ligase buffer. The entire ligation reaction was then transformed into DH5 α *E. coli* using methods described in section 2.3.7 to generate pOK264.09/-3764Δ.

pOK 264.07/-1278Δ and pOK264.05/-646 Δ were generated by digesting pOK205.01 with HindIII and XbaI respectively using similar methods described above.

-3601Δ/ pOK264.01 and -2472Δ/ pOK264.03 were generated by double digestion of pOK205.01 with Pst1, Nhe1 and Pst1, DraIII respectively using standard methods. Following the digest, the restriction enzymes were heat inactivated by incubating the reactions at 70°C for 15 minutes and an end filling reaction was performed by incubating these reactions using 0.5 µl

of T4 DNA polymerase, 1.2 µl of 25mM dNTP for 30 minutes at 37°C. The reactions were PCR purified, ligated and transformed to generate recombinant clones.

2.4.3 **Generating the *dbl-1* M4 enhancer**

The *dbl-1* M4 enhancer was PCR amplified from pOK205.01 template using primers PO1244 [TAATGTCCGTCTTTGGGGTC] and PO1245 [CCAAGAACTGCGTTCAGACA]. The following PCR program was used: 94°C - 2 min, 94°C - 30 secs, 54°C – 1 min, 72 – 40 secs, Goto 2- 34 times , 72°C – 5 min, 12°C – forever. The 715 bp PCR product was digested with HindIII and XbaI and cloned into the HindIII and XbaI sites of pOK147.01/ Δpes-10::gfp vector to generate pOK272.06.

2.4.4 **Site directed mutagenesis of the *dbl-1* promoter and the *dbl-1* M4 enhancer**

Site directed mutagenesis was performed using the Quik change lightning multi mutagenesis kit according to the manufacturer's protocols. Primers were designed such that they were 24-50 bases in length with a melting temperature ≥ 78°C and the bases to be mutated were roughly positioned in the middle of the primer sequence. A 25 µl PCR reaction containing 100 ng of each mutagenic primer, 50 ng of plasmid template DNA, 2.5 µl of 10X Quik Change lightning Multi reaction buffer, 0.075 µl of Quik Solution (provided), 1 µl of dNTP mix (provided) and 1 µl of QuikChange Lightning Multi enzyme blend. The following PCR program was used: 95°C - 2 minutes, 95°C - 20 seconds, 55°C - 30 seconds, 65°C - 30seconds/1kb plasmid length, goto 2 – 30 times, 65°C – 5 minutes, 12°C – forever. After the amplification, the reaction was placed on ice for 2 minutes and digested with 1 µl of DpnI at 37°C for an hour. The XL-10 ultra-competent cells were thawed on ice for 5 minutes and 2 µl of β-ME (provided) was added to the competent cells. 3 µl of the DpnI digested DNA was transformed into XL-10 ultracompetent gold cells (provided) using the heat shock transformation method described previously. The

transformed cells were recovered by adding 0.5 ml of preheated NZY+ broth, shaking for 1 hour at 37°C and spreading them on 2xTY plates containing ampicillin.

Pdbl-1$^{-2810\ mut}$, also called pOK270.02 was generated by site directed mutagenesis using the full length *dbl-1* promoter pOK205.01 as a template and primer pairs PO1170[CCATTCAACTGTCCATTCTCTGTTTTAAACAGATCATCTCACTGACCTT] and PO1171[AAGGTCAGTGAGATGATCTGTTTAAAACAGAGAATGGACAGTTGAATGG].

Pdbl-1$^{-2107\ mut}$, also known as pOK272.05 was generated using pOK205.01 as template and primer pairs PO1174 [ACACAATTGTTAGTTATCGTTTGATCTTGCCGCCGTCTCCG] and PO1175 [CGGAGACGGCGGCAAGATCAAACGATAACTAACAATTGTGT].

Pdbl-1$^{-2042\ mut}$ respectively was generated using pOK205.01 as template and primers pairs PO1176 [ATATGAGAAGAAAACATTCTTGATCTTGCGAGCAACTTCTTGCTGTC] and PO1177 [GACAGCAAGAAGTTGCTCGCAAGATCAAGAATGTTTTCTTCTCATAT].

-825 mut/ pOK277.01 was generated by site directed mutagenesis using pOK272.06[*dbl-1* M4 enhancer] as a template and primer pairs PO1248 [TGGAGCTATTGTTTTTCACACCCAGACGATGAATCTGGTGGG] and PO1249 [CCCACCAGATTCATCGTCTGGGTGTGAAAAACAATAGCTCCA]. -738 mut/ pOK277.03 was generated using primer pairs PO1178 [TTTTAAGCAACAGTGGTAGTAAGTTGACATCAGGCATTTCGAAAACC] and PO1179 [GGTTTTCGAAATGCCTGATGTCAACTTACTACCACTGTTGCTTAAAA] using site directed mutagenesis protocols described above.

2.5 Analyzing g1 gland cell morphology in TGF-β signaling pathway components

2.5.1 Construction of *daf-8(e1393) I; ivIs12/+ II* strain

The OK1014 strain containing *daf-8(e1393) I; ivIs12/+ [phat-1::yfp] II ,* was generated using the following steps: The worms were maintained at 16°C and the following steps were performed. In the P0 generation, N2 males were mated with rolling hermaphrodite from the OK0977 strain bearing an integrated *ivIs12 [phat-1::yfp]* gland cell reporter to generate an adequate number of *ivIs12/+* rolling males. In the F1 generation, *ivIs12/+* rolling males were mated with *daf-8(e1383)* mutants. In the F2 generation, cross progeny, rolling hermaphrodites which are double heterozygous for the *ivIs12* transgene and *daf-8(e1393)* (Genotype: *phat-1::yfp/+; daf-8(e1393/+*) were cloned onto individual plates and allowed to have progeny at 16°C. Approximately 40 F3 rolling hermaphrodites were cloned to individual plates and allowed to have progeny at 16°C for 3 days following which the F3 moms were shifted to new plates and allowed to have progeny at 25°C for 2 days. In the F4 generation, the plates at 25°C were screened to identify rolling dauers, that were homozygous for the *daf-8(e1393)* mutation and contained the *phat-1::yfp* transgene. These rolling dauers were cloned onto new plates and shifted to 16°C and allowed to have progeny and these plates were labelled as OK1014. This strain is heterozygous for the *ivIs12* transgene since the rolling dauers segregated 25% non-rollers.

2.5.2 Construction of *daf-14(m77) IV; ivIs12/+ II* strain

The OK1015 strain containing *daf-14(m77) IV; ivIs12/+ II* was generated using the methods described below: The worms were maintained at 16°C and the following steps were performed. In the P0 generation, N2 males were mated with rolling hermaphrodites from the OK0977 strain bearing an integrated *ivIs12 [phat-1::yfp]* gland cell reporter transgene to

generate adequate number of rolling males. In the F1 generation, *ivIs12/+* rolling males were mated with *daf-14(m77)* mutants. In the F2 generation, cross progeny rolling hermaphrodites which are double heterozygous for the *ivIs12* and *daf-14(m77)* (Genotype: *phat-1::yfp/+; daf-14(m77/+*) were cloned onto individual plates and allowed to have progeny at 16°C. Approximately 40 F3 rolling hermaphrodites were cloned to individual plates and allowed to have progeny at 16°C for 3 days following which the F3 moms were shifted to new plates and allowed to have progeny at 25°C for 2 days. In the F4 generation, the plates at 25°C were screened for rolling dauers, that were homozygous for the *daf-14(m77)* mutation and contained the *phat-1::yfp* transgene. These rolling dauers were cloned onto new plates and shifted to 16°C and allowed to have progeny and these plates were labelled OK1015. This strain is heterozygous for the *ivIs12* transgene.

2.5.3 **Examining the expression of *phat-1::yfp* in *sma-2* and *sma-3* mutants**

The g1 gland cell morphology in *sma-2* and *sma-3* mutants were visualized using the GD273 strain containing *sma-2(e502)III; ivIs12 II* and GD274 strain containing *sma-3(e491)III; ivIs12 II*. These strains were generously provided by Dr. Jeb Gaudet, University of Calgary, Canada.

2.5.4 **Construction of *sma-4(e729) III; ivIs12 II* strain**

The OK1017 strain containing *sma-4(e729) III; ivIs12 II* was generated using the following steps. In the P0 generation, N2 males were mated with the rolling hermaphrodites from the OK0977 strain expressing the integrated *phat-1::yfp* transgene gland cell marker to generate rolling males. In the F1 generation, the *ivIs12/+* rolling males were then mated with *sma-4(e729)* hermaphrodites to generate cross progeny rolling hermaphrodites. In the F2 generation, the rolling hermaphrodites were picked and cloned onto individual plates and allowed to have progeny. In the F3 generation, plates which contained Rolling Sma worms

were identified and these Rol Sma animals were cloned onto individual plates and allowed to have progeny. Plates which segregated 100% rolling Rol Sma animals were identified and these plates were named OK1017.

2.5.5 **Construction of *daf-3(mg90) X; ivEx[phat-3::yfp]***

The following steps were performed at 16°C. OK1016 containing *daf-3(mg90) X; ivEx[phat-3::yfp]* was generated by mating N2 males with the GD26 strain containing an extra chromosomal array for the gland cell marker *phat-3::yfp* in the PO generation. In the F1 generation, adequate rolling males were picked and mated with *daf-3(mg90)* mutants hermaphrodites and L4 stage cross progeny rolling males were picked. In the F2 generation, these cross progeny rolling males which are of the genotype *ivEx[phat-3::yfp]/+; daf-3/0* were then crossed with *daf-3(mg90)* mutant hermaphrodites to generate cross progeny rolling hermaphrodites. In the F3 generation these rolling hermaphrodites were cloned onto individual plates and allowed to have progeny and maintained at 16°C. These plates were named OK1016 and gland cell morphology was visualized by picking rollers and observing them under the fluorescence microscope.

2.5.6 **Construction of *cuEx611*[pOK230.01 + poK210.01+*pRF4*] strain**

To obtain rescue of gland cell morphology in *dbl-1* mutants, the following steps were performed. N2 animals were injected with 15 ng/µl of pOK210.01 *[phat-3::yfp]*, pOK230.01*[Pser-7b::dbl-1]* and 100 ng/µl of pRF4 to make OK0762 *cuEx611*. In the P0 generation, rolling hermaphrodites from OK0762 strain were crossed with N2 males to generate adequate number of rolling males. In the F1 generation, rolling males were mated with *dbl-1(ev480)* mutants to generate cross progeny rolling hermaphrodites. In the F2 generation, the rolling hermaphrodites were picked and cloned to individual plates and allowed to have progeny and plates were screened to identify Rol Sma animals, since *dbl-1* mutants exhibit the Sma

phenotype. In the F3 generation, Rol Sma worms were cloned to individual plates and plates which segregated 100% Rol Sma in the next generation were labelled as OK0792.

2.5.7 **Construction of *ceh-28(cu11); cuEx611* strain**

To rescue g1 gland cell morphology defects in *ceh-28(cu11)* mutants, we mated N2 males with rolling hermaphrodites from the OK0762 strain to generate adequate number of rolling males bearing the rescuing array. In the F1 generation, the rolling males were mated with *ceh-28(cu11)* mutants to generate an adequate number of cross progeny rolling hermaphrodites. In the F2 generation, the rolling hermaphrodites were cloned onto individual plates and allowed to have progeny. The F3 rolling progeny were cloned onto individual plates and allowed to have progeny for 3 days at 25°C, following which the F3 mom were genotyped to identify *ceh-28(cu11)* homozygotes using single worm PCR using methods described previously in section 2.4.1.

2.6 **Construction of *unc-31(e928); ivIs12* strain**

OK0973 containing *unc-31(e928); ivIs12* was generated using the following steps. In the P0 generation, N2 males were mated with rolling hermaphrodites from the OK0977 strain expressing the integrated *phat-1::yfp* transgene gland cell marker to generate rolling males. In the F1 generation, the rolling males were crossed with *unc-31(e928)* mutants to generate cross progeny rolling hermaphrodites. In the F2 generation, these rolling hermaphrodites were cloned onto individual plates and allowed to have progeny. The F3 progeny were screened under a dissecting scope to identify *unc-31(928)* animals which express GFP, since *unc-31(e928)* mutants are severely uncoordinated and don't exhibit a strong Rol phenotype. 30 Rol Uncs were cloned onto individual plates and allowed to have progeny. These plates were again screened under the dissecting scope to identify a plate which segregated 100% Rol Uncs and named OK0973.

2.7 Identification and characterization of downstream targets of CEH-28

2.7.1 Identifying CEH-28 binding sites in the downstream targets of CEH-28

The *egl-17* promoter containing bp 18977:21584 in cosmid F38G1 (Accession number FO080171), the *flp-5* promoter containing bp 6953:10452 in cosmid C03G5 (Accession number FO080313), the *flp-2* promoter containing bp 10095150-10096347 in cosmid WO7E11(Accession number # NC_003284), the *flp-21* promoter containing bp 33029:35724 of cosmid C26F1 (Accession number FO080683) and the *zag-1* promoter containing bp in fosmid wrm063aA08 were scanned on Wormbase for the presence of CEH-22 consensus binding sites described by Berger et al., 2006 by selecting the following options: Tools->Gbrowse-> Annotate Sequence Motif->Configure ->check the CEH-22 _Berger _2006 position weight matrix checkbox > paste the *ceh-22* Position Weight Matrix in the paste PWM here textbox, enter a Threshold of 0.82 -> select configure. The following *ceh-22* position weight matrix sequence shown below was used. The location and sequences of the CEH-22 binding sites present in the promoters of *egl-17*, *flp-5, flp-21* and *zag-1* are indicated in Appendix D, Figure 29 C-F.

```
A  [33  8  0 93  1  0  0  7 95 46 51 ]
C  [15 71 89  1 97  0 16 27  0 29 20 ]
G  [31 19  0  0  0  0  0 63  0 20 15 ]
T  [19  0  9  5  0 99 83  1  4  3 12 ]
```

2.7.2 Construction of *ayIs4; ceh-28(cu11)* strain

To visualize *egl-17::gfp* in *ceh-28(cu11)* mutants, in the P0 generation, the NH2466 strain *ayIs4; dpy-20(e1282)[egl-17::gfp]* bearing an integrated *egl-17* promoter fused to gfp, was crossed to N2 males to generate an adequate number of cross progeny males bearing the transgene. In the F1 generation, the *ayIs4/+* males were crossed into *ceh-28 (cu11)* hermaphrodites and 30 cross progeny L4 stage hermaphrodites, were cloned onto individual

plates and allowed to have progeny for 2 days at 25°C following which the moms were genotyped using primers PO640, PO641, and PO642 to identify worms which were heterozygous for *ceh-28(cu11)*. In the F2 generation, these *ceh-28(cu11)* heterozygotes were screened on a fluorescence scope to identify plates which contained GFP expressing progeny. 30 F2 progeny which are heterozygous for *ceh-28(cu11)* and the *ayIs4* transgene were identified and cloned onto individual plates and allowed to have progeny. In the F3 generation, animals were screened to *ceh-28(cu11)* homozygotes by single worm PCR genotyping. At this stage, the animals homozygous for *ceh-28(cu11)* and either heterozygous for the transgene in which case they segregated 75% GFP expressing animals in the F4 generation or segregated 100% GFP if they were homozygous for the transgene. 30 F3 moms homozygous for *ceh-28(cu11)* and expressed GFP were cloned onto individual plates and allowed to have progeny. In the F4 generation, a plate which segregated 100% GFP was identified by screening 30 L4 hermaphrodites in the F4 generation and this plate was named OK0978.

2.7.3 **Generating the *egl-17* M4 enhancer**

A 336 bp fragment from the *egl-17* promoter between bp -2589 and bp -2253 described to be necessary for M4 expression by Cui et al., 2003 was PCR amplified using primers PO1396 [AGCTCTAAGCTTCGAAATCACTGGAAGGCACT] and PO1397 [AGCTCTGTCGACGCCATAACTGACCTCATCCAA] using the following PCR program 94°C- 2 minutes, 94°C – 30 secs, 55°C – 30 secs, 72°C – 30 secs, goto 2 – 35 times, 72°C - 5 min, 12°C forever. The PCR product was digested with HindIII and SalI and cloned into the HindIII and SalI sites of pOK147.01/PD95.67. The resulting plasmid was named pOK291.06.

A 933 bp of the *egl-17* promoter containing sequences between bp -2638 and bp -1709 of cosmid F38G1 was PCR amplified using primers PO1396 [AGCTCTAAGCTTCGAAATCACTGGAAGGCACT]

and PO1398 [AGCTCTGTCGACGAGCGCTATTGGTTTTGTAC] using the following PCR program 94- 2 min, 94°C -30 secs , 55°C -1 sec,72°C -1 min, Goto 2 -35 times, 72°C – 5 min, 12° C forever. The PCR product was digested with HindIII and SalI and cloned into HindIII and SalI digested pOK147.01/PD95.67. The resulting plasmid was named pOK293.01 and was subsequently referred to as the *egl-17* M4 enhancer.

2.7.4 **Construction of strains expressing the FMRF neuropeptide genes in *ceh-28(cu11)* mutants**

To visualize the expression of the *flp* genes *flp-2, flp-5* and *flp-21* in M4 in *ceh-28(cu11)* mutants, the following methods were used. In the P0 generation, N2 males were mated with hermaphrodites from the following transgenic strains NY2049 *ynIs49 [flp-5::gfp]*, NY2057 *ynIs47 III; him-5(e1490) V,* NY2080 *ynIs80[flp-21::gfp],* to generate an adequate number of cross progeny transgenic males from each strain. In the F1 generation, transgenic males were then mated with *ceh-28(cu11)* hermaphrodites and allowed to have progeny. In the F2 generation, 20 L4 stage cross progeny hermaphrodites which expressed GFP and were double heterozygous for *ceh-28 (cu11)* and the transgenes of interest were identified by screening animals under a fluorescence dissecting scope and cloned on individual plates and allowed to have progeny for 5 days at 25°C following which the progeny were genotyped to identify *ceh-28(cu11)* homozygotes. 30 F3 progeny homozygous for *ceh-28(cu11)* and which expressed GFP were cloned on individual plates and their progeny were screened for animals which expressed 100% GFP in the F4 generation. These plates were named OK0979 *ynIs49 V; ceh-28(cu11) X*, OK0980 *ynIs57 III; ceh-28(cu11) X* and OK1013 *ynIs80; ceh-28(cu11) X*.

2.7.5 **Construction of *wgIs83; ceh-28(cu11)* strain**

In the P0 generation, N2 males were mated with hermaphrodites from the OP83 strain bearing an integrated *wgIs83 zag-1::yfp* transgene to generate an adequate number of

transgenic males. In the F1 generation the *wgIs83/+* males were crossed with *ceh-28(cu11)* hermaphrodites to generate cross progeny hermaphrodites. 30-40 F2 hermaphrodites were cloned on individual plates and allowed to have progeny for 5 days at 25°C, following which the mom were genotyped to identify *ceh-28* heterozygotes. After genotyping, 30 L4 stage hermaphrodites heterozygous for *ceh-28(cu11)* and the transgene were picked and cloned onto individual plates and allowed to have progeny for 2 days following which the moms were genotyped to identify *ceh-28(cu11)* homozygotes in the F3 generation. 30 F3 moms homozygous for *ceh-28(cu11)* were cloned onto individual plates and allowed to have progeny. In the F4 generation, a plate which segregated 100% GFP expressing animals was chosen by screening 30 L4 hermaphrodites on a fluorescence scope and named as OK0974.

2.8 **Characterizing the function of ZAG-1 in the M4 neuron**

2.8.1 **Identifying *zag-1(hd16)* homozygotes from the *zag-1/unc-17(ed113) dpy-13(e184)* strain**

zag-1(hd16) homozygotes arrest as L1 larvae and have severe locomotion defects. Since this strain is larval lethal, it is balanced over *unc-17 dpy-13*. To identify and recognize *zag-1* homozygotes, 8-10 non Unc hermaphrodites from the VH514 strain containing *zag-1(hd16)/unc-17(ed113) dpy-14(e184)* were bleached on an unseeded NGM plate and the L1 animals were analyzed the following day. *zag-1(hd16*) homozygotes have severe locomotion defects and adopt a coiled appearance and arrest as L1 larvae. These worms have a stuffed pharynx. This phenotype can be recognized by mounting the *zag-1(hd16)* mutants on a 2% agarose pad with M9 containing *E. coli* and imaging them on the microscope.

2.8.2 **Time lapse analysis of feeding behavior in wild-type and *zag-1(hd16)* mutants**

Pumping and peristalsis were recorded in untreated wild-type L1 larvae and *zag-1(hd16)* and in wild-type animals and L1 larvae treated with serotonin and arecoline respectively.

2.8.2.1 **Analysis of feeding behavior in untreated wild-type and *zag-1(hd16)* mutants**

To record pumping and peristalsis in untreated wild-type animals and *zag-1(hd16)* mutants, 8-10 adult hermaphrodites from N2 and the VH514 strain were bleached on an unseeded NGM plate respectively. L1 larvae from wild-type and *zag-1(hd16*) mutants which hatched in the absence of food were identified and mounted on a 2% agarose pad in a drop of M9 containing *E coli* and a coverslip was placed on top before imaging them. This protocol was done to ensure that the *zag-1(hd16)* animals don't get stuffed with too much bacteria while recording pumping and peristalsis. The animals were imaged on a Zeiss AxioImager using an Mrm Camera.

2.8.2.2 **Drug studies on wild-type and *zag-1(hd16)* mutants**

To record pumping and peristalsis behavior in drug treated animals, L1 larvae from N2 and *zag-1(hd16)* mutants were picked from a plate containing a mixed stage population of worms from N2 and VH514 strain respectively. They were placed on an unseeded NGM plate for 20 minutes following which they were treated with serotonin or arecoline respectively.

20 mM Serotonin solution was prepared by dissolving 0.0232 g of Serotonin (H7752, Sigma-Aldrich, Inc) in 3 ml of M9. Serotonin treatment of wild-type and *zag-1(hd16)* mutants was performed by soaking worms in 5 µl of 20 mM Serotonin solution for 20 minutes on a 2% agarose pad. An additional 5 µl of serotonin was added before imaging to keep the worms hydrated.

To incubate worms with arecoline, 50 µl of 1 M arecoline solution was plated onto a small NGM plate and allowed to dry overnight to arrive at a 5mM final concentration of arecoline. The next day, L1 animals from wild type and *zag-1(hd16)* mutants were incubated on this arecoline containing NGM plate for 20 minutes following which they were mounted on a 2% agarose slide with 5 µl of M9 solution containing OP50 and a coverslip was placed on top. The animals were imaged using a Zeiss AxioImager microscope equipped with an MRm camera and processed with ZEN 2011 software.

2.8.2.3 **Quantification of pumping and peristalsis behavior**

The feeding behavior in every animal was recorded at a speed of 25 frames /sec for a total time of 2 min. To quantify the feeding behavior in every animal, a region of every recorded movie, usually 200-300 frames during which the animal exhibited a consistent pumping rate was chosen and these frames were analyzed to determine pumping rate, peristalsis frequency, duration of pump and peristalsis whenever applicable. The duration of each frame was calculated using the relative time function on Axiovision and these values were exported into an Excel spreadsheet.

Pumping rate was measured using the formula: total number of pumps (n)/ total time for (n) pumps. To determine the duration of a procorpus contraction during a pump, the number of frames between the beginning and ending of a contraction in the procorpus was calculated. Similarly, to determine the duration of a terminal bulb contraction, the number of frames during which the grinder moved and returned to its original position was calculated. Duration of a peristalsis was determined by measuring the frames during which the isthmus lumen opened and closed. Frequency of peristalsis was calculated as a percent of pumps followed by peristalsis using the formula: total number of peristalsis x100/total number of pumps. The average and standard deviation for pump rate, duration of a corpus contraction, duration of terminal bulb contraction, and peristalsis frequency was calculated using Microsoft Excel.

2.8.3 **Analysis of M4 differentiation defects in *zag-1(hd16)* mutants**

The following transgenic strains were used as markers to visualize M4 differentiation in *zag-1(hd16*) mutants. MT15672 *nIs177[ceh-28::4xNLS::gfp]* (kindly provided by Bob Horvitz, MIT), BW1946 *ctIs43[Pdbl-1::gfp]; unc-42(e270) V* (kindly provided by Dr. Yo Suzuki, University of Colorado), (Suzuki, 1999), NH2466 *ayIs4[egl-17::GFP dpy-20(+)] I; dpy-20(e1282ts) IV* (Burdine et al., 1998), NY2049 *ynIs49[flp-5::gfp]* (Kim and Li, 2004), *cuEx469[ser-7b::gfp],* NY2047 *ynIs47 III; him-5(e1490) V* (Kim and Li, 2004)2057, NY2080 *ynIs80[flp-21::gfp]*, RM2258 *pha-1(e2132ts); mdIs18[unc-17::gfp]* (Alfonso et al., 1993).

To visualize the expression of *ser-7b::gfp* in *zag-1(hd16*) mutants, transgenic animals bearing the extra chromosomal array *cuEx469[ser-7b::gfp] ; rol-6(su1006)* were mated with N2 males to generate adequate number of rolling males. The rolling transgenic males were mated with *zag-1(hd16)/ unc-17(ed113) dpy-14(e184)* hermaphrodites and 25 cross progeny rolling hermaphrodites which were heterozygous for *zag-1* and contained the *ser-7b* transgene (*zag-1/*+ ; *cuEx469*) or heterozygous for *unc-17(ed113) dpy-14(e184)* and contained the *ser-7b* transgene (*unc-17(ed113) dpy-14(e184)/*+ ; *cuEx469)* were cloned onto individual plates and allowed to have progeny for 2 days at 25°C after which the mom was removed. Plates that segregated *zag-1(hd16)* homozygotes were identified and GFP expression was scored in *zag-1(hd16)* homozygotes and their siblings which were +/+ or *zag-1/*+ and we refer to these animals as *zag-1(+)* animals.

To visualize the expression of various other M4 differentiation markers in *zag-1(hd16)* mutants, animals bearing the following integrated transgenes: *nIs177[ceh-28::gfp], ctIs43[dbl-1::gfp],], ayIs4[egl-17:gfp], ynIs49[flp-5::gfp], ynIs57[flp-2::gfp], ynIs80[flp-21::gfp], mdIs18[unc-17::gfp]* were crossed into N2 males to generate cross progeny males bearing the transgene of interest. The transgenic males were mated with *zag-1(hd16)*/ *unc-17(ed113) dpy-14(e184)* hermaphrodites and allowed to have progeny. 30 GFP expressing cross progeny

hermaphrodites which were either double heterozygous for the transgene and *zag-1* or double heterozygous for the transgene and *unc-17* and *dpy-13* were cloned onto individual plates and allowed to have progeny for 2 days at 25°C after which the mom was removed. Plates containing animals that segregated *zag-1(hd16)* homozygotes were identified and GFP expression were scored in *zag-1(hd16)* homozygotes and *zag-1(+)* animals as described above. A maximum of 75% of all the progeny are expected to be transgenic.

2.9 **Miscellaneous methods**

2.9.1 **Isolation of M4 cells by fluorescence activated cell sorting (FACS)**

A synchronous population of L1 animals from the MT1572 strain *nIs177 I* [*ceh-28::4XNLS::gfp*] and the OK0944 strain *nIs177 I; ceh-28(cu11)* were used to perform the cell isolation and sorting. For typical cell isolation, approximately 500,000-800,000 L1 animals from each wild-type and *ceh-28* mutants is required to obtain a sufficient number of M4 cells that can be sorted by a flow cytometer. For each sorting experiment either a negative control (cells isolated from N2 worms) or a positive control (cells isolated from a pan neuronal GFP expressing strain) was used. Since cells from the negative and positive control were only used to set the gates for the flow cytometer and not used to collect cells, fewer number of L1s, typically, 100,000 or lesser animals were used to isolate cells for controls using similar conditions described below.

Five to six 15 cm diameter NEP plates seeded with NA22 containing lots of young adults from each wild-type and *ceh-28* mutants were prepared to yield sufficient number embryos that be can be hatched in M9 to obtain 500,000-600,000 L1s to be used in a typical cell isolation and sorting experiment.

2.9.2 **Obtaining a synchronous population of L1 animals to perform the cell isolation**

To obtain a large number of L1 animals the following protocol was used: worms from each strain were grown on five to six 10 cm diameter NEP plates seeded with NA22 for 5 days at 25°C. The worms from these plates were then expanded to five or six 15 cm diameter NEP plates seeded with NA22 and grown for 5-6 days at 25°C till you see a lot of young adults. Worms from these five 15cm plates were washed off and resuspended in 15 ml of M9 and 3 ml of worms were plated onto each 15 cm NEP plate. The plates were incubated for 3-5 days at 25°C.

Worms from each 15 cm diameter NEP plate were washed off into a sterile 15 ml conical tube with distilled water and centrifuged at 2 minutes at 2500 rpm to pellet the worms and the supernatant was removed. The washing step was repeated one more time and most of the supernatant was removed leaving only the worm pellet intact. The worm pellet was treat with 5 ml of bleach solution (2 ml Chlorox, 7.5ml d H_20, 0.5 ml 10 N NaOH) for 6 minutes and the tube was shaken by inverting it up and down continuously, several times throughout the incubation to ensure proper lysis. The bleach solution usually turns deep yellow by the end of the 6 min incubation,and the reaction was completely stopped by adding 10 ml of Egg Buffer (118 mM NaCl, 48 mM KCl, 2 Mm $Cacl_2$. 2H20, 2 mM $MgCl_2$. 6H20 and 25 mM HEPES) and centrifuging it for 2.5 minutes at 2500 rpm. The wash with egg buffer was repeated 3 times to remove all the bleach. The embryos were separated from the worm debris by thoroughly resuspending the worm pellet in 10 ml of 30% sucrose and centrifuging at 2500 rpm for 2.5 minutes at 4°C. At the end of this step, the embryos will float on the top while the worm debris settles at the bottom. 5 ml of sucrose solution containing the embryos was transferred to a new tube and diluted to 15 ml with distilled water. The solution was centrifuged at 2500 rpm for 2 minutes to pellet the embryos. The wash with water was repeated to remove any residual sucrose. The supernatant was removed and the pellet of embryos was suspended in 10 ml of M9 in a conical tube and

placed on a Nutator shaker. The embryos were hatched for 15 hours at room temperature. The total number of L1s in the 10 ml solution can be estimated by counting the number of L1s present in 1 µl of M9 under a microscope.

2.9.3 **Optimized larval cell isolation protocol to dissociate cells from L1 larva**

The larval isolation protocol described by Zhang et al., 2011, was used to prepare stock solutions and necessary reagents. We optimized the duration of detergent and protease treatment conditions to achieve sufficient release of cells from the L1 larvae from both wild-type and *ceh-28* mutants.

The following modified larval cell isolation protocol was used. After the 15 hour incubation of embryos in M9, the number of L1's that hatched in the 10 ml M9 solution was estimated by counting the number of L1s in 2-3 µl drop of the solution under a microscope. The L1s in the 15 ml conical tubes were pelleted by centrifuging them at 3000 rpm for 5 minutes at 4°C and the worm pellet was transferred to a 1.5 ml microcentrifuge tube. The pellet was washed once with 1 ml of M9 by centrifuging at 3000 rpm for 2 min and the supernatant was removed. 200 µl of freshly thawed SDS-DTT (20 mM HEPES, 0.25 % SDS, 200Mm DTT and 3 % sucrose) was added to the pellet and incubated for 3.5 min and the reaction was stopped by adding 800 µl of egg buffer. The tube was centrifuged at 13,000 rpm for 1 min and the wash with 1 ml egg buffer was repeated 5 times to remove any traces of SDS in the pellet. Following the wash, the worm pellet was treated with 100 µl of 15 mg/ml Pronase E (Sigma, P8811) for 25 minutes. During the Pronase incubation, the pellet was pipetted repeatedly and vigorously 50 times every 3 minutes with a P200 pipette tip by touching the bottom of the tube. The pipetting is believed to provide the mechanical disruption force to break up the worms. The digestion with Pronase was stopped by adding 900 µl of L-15 media (Life technologies 2013-027) supplemented with 10 % Fetal Bovine Serum (FBS). Cells were centrifuged at 10,000 rpm for 5

minutes at 4°C and the supernatant was removed. The pellet washing with L-15/FBS was repeated twice the cell pellet was resuspended in 1ml of L-15/FBS. The cell suspension was filtered using a 21G1 ½" needle and a 5 µm Durapore filter (Millipore, SLSV R25 LS) by filtering 500 µl of cell suspension at a time into a new tube and washing the filtered contents with additional L-15/FBS solution. Cells were spun at 6000 rpm for 3 min and the supernatant was removed. The cells from all the other tubes were combined into one tube and resuspended in 1 ml egg buffer and placed on ice until they are ready to sort.

2.9.4 **Using Fluorescence activated cell sorting to isolate GFP tagged M4 neurons**

The cell sorting was performed using the BeckMan Coulter Mo Flo instrument at the Research Resource facility (RRC) at UIC. Right before the sort, 1 mg/ml of propidium iodide was added to the tube to ensure cell viability. N2 cells were used as a negative control and a pan-neuronal gfp reporter was used as a postive control. The gating parameters and cell sort experiments were performed by the RRC research personnel. The gating parameters which were determined using the cells from the N2 strain or the *evIs111[[PF25B3.3::GFP]* were applied to the experimental sort of M4 cells from wild-type and *ceh-28(cu11)*. Size and granularity of the experimental cells are determined by plotting the Linear Function of Forward Scatter (FS Lin) versus Linear function of Side Scatter (SS Lin). The pulse width function was determined by plotting pulse width against side scatter. The amount of autoflourescence in the sample was determined and background subtraction was performed by plotting Log function of GFP compensation versus Log function of Auto fluorescence compensation. After the background subtraction, the threshold levels were set to separate signal from noise. The parameters determined using control cells were applied to the experimental cells and the sorting experiment was perfromd by collecting cells in 500 µl of TRIzol.

2.10 **Total RNA isolation from L1 stage animals using TRIzol Reagent**

Synchronized populations of L1 animals were obtained by bleaching gravid adults from N2, MT15672 and OK0944 strains and hatching them in M9 using methods described in section 2.9.2 and total L1 RNA from these animals was isolated using the following protocol. The L1 worms were pelleted by centrifuging them at 2500 rpm for 3 min and the supernatant was removed. TRIzol reagent was added in a 10:1 ratio (1 ml of TRIzol for 100 µl of worm pellet) and vortexed for 15 minutes at room temperature. The mixture was then centrifuged at 14,000 rpm using an Eppendorf centrifuge (5804 R, rotor F45-30-11) for 10 min at 4C and the supernatant was transferred to a fresh 1.5 ml microcentrifuge tube and 200 µl of Cholorofom was added and incubated at room temperature for 3 minutes. The tubes were then centrifuged at 14,000 rpm for 15 minutes at 4°C. The clear aqueous phase containing the RNA was carefully transferred to a fresh microcentrifuge tube, and 0.5 ml of isopropanol was added to precipitate the RNA. The tubes were incubated at room temperature for 10 minutes and centrifuged at 14,000 rpm for 10 minutes. A white pellet should be visible at this stage. The supernatant was decanted carefully without dislodging the pellet and the pellet was washed with 75% ethanol in DEPC treated water. The samples were centrifuged at 7,500 rpm for 5 minutes at 4°C and the supernatant was removed and the pellet was air dried for 20 minutes. Following the drying, the pellet was dissolved in 30 µl of DEPC treated water and incubated at 60°C for 10 minutes. The RNA samples were then subjected to DNAse treatment (Life technologies, AM1907) and further purified using an RNeasy clean-up kit (Qiagen). The purified RNA was then quantified using a Nanodrop to estimate the concentration.

2.11 **Performing quantitative RT- PCR using L1 RNA**

q RT-PCR was performed using the Power SYBR Green RNA-to-CT 1-Step kit (Life technologies) using L1 RNA from wild-type and *ceh-28* mutants according to manufacturer's protocol. Primers were designed according to manufacturer's guidelines such that they span an intron and detect 150-200 bp amplicons from the gene of interest while using a cDNA template. Primer pairs PO1317 [AAGCATCATAACACCGAGGC] and PO1318 [ACTGAGCTGGCATTGGATTT] were used to detect a 157 bp *dbl-1* amplicon, PO1399[ACTTTTCACTGGAGTTGTCCCA]/PO1400[GGTAGTTTTCCAGTAGTGCA] were used to detect a 144 bp *gfp* amplicon, PO1401/PO1402 were used to detect a 174 bp *ser*-7 amplicon and PO1061[AGGCGAAGGATGTGTTGTG]/PO1062[TCACCGTGTTCTTTGGGTC] were used to detect a 120 bp *ama-1* amplicon. A 20 µl reaction containing 200 nM of forward and reverse primer corresponding to each gene of interest, 0.16 µl RT enzyme super mix, 1 µl of template RNA (1 ng/µl), 10 µl of 2X SYBR Green and required amounts of distilled H_2O to constitute a final volume of 20 µl. For every gene that was assayed, the reactions were performed in triplicate to account for variations. The PCR reaction was set up in white PCR tubes (Bio-rad, TLS0851) and covered with optically clear caps (Bio-Rad TCS0803). The q RT-PCR was performed using DNA engine Opticon 2 (MJ Research) present in Dr. Jennifer Schmidt's lab, UIC and the tubes were placed in the center avoiding the outside rows and columns on the PCR machine. The following program was used: 1. 48°C - 30 min, 2. 95°C - 10 min, 3. 95°C - 15 secs, 54°C - 1 min, Plate read, Incubate at 80°C - 1 sec, Plate read, Go to STEP 3 - 39 times, Incubate at 95°C - 2 min, melting curve from 60°C- 95°C read every 0.2C, hold for 1 sec, End.

2.11.1 **Quantification and analysis of q-PCR data**

After the PCR program was completed, the q-PCR data was analyzed using the MJ Opticon Monitor Analysis Software. The cells corresponding to a single primer set was selected

on the screen. In the quantitation window, the autoscale was unchecked and the log scale option was selected. The 'trend' under 'options' was selected in the top right corner of the window. The threshold bar was set above the background noise by manually moving it above. The 'melting curve' tab on the screen was selected and the -dI/dT dot in the 'Display' box to the right was selected. We ensured that there was only a single peak in the melting curve graph around 75°C and that there was no multiple peaks corresponding to primer dimers at lower melting temperatures. If the melting curve looked good, we returned to the quantitation window and clicked the 'calculations' tab on the lower right part of the window and selected 'copy to clipboard' option and pasted the values to an Excel spreadsheet. This was repeated for every primer set. To calculate the relative fold change, the $2^{-\Delta\Delta Ct}$ method was used (Livak and Schmittgen, 2001).

2.12 **PCR and sequencing to verify RNAi clones in the feeding library**

The potential list of downstream targets of TBX-2 were knockdown using feeding RNAi. The list of genes screened and the respective feeding RNAi clones used to knockdown these genes listed in Appendix D, Table XIII. The RNAi clone for each gene was streaked onto a 2xTY plate containing ampicillin and tetracycline and incubated at 37°Cr overnight to allow the growth of individual colonies. A colony PCR was performed to verify the right inserts in the library by picking a colony with a sterile pipette tip onto a PCR tube containing 2 µl of dH_20 heated to 95°C for 15 minutes followed by 4°C for 10 minutes. This denatured DNA was used as template and the PCR reaction was performed in a 50 µl reaction using primers PO9017 and PO918 and the following PCR program was used: 94°C - 10 min, 94°C- 30 secs, 59.6°C - 30 secs, 72°C for 3 minutes, goto 2 - 39X, 72°C - 5 min, 12°C forever. 5 µl of the PCR reaction was analyzed on a 1% agarose gel to ensure the presence of a single 3 kb amplification product. After the PCR verification, single colonies were picked and grown to isolate the plasmids and the samples were sequence verified using M13 F(-20) primers. The sequence

results were subject to a BLAST search in the *C .elegans* genome to ensure they targeted the desired gene.

2.13 **Feeding RNAi protocol**

The feeding RNAi was performed for each gene listed in Appendix D, Table XIII using protocols described (Kamath and Ahringer, 2003) previously. The required RNAi clones were grown on liquid culture and seeded onto 6 cm NGM/Carbenicllin/IPTG plates and incubated for 12-24 hours at room temperature to allow the bacteria to grow and begin induction. 10 L4 stage N2 or rollers were picked onto to 1 NGM RNAi plate for 24 hours at 20°C. After the incubation, 3 worms were passaged to individual NGM RNAi plates from the prefed RNAi plate. These plates were incubated for 24 hours at 20°C after which the moms from each plate were removed, leaving behind embryos. These plates were incubated for an additional 24 hours at 20°C. After incubation, worms were scored for RNAi phenotypes by examining these animals under DIC to look for changes in morphology or GFP expression. Embryonic lethality could be estimated by counting the number of embryos that were present on an RNAi plate and estimating the number of unhatched embryos the following day as a result of RNAi.

3 CEH-28 activates *dbl-1* expression and TGF-ß signaling in the *C. elegans* M4 neuron

3.1 Publication information

This work titled ‘CEH-28 activates *dbl-1* expression and TGF-beta signaling in the *C. elegans* M4 neuron’ was published in the *Journal of Developmental Biology* in March 2014 (Ramakrishnan et al., 2014).

Figures 10, 11, 14 15 B-J, and Table III, Contributing Author: Paramita Ray.

Figures 12, 13, 15 I-K 16, 17, 18 and Tables I &II Contributing Author: Kalpana Ramakrishnan.

The data for Table IV was contributed by Kalpana Ramakrishnan and Paramita Ray.

3.2 **Abstract**

M4 is a multifunctional neuron in the *C. elegans* pharynx that can both stimulate peristaltic contractions of the muscles in the pharyngeal isthmus and function systemically to regulate an enhanced sensory response under hypoxic conditions. Here we identify a third function for M4 that depends on activation of the TGF-ß family gene, *dbl-1,* by the homeodomain transcription factor CEH-28. *dbl-1* is expressed in M4 and a subset of other neurons, and we show CEH-28 specifically activates *dbl-1* expression in M4. Characterization of the *dbl-1* promoter indicates that CEH-28 targets an M4-specific enhancer within the *dbl-1* promoter region, while expression in other neurons is mediated by separate regulatory sequences. Unlike (Ramakrishnan et al., 2014) *ceh-28* mutants, *dbl-1* mutants do not exhibit M4 synaptic and signaling defects. Instead, both *ceh-28* and *dbl-1* mutants exhibit morphological defects in the g1 gland cells located adjacent to M4 in the pharynx, and these defects can be partially rescued by M4-specific expression of *dbl-1* in these mutants. Identical gland cell defects are observed in *sma-6* and *daf-4* mutants defective in the receptor for DBL-1, but they are not observed in *sma-2* and *sma-3* mutants lacking the R-Smads functioning downstream of this receptor. Together these results identify a novel neuroendocrine function for M4 and provide evidence for an R-Smad-independent mechanism for DBL-1 signaling in *C. elegans*.

3.3 Introduction

At the cellular level, the *C. elegans* nervous system is remarkably simple and well characterized. In adult hermaphrodites, the nervous system consists of 302 cells that can be divided into a pharyngeal nervous system of 20 cells and an extra-pharyngeal nervous system of 282 cells. Electron micrographic reconstructions have produced a wiring diagram describing cellular morphology and synaptic connectivity throughout both the pharyngeal and extra-pharyngeal nervous systems (Albertson and Thomson, 1976; White et al., 1986b). While many excellent studies have revealed a great deal about how this nervous system senses the environment, controls various behaviors, and affects development (Ardiel and Rankin, 2010; Avery and You, 2012; Schafer, 2005), we still do not understand how such a simple nervous system carries out so many complex functions.

Many *C. elegans* neurons appear multifunctional and cannot be easily classified as a single morphological type, such as motor neuron, sensory neuron, or interneuron (Albertson and Thomson, 1976; White et al., 1986b). In addition, a variety of neurons also synthesize factors controlling developmental and homeostatic processes such as dauer formation, fat storage, and body size (Ashrafi, 2007; Gumienny and Savage-Dunn, 2013; Hu, 2007). Such multifunctionality may be one mechanism by which this simple nervous system controls many complex behaviors (Avery and Thomas, 1997b).

The pharyngeal motor neuron M4 is a multifunctional neuron that stimulates contraction of the muscles in a region of the pharynx called the isthmus and regulates enhanced sensory perception during hypoxia (Avery and Horvitz, 1989; Pocock and Hobert, 2010). M4 forms en passant synapses on the muscles in the posterior isthmus, and synaptic vesicles at these synapses are believed to release acetylcholine onto the isthmus muscles to stimulate a wave-

like, peristaltic contraction in these muscles (Albertson and Thomson, 1976; Ray et al., 2008). M4 also contains larger dense core vesicles (DCVs) that are not found in other pharyngeal motor neurons (Albertson and Thomson, 1976). DCVs are believed to secrete neuropeptides and hormones (Burgoyne and Morgan, 2003), and the M4 DCVs likely release the FMRFamide neurotransmitter FLP-21 to affect the extra-pharyngeal nervous system under hypoxic conditions (Pocock and Hobert, 2010). In addition, both morphological features and gene expression patterns suggest M4 has other signaling functions. First M4 synapses onto the pharyngeal g1 gland cells, which are secretory cells that extend ducts through the isthmus that join the pharyngeal lumen (Albertson and Thomson, 1976). The gland cells secrete a variety of mucin-like proteins that facilitate bacterial transport through the pharyngeal lumen during feeding (Smit et al., 2008). Second, M4 expresses genes encoding signaling molecules such as the FGF-family member *egl-17* and the TGF-ß family member *dbl-1* suggesting M4 may have other signaling functions (Burdine et al., 1998; Suzuki et al., 1999).

We are interested in the role the NK-2 homeodomain transcription factor CEH-28 plays in M4. CEH-28 is expressed exclusively in M4 from mid-embryogenesis through adulthood, and it plays a crucial role in regulating M4 synapse formation and stimulation of isthmus peristalsis (Ray et al., 2008). In *ceh-28* mutants, synapses are morphologically abnormal, and they are inappropriately located in regions that normally exhibit dendritic characteristics (Albertson and Thomson, 1976). *ceh-28* mutants can hyper-stimulate peristaltic contractions of the pm5 muscles that make up the pharyngeal isthmus (Ray et al., 2008).

In this work we investigate the function and regulation of *dbl-1* gene expression in M4. *dbl-1* encodes a TGF-ß family factor that is part of the Sma/Mab pathway, and it is expressed in M4 and a subset of pharyngeal and extra-pharyngeal neurons (Gumienny and Savage-Dunn, 2013). *dbl-1* was initially characterized based on its developmental role as a regulator of body size and male tail morphogenesis (Morita et al., 1999; Suzuki et al., 1999), but more recently it

has been found to function throughout the life-cycle as a regulator of innate immunity, reproductive aging, and aversive olfactory learning (Luo et al., 2010; Zhang and Zhang, 2012; Zugasti and Ewbank, 2009).

Here we show that *dbl-1* expression in M4 depends on CEH-28, and that *dbl-1* expression in M4 regulates g1 gland cell morphology. CEH-28 activates *dbl-1* expression in M4 by targeting a cell-specific enhancer, and mutation of CEH-28 binding sites in this enhancer strongly reduces its activity. The g1 gland cells exhibit abnormal morphology in both *ceh-28* and *dbl-1* mutants, and restoring expression of *dbl-1* in M4 partially rescues these mutant defects. DBL-1 secretion does not depend on DCV release as *unc-31* mutants defective in this process exhibit normal gland cell morphology. DBL-1 signaling affecting gland cells requires the Sma/Mab pathway receptors SMA-6 and DAF-4 but does not require the receptor-regulated Smads SMA-2 and SMA-3. These results identify a novel function for DBL-1 and the M4 cell, and we suggest DBL-1 protein secreted from M4 non-autonomously activates a Smad-independent TGF-ß signaling pathway affecting gland cell morphology.

3.4 **Materials and Methods**

3.4.1 **Nematode handling, transformation and strains**

C. elegans were grown under standard conditions (Lewis and Fleming, 1995). Germline transformations were performed using standard techniques (Mello and Fire, 1995) using injection mixes containing pRF4 rol-6(su1006) (100 ng/µl) and gfp or other plasmids (10-25 ng/ µl).

The following strains were used in this study: BW1946 ctIs43*[Pdbl-1::gfp*]; *unc-42(e270)* V, BW1806 *dbl-1(ev580) V* (kindly provided by Y. Suzuki, University of Colorado), (Suzuki et al., 1999), OK0542 *ctIs43; unc-42(e270) V; ceh-28(cu11) X,* OK0543 *ctIs43; unc-42(e270) V;*

ceh-28(tm1258) X , OK0435 *cuEx324[ceh-28::gfp]* (Ray et al., 2008), OK0545 *dbl-1(ev580); cuEx324.*

The following strains were used to analyze 5' deletions of the *dbl-1* promoter:

OK0830 *cuEx659[Pdbl-1::gfp -3764Δ],* OK0833 *cuEx662[Pdbl-1::gfp -3061Δ]*, OK0837 *cuEx666[Pdbl-1::gfp -2472Δ], OK0839 cuEx668[Pdbl-1::gfp -1278Δ]; OK0842 cuEx671[Pdbl-1::gfp -646Δ].*

The following strains were used to assay *dbl-1* M4 enhancer activity in wild-type and *ceh-28(cu11)* mutants respectively: OK0765 *cuEx613[dbl-1 M4 enhancer wild-type]*

OK0766 *ceh-28(cu11); cuEx613*, OK0772 *cuEx619[M4 enhancer -825mut*], OK0774 *cuEx621[M4 enhancer -738mut*], OK0780 *cuEx627[M4 enhancer double_mut]*

The following strains were used to examine pharyngeal g1 gland cell morphology:

GD26 *ivEx[phat-3::yfp*] (kindly provided by J. Gaudet, University of Calgary), OK0567 *ceh-28(cu11); ivEx[phat-3::yfp],* OK571 *ceh-28(tm1258); ivEx[phat-3::yfp*], OK0792 *dbl-1(ev580); phat-3::yfp*, OK585 *daf-1(m40) IV; ivEx[phat-3::yfp*], OK586 *daf-4(m72)III; ivEx[phat-3::yfp]*, OK584 *sma-6(wk7); ivEx[phat-3::yfp]*, OK0977 *ivIs12[phat-1::yfp]* (kindly provided by J. Gaudet, University of Calgary, Canada), GD273 *sma-2(e502) III; ivIs12 II*, GD274 *sma-3(e491) III; ivIs12 II* (Raharjo et al., 2011), OK1014 *daf-8(e1393) I; ivIs12 II*, OK1015 *daf-14(m77) IV; ivIs12 II*, OK1016 *daf-3(mg90) X*; *ivEx[phat-3::yfp],* OK1017 *sma-4(e729) III; ivIs12 II,* OK0762 *cuEx611[pser-7b::dbl-1; phat-3::yfp*], OK0763 *dbl-1(ev580); cuEx611*, OK0859 *ceh-28(cu11); cuEx611*. N2 worms were injected with 15 ng/µl of pOK210.01 [*phat-3::yfp],* pOK230.01*[Pser-7b::dbl-1*] and 100 ng/µl of pRF4 to make OK0762.

To investigate gland morphology in *unc-31* mutants, the following strains were used CB928 *unc-31(e928)* (kindly provided by J. Richmond, UIC), and OK0973 *unc-31(e928); ivIs12*.

3.4.2 General methods for nucleic acid manipulations and plasmid construction

Standard methods were used to manipulate all DNA sequences (Ausubel, 1990) and all plasmids are available from the authors.

The full-length *Pdbl-1*::gfp pMY+NLS/pOK205.01 containing bp 11,900-16,530 of T25F10 cosmid (Accession #U64856) was provided by W. Wood (University of Colorado) (Suzuki et al., 1999). Deletions in *Pdbl-1::gfp* are named to indicate the number of base-pairs upstream of the *dbl-1* translational start site and were generated by restriction digestion to the following sites in the *dbl-1* promoter: SphI (-3764Δ; pOK264.09), NheI (-3601Δ; pOK264.01), DraIII (-2472Δ; pOK264.03), HindIII (-1278Δ; pOK 264.07), and XbaI (-646Δ; pOK264.05).

The M4 enhancer wild-type was amplified from pOK205.01, and a HindIII-XbaI fragment (bp 15,281-15,916 of cosmid T25F10) was inserted upstream of the ∆pes-10::gfp to make pOK272.06. CEH-28 binding sites in the enhancer where separately mutated using Quik Change Lightning Multi Kit (Stratagene) in pOK272.06 to produce M4 enhancer -825mut plasmid pOK277.01 and M4 enhancer -738mut plasmid pOK277.03, respectively. The M4 enhancer double_mut plasmid pOK277.05 was created by mutating the site at -738bp in pOK277.01. The constructs were sequenced to confirm the presence of targeted mutations. The adjacent fragment of the *dbl-1* promoter (bp 13,502-15,284 of cosmid T25F10) was amplified and a HindIII-NheI was inserted upstream of ∆*pes-10::gfp* to generate pOK274.19.

The *Pser-7b*::*dbl-1* expression plasmid pOK230.01 was constructed by amplifying the full-length *dbl-1* orf from yk1350b03/pOK227.03 (provided by Y. Kohara) with primers PO801 [AGGTACCAAAATGAACGACTCTGTGCGGAC]

and PO803 [CCAGAATTCTAATGTGCGACGACGATGG] digesting with KpnI and EcoRI, and inserting this fragment downstream of the *ser-7b* promoter in KpnI-EcoRI digested pOK197.03 (Hobson et al., 2003).

3.4.3 **Identification of candidate CEH-28 binding sites in the *dbl-1* promoter**

Candidate CEH-28 binding sites were identified by scanning the *dbl-1* promoter using the WormBase function Annotate Sequence Motif (www.wormbase.org) with the JASPAR position-frequency-matrix MA0264.1 (jaspar.cgb.ki.se) at a threshold of 0.82 (Berger et al., 2006). We identified 8 CEH-28 binding sites starting at base pair -2810, -2668, -2441, -2107, -2042, -835, -738, and -497 bp upstream of the *dbl-1* translational start site. Conserved sites were identified in the *dbl-1* promoter using multiz alignments of the *C. elegans*, *C. briggsae, C. remanei, C. brenneri* and *C. sp. 11* genomes (http://genome.ucsc.edu/).

3.4.4 **Microscopy**

Micrographs of wild-type and mutant animals were acquired using a Zeiss Axioskop microscope using an Axiocam MRm camera. Images were analyzed using AxioVision software and processed using Adobe Photoshop.

To analyze pharyngeal pumping and peristalsis, L1 larvae from wild-type and *dbl-1*(ev580) were selected and recorded as described previously (Ray et al., 2008). For each genotype, pumping and peristalsis were analyzed in at least 5 animals for approximately 30 seconds.

M4 synapses in wild-type and *dbl-1(ev580)* mutants were visualized using a *ser-7b::snb-1::gfp* fusion described previously (Ray et al., 2008). Z-stacks of SNB-1::GFP were acquired using a Zeiss Axiovert 200 microscope and deconvolved using AxioVision 4.3 software. Adjacent focal planes exhibiting GFP throughout two pharyngeal nerve cords were Z-projected

using maximum fluorescence and fluorescence intensity profiles were generated on a Macintosh computer using ImageJ (developed at the US NIH and available at http://rsb.info.nih.gov/nih-image/) (Figure 16).

3.5 Results

3.5.1 *dbl-1::gfp* is not expressed in *ceh-28* mutant M4 cells

A *dbl-1* promoter::gfp fusion *(Pdbl-1::gfp)* containing a 4.6 kb promoter fragment was previously shown to be expressed in a subset of neurons, including the pharyngeal neurons M1, M2, M4, M5 and I5, as well as non-pharyngeal neurons including some amphid neurons and neurons of the ventral nerve cord (Suzuki et al., 1999). To determine if *dbl-1* expression in M4 requires CEH-28, we compared expression of *Pdbl-1::gfp* in wild-type animals and *ceh-28* mutants. In wild-type animals, strong *Pdbl-1::gfp* expression was observed in the M4 cell in 96% of transgenic adults (Figure 12 B,C; n=57). In comparison, strong *Pdbl-1::gfp* expression in M4 was observed in only 17% of *ceh-28(cu11)* adults (n=53) (Figure 12 D,E) and 19% of *ceh-28(tm1258)* adults (n=47). Thus, *ceh-28* functions upstream of *dbl-1* and is specifically required for *Pdbl-1::gfp* expression in M4. A *ceh-28*::gfp reporter is expressed normally in the M4 neuron of *dbl-1(ev580)* mutants (Figure 13), indicating that DBL-1 is not necessary for M4 differentiation.

3.5.2 The *dbl-1* promoter contains separable regulatory regions controlling expression in M4 and other neurons

To determine if the *dbl-1* promoter could be directly targeted by CEH-28, we searched for sequences matching the binding site for the related NK-2 homeodomain factor CEH-22 (jaspar.genereg.net; ID MA0264.1; (Berger et al., 2006)). NK-2 family factors are characterized by a tyrosine residue at homeodomain position 54 that is crucial to DNA-binding specificity

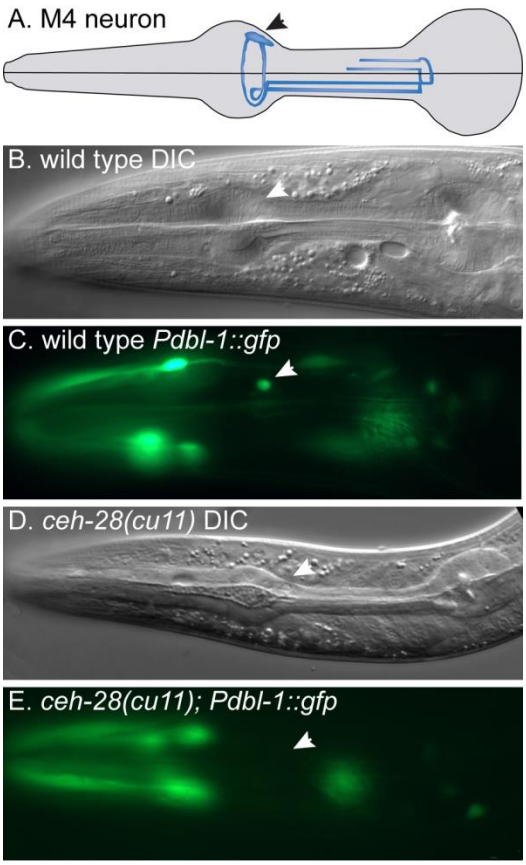

Figure 12 *Pdbl-1::gfp* expression in wild type and *ceh-28* mutants

(A) Schematic diagram of the pharynx indicating the M4 neuron (blue) (adapted from Albertson and Thompson, 1976). The M4 cell body (arrowhead) is located in the pharyngeal metacorpus, and it extends two processes through the pharyngeal isthmus. (B-E) DIC and fluorescence micrographs of a wild-type animal (B, C) and a *ceh-28(cu11)* mutant (D, E) expressing *Pdbl-1::gfp*. The M4 neuron is marked (arrowheads).

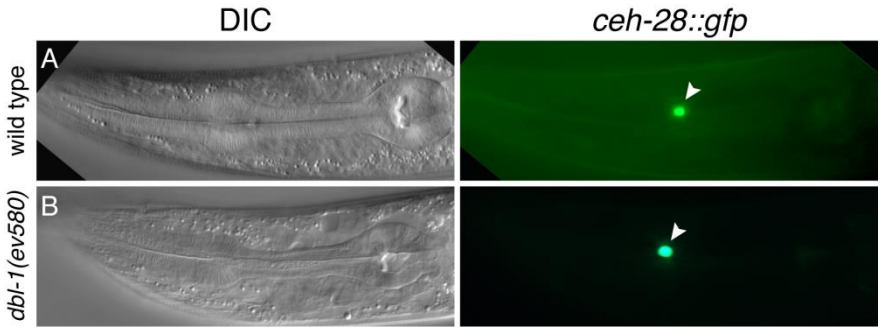

Figure 13 *dbl-1 mutants* express *ceh-28::gfp* normally

DIC and fluorescence micrographs of wild-type (A) and *dbl-1(ev580)* (B) adults expressing *ceh-28::gfp* in the M4 cell. *ceh-28::gfp* (arrowheads) was expressed in M4 in 100% of wild-type (n=23) and *dbl-1(ev580)* (n=27) animals.

(Harvey, 1996; Pradhan et al., 2012), and CEH-22 and all characterized members of this family bind similar DNA sites (Berger et al., 2006; Okkema and Fire, 1994). The CEH-22 and CEH-28 homeodomains are 62% identical, and it is likely they exhibit very similar DNA-binding specificity. We found 8 candidate CEH-28 binding sites in the *dbl-1* promoter (Figure 14 A), with three of these sites conserved in the *dbl-1* promoter in related nematodes based on multiz alignments (http://genome.ucsc.edu/).

To identify sequences regulating *dbl-1* expression, we examined the intensity and frequency of GFP expression in transgenic animals bearing 5'-deletions of *Pdbl-1*::*gfp*. Notably, a deletion to -2472 largely eliminated *Pdbl-1::gfp* expression in most neurons but retained strong expression in M4 (Figure 14 A,D; Table 1). This suggests separable regulatory sequences control *dbl-1* expression in M4 and other neurons. A moderate decrease in the frequency and intensity of *Pdbl-1::gfp* expression was observed when sequences were further deleted to -1278, and expression was completely lost when deleted to -646 (Figure 14 E,F; Table I). These results suggest that the candidate CEH-28 binding sites in the *dbl-1* promoter contribute additively to expression in M4, and indicate that the region between -1278 to -646 contains sequences necessary for activating *dbl-1* expression in M4.

3.5.3 **The *dbl-1* promoter contains an M4-specific enhancer activated by CEH-28**

We next tested fragments of the *dbl-1* promoter containing candidate CEH-28 binding sites for enhancer activity by asking if they could activate expression of a Δ*pes-10::gfp* reporter. The Δ*pes-10::gfp* alone is not expressed in transgenic *C. elegans*, but it is sensitive to upstream enhancers (Okkema and Fire, 1994). A 1783 bp fragment between regions -3061 bp to -1278

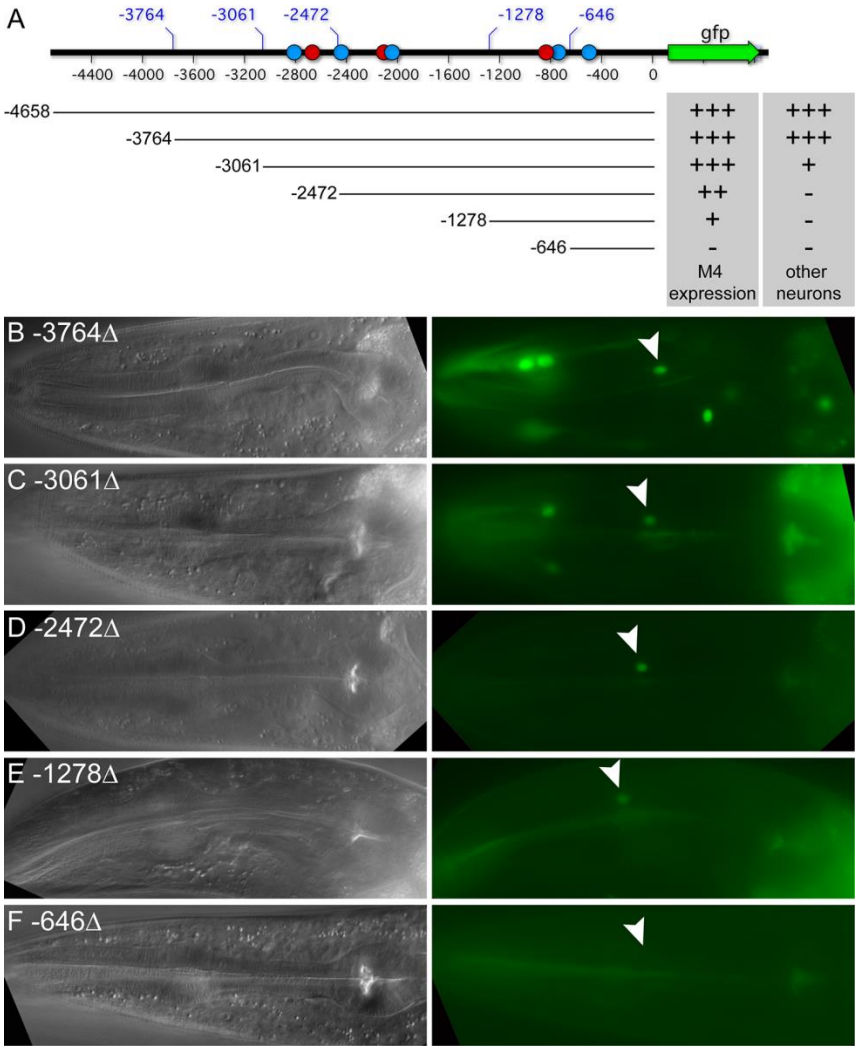

Figure 14 Deletion analysis of the *dbl-1* promoter

(A) Schematic diagram of the *Pdbl-1::gfp* indicating candidate CEH-28 binding sites (circles; red indicate conserved) and the endpoints of promoter deletions. Relative expression levels and frequency in M4 and other neurons inside and outside the pharynx are indicated. Deletion endpoints are numbered by distance upstream of the *dbl-1* ATG codon. (B-F) DIC (left) and fluorescence (right) micrographs of adult animals expressing the indicated *Pdbl-1::gfp* deletions numbered as in (A). The M4 cell body is marked with an arrowhead.

Table I: FREQUENCY OF *Pdbl-1::gfp* EXPRESSION IN M4

Pdbl-1::gfp promoter deletions	Frequency of expression in M4 (n) [a]
-4658Δ	85% (40)
-2472Δ	64% (50)
-1278Δ	40% (45)
-646Δ	0% (40)

[a] M4 GFP expression was scored in transgenic adults

bp containing 5 candidate CEH-28 binding sites had no detectable enhancer activity (Figure 15A; data not shown).

In contrast, the adjacent 632 bp fragment between regions -1278 bp to -646 bp containing 2 candidate CEH-28 sites exhibited strong, M4-specific enhancer activity, and we refer to this fragment as the M4 enhancer (Figure 15 A,B; Table II). When examined in a *ceh-28(cu11)* null mutant background, activity of the M4 enhancer was completely lost (Figure 15C; Table II). Thus the M4 enhancer depends on CEH-28.

The M4 enhancer contains two candidate CEH-28 binding sites: one located at bp -825, which is conserved in other *Caenorhabditis* species, and a second at bp -738. We tested the effect of mutations in each of these sites on M4 enhancer activity either alone or in a double mutant. Mutation of the site at -825 led to a decrease in the intensity of GFP expression level and a moderate decrease in the frequency of animals expressing GFP, whereas mutation of the site at -738 had little effect on enhancer activity (Figure 15 D, E; Table II). In comparison, a double mutant affecting both of these sites had a stronger reduction in both the intensity and frequency of GFP expression in M4, although weak expression was still observed in some animals (Figure 15 F; Table II). These results indicate that both sites contribute to activity of the M4 enhancer, and strongly suggest that CEH-28 directly activates *dbl-1* expression in M4.

3.5.4 **M4 neuronal function and synapses are normal in *dbl-1* mutants**

ceh-28 mutants exhibit frequent and prolonged peristalses of the pharyngeal isthmus muscles and a stuffed pharynx phenotype, and we believe these phenotypes result from abnormal and mispositioned synapses in M4 throughout the isthmus (Ray et al., 2008). Because, TGF-ß mediated signals have been implicated in synapse assembly and positioning

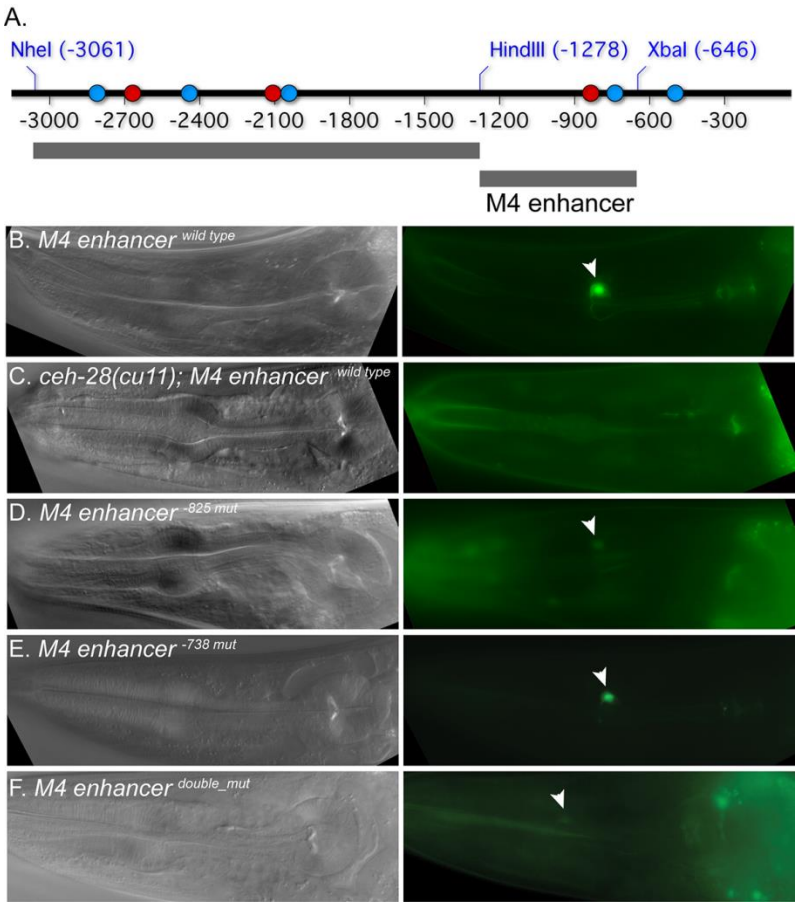

Figure 15 Identification and analysis of the M4 enhancer

(A) Schematic diagram of the *dbl-1* promoter region and fragments tested for enhancer activity (gray bars; numbered as in Figure 1). (B, C) DIC and fluorescence micrographs of wild-type (B) and *ceh-28(cu11)* (C) adult animals expressing Δ*pes-10::gfp* containing the wild-type M4 enhancer. (D-E) Micrographs of wild-type adults expressing Δ*pes-10::gfp* containing mutated M4 enhancers. The M4 cell body is marked with an arrowhead.

Table II ACTIVITY OF THE M4 ENHANCER DEPENDS ON CEH-28 BINDING SITES

Genotype	Percent animals expressing GFP in M4 (n) [a]
cuEx613 [M4 enhancer $^{wild\ type}$]	100% (30)
ceh-28(cu11); cuEx613 [M4 enhancer $^{wild\ type}$]	0% (20)
cuEx619 [M4 enhancer $^{-825\ mut}$]	63% (30)
cuEx621 [M4 enhancer $^{--738\ mut}$]	95% (40)
cuEx627 [M4 enhancer $^{double\_mut}$]	30% (37)

[a] transgenic adults were scored for GFP expression in M4

in other organisms (Marques, 2005), we examined M4 neuronal function and synapses in *dbl-1(ev580)* mutants. However, in both assays, *dbl-1* mutants appear normal.

We used video microscopy to examine pharyngeal contractions in wild-type and *dbl-1(ev580)* mutant L1 larvae, and found *dbl-1* mutants exhibit normal pharyngeal pumping and peristalses In particular, the length of isthmus peristalses are very similar in wild type and *dbl-1* mutants (Table III). Consistent with normal pharyngeal function, we never observed a stuffed pharynx phenotype *in dbl-1(ev580)* mutant adults (n=74) (data not shown).

We next examined synapses in *dbl-1(ev580)* mutants using a *snb-1::gfp* fusion gene expressed specifically in the M4 cell using the *ser-7b* promoter (Ray et al., 2008). SNB-1::GFP is a functional synaptobrevin that marks synaptic vesicles (Nonet, 1999). In both wild-type and *dbl-1*(ev580) animals SNB-1::GFP marked synapses are appropriately localized in the posterior region of the pharyngeal isthmus and these synapses appear more uniformly sized and spaced than we have previously observed in *ceh-28* mutants (Figure 16) (Ray et al., 2008).

In summary, the M4 cell function and synaptic morphology in *dbl-1*(ev580) mutants appears similar to that of wild-type animals. These observations are in sharp contrast with those from similar analyses of *ceh-28* mutants (Ray et al., 2008), and they indicate *dbl-1* is not necessary for M4 synapse formation or neuronal function.

3.5.5 ***ceh-28* and *dbl-1* mutants exhibit similar defects in pharyngeal g1 gland cell morphology**

The function of DBL-1 in M4 is unknown, but, as a secreted growth factor, it likely affects nearby cells. The g1 pharyngeal gland cells are in close proximity to M4, and M4 forms synapses on g1 (Albertson and Thomson, 1976). The g1 cell bodies are located in the posterior bulb of the pharynx, and they extend processes anteriorly along the dorsal and subventral

Table III PHARYNGEAL PUMPING AND PERISTALSIS IN *dbl-1* MUTANTS

	Wild type [a]	*dbl-1(ev580)* [b]
Pump rate (pumps/min)	174 ± 39	179 ± 25
Procorpus contraction length (msec)	74 ± 14	79 ± 19
Posterior bulb contraction length (msec)	129 ± 28	118 ± 20
Isthmus peristalsis length (msec)	215 ± 38	210 ± 90
% pumps followed by isthmus peristalsis	2.5%	10.5%

[a] Five N2 L1s were recorded for 29-30 sec each, and a total of 442 pumps were analyzed.

[b] Five *dbl-1(ev580)* L1s were recorded for 20-30 sec each, and a total of 352 pumps were analyzed.

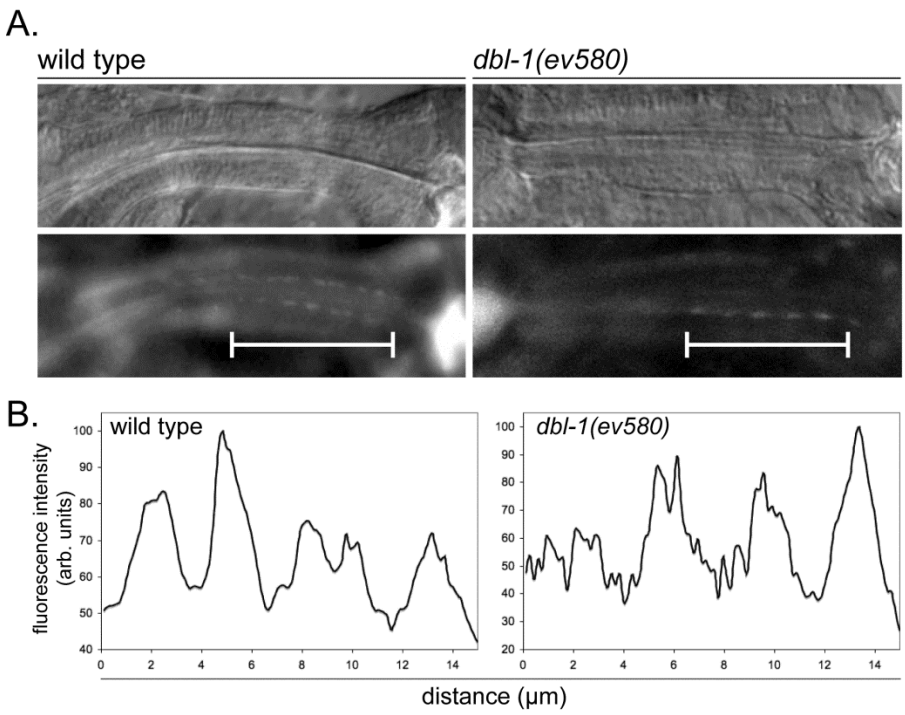

Figure 16 Characterization of SNB-1::GFP marked synapses in *dbl-1* mutants

(A) DIC and Fluorescence micrographs showing the pharyngeal isthmus of wild-type and *dbl-1(ev580)* mutant adults expressing SNB-1::GFP. M4 synapses appear as fluorescent dashes in the M4 processes in the posterior half of the isthmus (bar). Anterior is left. Two processes are visible in wild type while a single process is visible in *dbl-1(ev580)*. (B) Representative profiles of SNB-1::GFP fluorescence intensity in M4 processes.

pharyngeal nerve cords, where they contact the M4 neuronal processes (Figure 17A). The dorsal process extends the length of the pharynx and connects to the pharyngeal lumen near the anterior tip of the pharynx, whereas the subventral processes extend through the isthmus and connect to the lumen near the anterior bulb.

We examined the g1 gland cells in *ceh-28* and *dbl-1* mutants and found these animals had nearly identical defects in gland cell morphology. The g1 gland cells were visualized using *phat-3::yfp* and *phat-1::yfp* reporters labeling the g1 gland cell bodies and processes (kindly provided by J. Gaudet), and identical results were obtained using *hlh-6::gfp* and *kel-1::gfp* reporters as markers (data not shown). In wild-type animals, the gland cell processes are thin and have a uniform diameter along their entire length (Figure 17 B). In comparison, we found these processes in the mutants often appeared thicker than in wild-type animals and often exhibited abnormal swellings near the M4 cell body (Figure 17 C-E). To rule out the possibility that gland cell defects result from the reporter genes themselves, we directly compared wild type and *ceh-28(cu11)* mutant gland cell processes in non-transgenic animals using DIC microscopy and found that *ceh-28(cu11)* mutants had g1 gland cell processes that were wider than those in wild-type animals (Figure 18). While the *ceh-28(cu11)* gland cell processes contained vesicles similar to those of wild type animals, these processes did not appear stuffed with vesicles, as has been previously observed in *daf-9* and *peb-1* mutants that also exhibit enlarged gland cell processes (Albert and Riddle, 1988; Fernandez et al., 2004).

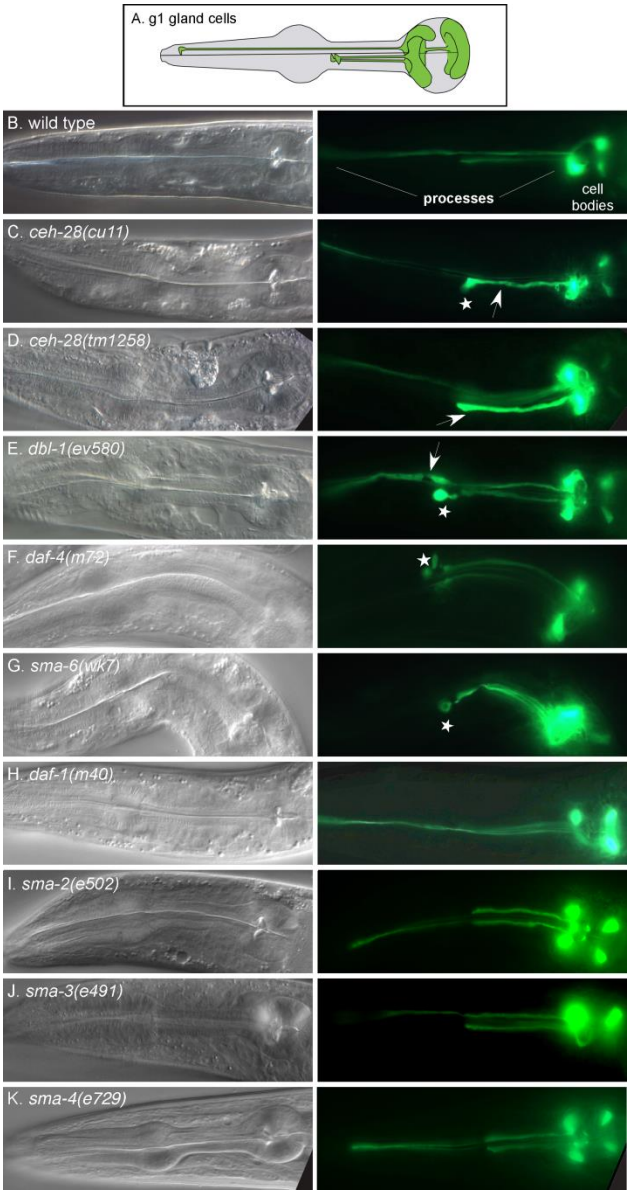

Figure 17 g1 gland cell defects in *ceh-28* and TGF-ß signaling mutants

(A) Schematic diagram of the pharynx indicating the g1 gland cells (green) (adapted from (Albertson and Thomson, 1976)). (B-K) DIC and fluorescence micrographs of the indicated mutants expressing the g1 gland cell markers *phat-3::yfp* (B-H) or *phat-1::yfp* (I-K). In wild-type animals, the gland cell processes are thin and a uniform diameter. Thickened processes (arrowheads) and abnormal swellings (stars) are indicated. In some cases only the subventral process are in focus.

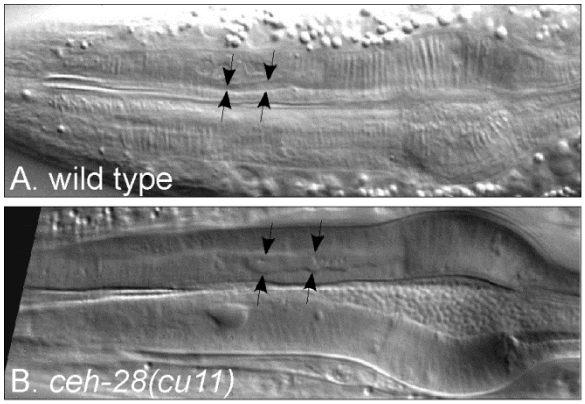

Figure 18 gland cell defects in untransformed *ceh-28* mutants

DIC micrographs of the anterior pharynx with the width of the dorsal g1 gland cell process marked (arrows).

3.5.6 **Normal gland cell morphology depends on the SMA-6 and DAF-4 receptors but is independent of R-Smads**

DBL-1 is a TGF-ß family ligand that is known to regulate body size and male tail morphogenesis through the Sma/Mab signaling pathway (Gumienny and Savage-Dunn, 2013). We asked if other components of this pathway also affect gland cell morphology. *sma-6* and *daf*-4 encode Type I and Type II receptor subunits, respectively, that bind DBL-1, and we find that both *sma-6* and *daf-4* mutants exhibit g1 gland cell abnormalities similar to those observed in *dbl-1* mutants (Figure 17 F,G, Table IV).

DAF-4 also functions in another TGF-ß signaling pathway regulating dauer larvae formation with the DAF-1 Type I receptor subunit (Gumienny and Savage-Dunn, 2013), and we asked if this pathway also regulates gland cell morphology. We found that *daf-1* mutants exhibit only a weak gland cell defect, and most *daf-1* mutants have normal g1 gland cell morphology (Figure 17H, Table IV).

Downstream signaling in response to TGF-ß receptor activation can occur via either Smad-dependent or Smad-independent pathways (Sieber et al., 2009). *sma-2* and *sma-3* encode R-Smads that function in the Sma/Mab pathway, while *sma-4* encodes a co-Smad in this pathway (Gumienny and Savage-Dunn, 2013). *sma-2* and *sma-3* mutants were previously shown to have normal g1 gland cells (Raharjo et al., 2011), and we made similar observations (Figure 17 I,J, Table IV). *sma-4* mutants exhibited g1 gland cell defects at a low frequency comparable to those observed in *daf-1* mutants, but most *sma-4* animals had a normal gland cell morphology (Table IV; Figure 17 K; Figure 19 E). *daf-8* and *daf-14* encode R-Smads that function in the dauer formation pathway, while *daf-3* encodes the co-Smad in this pathway (Gumienny and Savage-Dunn, 2013), and mutants affecting each of these genes exhibited normal gland cell morphology (Table IV; Figure 19 B-D). Thus DBL-1 affects gland cell

morphology independently of the known R-Smads and functions through a Smad-independent signaling pathway mediated by the SMA-6 and DAF-4 receptors.

Table IV FREQUENCY OF g1 GLAND CELL ABNORMALITIES IN *ceh-28* MUTANTS AND TGF-ß SIGNALING MUTANTS

Genotype	% adults exhibiting abnormal g1 gland cell processes (n) [a, b]
Wild type [c]	9 (98)
ceh-28(cu11) [c]	64 (22)
dbl-1(ev580) [c]	76 (50)
daf-4(m72) [c]	72 (36)
sma-6(wk7) [c]	68 (37)
daf-1(m40) [c]	25 (24)
sma-2(e502) [d]	8 (37)
sma-3(e491) [d]	10 (35)
sma-4(e729)[d]	30 (60)
daf-8(e1393)[d]	9 (43)
daf-14(dr77)[d]	10 (42)
daf-3(mg90)[c]	7 (28)
cuEx611[ser-7b::dbl-1 + phat-3::yfp] [e]	11 (38)
dbl-1(ev580); cuEx611 [e]	36 (68)
ceh-28(cu11); cuEx611 [e]	30 (20)

[a] g1 gland cell abnormalities include thick gland cell processes, or abnormal knobs or projections on the gland cell process.

[b] n = the total number of adult animals scored using the *yfp* reporters to visualize g1 gland cells

[c, d] gland cell morphology was scored using a *phat-3::yfp* transgene *ivEx[C49G7.4::YFP]* or a *phat-1::yfp* transgene *ivIs12* (d).

[e] *cuEx611* is an extrachromosomal transgene containing *phat-3::yfp* and *ser-7b::dbl-1*.

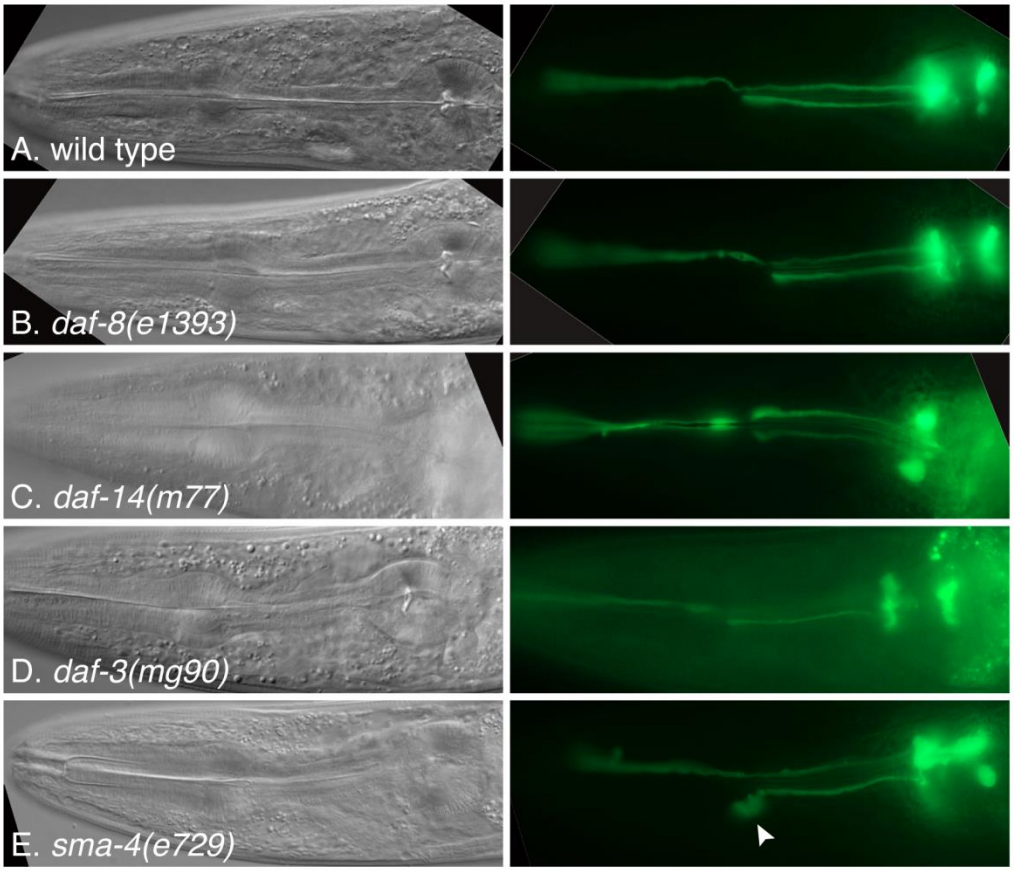

Figure 19 g1 gland cell morphology is normal in *daf-8, daf-14,* and *daf-3* mutants, but can be abnormal in some *sma-4* mutants

DIC and fluorescence images indicating g1 gland cell morphology in animals of the indicated genotypes. In A, B, C and E gland cells are marked with *phat-1::yfp*, while in D gland cells are marked with *phat-3::yfp*. Note that gland cell defects were relatively infrequent in *sma-4* mutants, and these defects were limited to swelling near the anterior tip of the sub-ventral gland cell process (arrowhead).

3.5.7 ***dbl-1* expression in M4 partially rescues gland cell defects in *ceh-28* and *dbl-1* mutants**

We hypothesize that DBL-1 is expressed and secreted from M4 to affect gland cell morphology. To test this hypothesis, we asked if expressing *dbl-1* in the M4 cell using the *ser-7b* promoter would rescue gland cell defects of *dbl-1* and *ceh-28* mutants. The *ser-7b* promoter is active exclusively in M4, and we have previously shown it remains active in *ceh-28* mutants (Hobson et al., 2003; Ray et al., 2008). Wild-type animals bearing this transgene exhibited normal gland cell morphology, indicating that *ser-7b::dbl-1* expression did not adversely affect gland cell morphology (Figure 20 A; Table IV).

ser-7b::*dbl-1* partially rescued gland cell defects in both *dbl-1* and *ceh-28* mutants (Figure 20 B,C; Table IV), although some animals still exhibited gland cell abnormalities. These results indicate *dbl-1* expression in M4 does affect gland cell morphology. Because both the *dbl-1* mutants lacking all DBL-1 activity and *ceh-28* mutants lacking DBL-1 only in M4 exhibited similar levels of rescue, we conclude that M4 is the major source of DBL-1 affecting gland cell morphology.

3.5.8 **DBL-1 secretion from M4 is not mediated by dense core vesicles**

Neurons use dense core vesicles (DCVs) to secrete neuropeptides and proteins from their cell somas using the regulated pathway of secretion (Burgoyne and Morgan, 2003). The M4 neuron contains dense core vesicles, and these DCVs are likely involved in secreting the FLP-21 peptide that controls feeding behavior under hypoxic conditions (Albertson and Thomson, 1976; Pocock and Hobert, 2010). DCVs have been previously implicated in secreting TGF-ßs in mammals (Krieglstein and Unsicker, 1995; Lacmann et al., 2007; Specht et al., 2003), and we were interested in determining if DBL-1 secretion from M4 might be similarly mediated by DCVs.

unc-31 encodes the only form of the calcium-activated protein for secretion (CAPS) in *C. elegans*, and it is specifically required for DCV release (Sieburth et al., 2007; Speese et al., 2007). To investigate if DBL-1 secretion from M4 to the gland cells is mediated by DCVs, we visualized g1 gland cell morphology in *unc-31(e928)* null mutants using a *phat-1::yfp* gland cell reporter. However, none of the mutants exhibited gland cell abnormalities (Figure 20; n=35). This result indicates DCV release is not necessary for DBL-1 secretion from M4 via the regulated pathway and suggests that DBL-1 secretion is mediated by other secretory mechanisms.

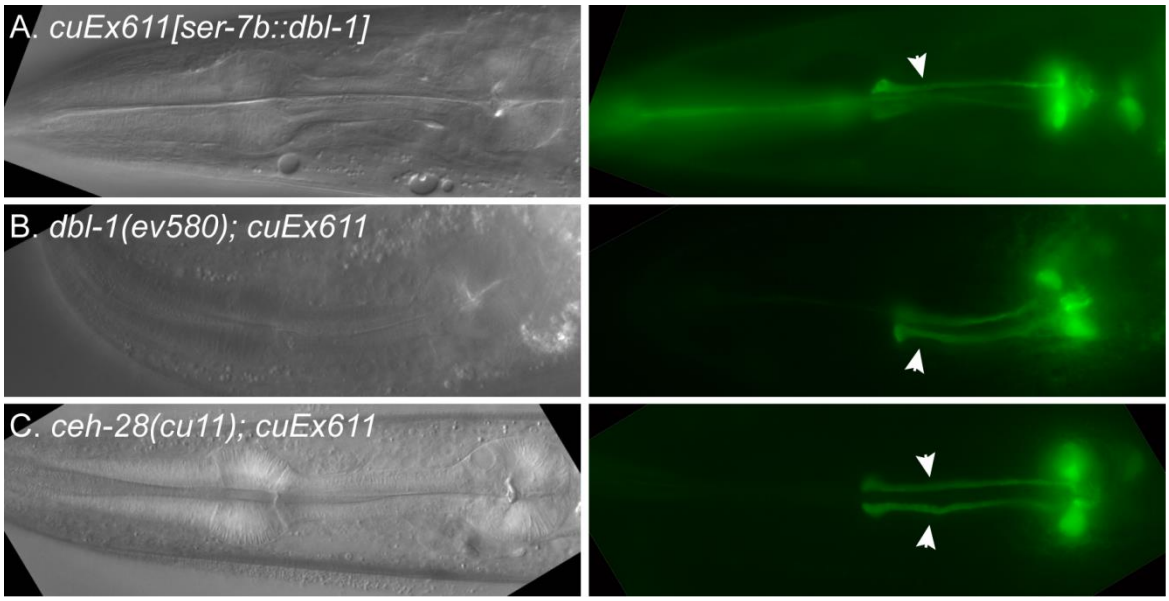

Figure 20 Rescue of gland cell morphology

DIC and fluorescence micrographs of animals of the indicated genotypes expressing *phat-3::yfp* in the g1 gland cells. Arrowhead mark in focus g1 processes.

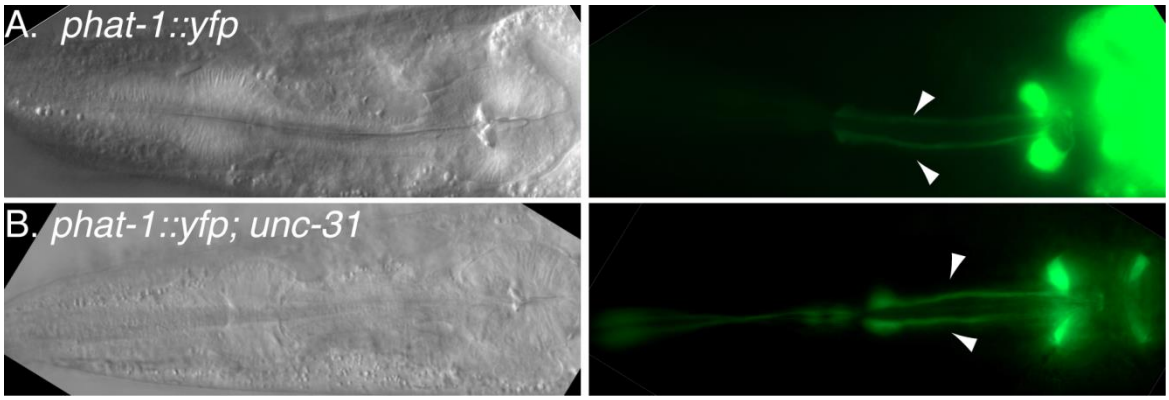

Figure 21 *unc-31* mutants have normal g1 gland cell morphology

DIC and fluorescence micrographs of wild-type (A) and *unc-31(e928)* mutant animals (B) expressing *phat-1::yfp* in the g1 gland cells. Ventral view with arrowheads marking the left and right subventral processes of these cells.

3.6 **Discussion:**

Here we show that the NK-2 homeodomain transcription factor CEH-28 functions specifically in M4 and regulates a previously unidentified neurosecretory function of M4 by activating the TGF-ß family gene *dbl-1*. The *dbl-1* promoter contains largely separable sequences activating *dbl-1* expression in M4 and other neurons, and CEH-28 directly targets an M4 specific enhancer within the *dbl-1* promoter. *dbl-1* expression in M4 affects morphology of the g1 gland cells, which directly contact M4. Despite being enriched in DCVs, M4 does not require DCV secretion to affect the gland cells, suggesting that DBL-1 is secreted through the constitutive exocytic pathway rather than through regulated release of DCVs (reviewed in (Burgoyne and Morgan, 2003)). Finally we demonstrate that DBL-1 affects gland cells through a Smad-independent, non-canonical TGF-ß signaling pathway (reviewed in (Zhang, 2009)).

3.6.1 **CEH-28 is an upstream regulator of TGF-ß signaling in M4**

Our results strongly suggest that CEH-28 directly activates *dbl-1* expression in M4. The *dbl-1* promoter contains separate regions that control expression in M4 and other neurons, and we identified a transcriptional enhancer that specifically activates transcription in the M4 cell. Activity of this enhancer was completely dependent on wild-type CEH-28, and mutation of two candidate CEH-28 binding sites strongly reduced enhancer activity. These CEH-28 binding sites appear partially redundant, as single mutants retain more enhancer activity than the double mutant. Interestingly, the site at -825 has the strongest effect on enhancer activity and this site is conserved in Multiz alignments of the *C. elegans*, *C. briggsae*, *C. remanei, C. brenneri and C. sp. 11 genomes* (Kent et al., 2002). In comparison, the site at -738 is not conserved at this position in alignments with other species, and mutation of this site affects enhancer activity only when both it and the -825 site are mutated. The observation that

enhancer activity is lost in *ceh-28* mutants, while low level enhancer activity remains when these binding sites are mutated suggests additional sequences contribute to enhancer activity in M4. These sequences might contain more highly diverged CEH-28 binding sites, or alternatively a site for another transcription factor that is dependent on CEH-28.

In mammals, the CEH-28 related factor NKX2.1 directly activates expression of the TGF-ß family gene Bmp4 in lung epithelial cells (Zhu et al., 2004), suggesting that TGF-ß family gene regulation by NK-2 homeodomain factors is conserved in some contexts. In the developing mouse lung, Nkx2.1 and Bmp4 are co-expressed only in the distal branching epithelium (Zhu et al., 2004), and decreased activity of either Nkx2.1 or Bmp4 results in similar defects in distal lung morphogenesis (Minoo et al., 1999; Weaver et al., 1999). While the processes of the pharyngeal gland cells in *C. elegans* are structurally very different than branching epithelia in the lung, it is tempting to speculate that TGF-ß family gene regulation may have a conserved function in morphogenesis of tubular structures.

3.6.2 **Analysis of gland cell morphology in *ceh-28* and *dbl-1* mutants reveals a new function for M4**

M4 has two previously recognized functions. Ultrastructural and functional studies demonstrated M4 functions as a motor neuron to stimulate peristaltic contraction of the muscles in the isthmus of the pharynx (Albertson and Thomson, 1976; Avery and Horvitz, 1989), and this function likely depends on the release of acetylcholine from M4 (Ray et al., 2008). More recently, a second function of M4 was described in an enhanced sensory response under hypoxic conditions (Pocock and Hobert, 2010), and this function depends on release of the FMRFamide related neuropeptide FLP-21.

In this work, we describe a third function for M4 in which secretion of the TGF-ß family factor DBL-1 affects the morphology of the g1 gland cells. *ceh-28* mutants and *dbl-1* mutants

exhibit abnormal gland cell morphology that include thicker processes and swellings near the M4 cell body. It is unlikely that the gland cells are enlarged due to increased secretion of gland cell-specific mucin-like proteins because the *phat* genes encoding these proteins are not over expressed in *dbl-1* mutants (Ghai and Gaudet, 2008; Roberts et al., 2010). Likewise the *dbl-1* mutant gland cell processes are not filled with vesicles as has been observed in *daf-9* and *peb-1* mutants, which have enlarged gland cells resulting from molting defects (Albert and Riddle, 1988; Fernandez et al., 2004; Jia et al., 2002). g1 gland cell secretory activity is increased prior to molting, and these secretions are believed to aid in shedding the cuticle lining the pharynx (Hall and Hedgecock, 1991). However, neither *ceh-28* nor *dbl-1* mutants have any obvious molting defects, suggesting *dbl-1* expression in M4 does not stimulate this pre-molt secretory activity.

Our data indicates that M4 is the major source of DBL-1 signal that affects gland cell morphology. However it is not clear whether DBL-1 secreted from M4 affects the gland cells directly, or whether its effect could be indirect. M4 forms synapses on the g1 gland cells, and these synapses have been suggested to stimulate gland cell activity during molting and feeding (Albertson and Thomson, 1976). However, DBL-1 secreted from M4 could also indirectly affect gland cell morphology by altering the integrity of the pharyngeal muscle cells that surround the gland cell processes. Both M4 and the g1 gland cell processes contact pharyngeal muscles in the isthmus, and mutants that have weakened pharyngeal muscles exhibit abnormalities in gland cell morphology similar to those we observe in *ceh-28* and *dbl-1* mutants (Raharjo et al., 2011; Albertson and Thomson, 1976). The pharyngeal muscles have been shown to express the receptor protein SMA-6, while expression has not yet been reported in the gland cells (Krishna et al., 1999; Yoshida et al., 2001).

3.6.3 **DBL-1 affects gland cell morphology through an R-Smad independent pathway**

Many characterized effects of TGF-ß signaling depend on the canonical TGF-ß signaling pathway in which activated receptors phosphorylate receptor regulated Smads (R-Smads), leading to complex formation with a co-Smad and translocation into the nucleus (Sieber et al., 2009). More recently, a number of noncanonical, Smad-independent responses to TGF-ß signaling have been identified in which activated receptors instead target other signaling pathways, including branches of the MAPK, PI3K-Akt, RhoA-like small GTPase pathways (reviewed in (Mu et al., 2012; Zhang, 2009)).

Both canonical and noncanonical responses to DBL-1 have been described in *C. elegans* (reviewed in (Gumienny and Savage-Dunn, 2013)). DBL-1 functions through the canonical Sma/Mab pathway and depends on the R-Smads SMA-2 and SMA-3 to regulate body size, male tail morphogenesis and aversive olfactory learning (Savage et al., 1996; Zhang and Zhang, 2012). In contrast, a noncanonical pathway that only requires SMA-3 mediates DBL-1 regulation of innate immunity (Zugasti and Ewbank, 2009).

Here we show that DBL-1 affects gland cell morphology independently of the Sma/Mab pathway R-Smads SMA-2 and SMA-3, as well as the dauer formation pathway R-Smads DAF-8 and DAF-14. These observations are consistent with results of previous studies examining gland cell morphology in mutants with small body size (Raharjo et al., 2011). While we do see a minor role for the co-Smad SMA-4 in affecting gland cells, this work suggests an R-Smad independent pathway for DBL-1 signaling through the SMA-6 and DAF-4 receptors exists in *C. elegans*, and this pathway plays a key role in M4 regulation of gland cell morphology.

3.6.4 **Dense core vesicle release is not necessary for DBL-1 secretion from M4**

M4 is unique among pharyngeal neurons in that it contains dense core vesicles (Albertson and Thomson, 1976), and neuronal DCVs are often associated with neuropeptide secretion (Burgoyne and Morgan, 2003). DCVs have also been shown to mediate regulated secretion of TGF-ß family ligands in chromaffin and PC12 cells (Krieglstein and Unsicker, 1995; Specht et al., 2003), and activity-dependent TGF-ß secretion affecting synaptic plasticity in hippocampal neurons (Lacmann et al., 2007). Active movement of vesicles is visible in the g1 gland cell ducts prior to molting and during feeding (Albertson and Thomson, 1976; Hall and Hedgecock, 1991), and this activity could in principle be controlled by regulated secretion of DBL-1 from M4 via DCVs. However, our results indicate DBL-1 is secreted from M4 independently of DCVs, as *unc-31* null mutants lacking DCV secretion exhibit normal gland cell morphology. These results suggest that DBL-1 is secreted through the constitutive secretory pathway, rather than through regulated release of DCV.

.

4 *C. elegans* ZAG-1 and CEH-28 function to regulate M4 motor neuron differentiation

4.1 Abstract

Nervous system development is achieved by a complex network of transcription factors which regulate neuronal specification and differentiation programs at the single neuron level. Here we show that the *C. elegans* zinc-finger/homeodomain transcription factor ZAG-1 and the NK-2 homeodomain transcription factor CEH-28 function in a hierarchy and regulate differentiation of the M4 pharyngeal motor neuron. CEH-28 regulates M4 synapse formation and activates the expression of its downstream targets *dbl-1*, *egl-17*, *flp-5* and *flp-2*. ZAG-1 acts as a broad regulator of M4 differentiation, and it activates isthmus muscle contractions called peristalsis, which facilitates proper feeding. *zag-1* null mutants completely lack M4 isthmus peristalses and are unable to feed normally. The failure of peristalsis in *zag-1* mutants occurs mainly due to a defective M4 neuron which cannot be stimulated by exogenous serotonin indicating that M4 lacks signaling functions. The isthmus muscles of *zag-1* mutants are functional and can be stimulated by arecoline to produce peristalses even in the absence of M4 signaling. These results indicate that ZAG-1 mainly functions in the M4 neuron to activate peristalsis. We find that the expression of several M4 differentiation markers that include *ceh-28* and its downstream targets and other M4 markers such as *flp-2* and *ser-7* are lost in *zag-1* mutants. Together, we identify a hierarchical gene network in the M4 neuron that regulates multiple aspects of neuronal differentiation.

4.2 Introduction

Motor neuron differentiation is a crucial step required for the formation of a fully functional nervous system. This process requires generation of neuron specific gene expression patterns and action of transcription factors which function in cell fate specification, neuronal differentiation and signaling. While a number of studies in vertebrates and invertebrates have shown that combinatorial codes of transcription factors function in cell fate specification and neuronal differentiation (Briscoe and Ericson, 2001; Shirasaki and Pfaff, 2002; Thor and Thomas, 2002), how individual motor neurons differentiate and function in a nervous system is only beginning to be understood.

The *C. elegans* pharynx is an excellent model system to understand mechanisms that regulate differentiation of individual motor neurons. It is a neuromuscular feeding organ consisting of 20 neurons and 20 muscles (Albertson and Thomson, 1976). The pharynx contracts rhythmically to produce two types of muscle contractions called a pump and a peristalsis which facilitate feeding behavior [reviewed in (Avery and You, 2012)]. Pumping is a simultaneous contraction of muscles in the anterior pharynx and the terminal bulb, which allows the worm to ingest bacteria, and a peristalsis is a wave like relaxation of the isthmus muscles that transports food across the pharynx. Pumping is a frequent event that can be increased by the presence of food and exogenous serotonin, and the pharyngeal MC neurons regulate the frequency of pumping. In comparison, peristalsis is a relatively infrequent event which occurs after a series of pumps.

The pharyngeal M4 neuron activates isthmus peristalsis, and laser ablation of M4 in larvae eliminates isthmus peristalsis and results in a stuffed pharynx phenotype that causes larval lethality (Avery and Horvitz, 1987). M4 is a cholinergic neuron which activates isthmus peristalsis presumably by releasing acetylcholine at the isthmus muscles. While the regulation

of peristalsis is not fully understood, exogenously added serotonin has been shown to increase peristalsis (Song and Avery, 2012) and the requirement of M4 in peristalsis can be partially bypassed by activating muscarinic acetylcholine receptors (mAChRs) in the isthmus through the addition of mAChR agonist arecoline (Raizen et al., 1995).

We are interested in understanding the factors that control differentiation of the M4 neuron. We previously showed that the NK-2 homeodomain factor CEH-28 functions in the M4 where it regulates M4 synapse assembly and morphology (Ray et al., 2008). However, it is not required for the specification of the M4 neuron or maintaining the cholinergic fate of the M4 neuron since *ceh-28* mutants express M4 differentiation markers such as *ser-7b* and *unc-17* normally. To further understand the mechanisms that regulate M4 differentiation we were interested in identifying downstream targets of CEH-28.

We find that ZAG-1 plays a major role in M4 differentiation. *zag-1* is a zinc-finger homeodomain transcription factor which was initially characterized based on its role in regulating axonal path finding, neuronal differentiation and locomotion (Clark and Chiu, 2003; Wacker et al., 2003). More recently it has been shown to act as a transcriptional switch that maintains sensory neuron fates (Smith et al., 2013). Previous studies by Wacker et al., 2003 reported that *zag-1(hd16)* mutants develop stuffed pharynx and die consequently and suggested additional roles for *zag-1* in the pharynx (Wacker et al., 2003).

In this work, we show that *zag-1* and *ceh-28* function in a sequential pathway to regulate M4 differentiation. *zag-1* null mutants completely lack isthmus peristalsis and they contain a defective M4 neuron which cannot be stimulated with exogenous serotonin. However, the isthmus muscles of *zag-1* mutants can be stimulated with arecoline to induce peristalsis, suggesting that they don't have any gross muscle development defects. We also show that *zag-1* acts as a major regulator of M4 differentiation by activating an M4 gene regulatory

network that includes *ceh-28* and its downstream targets and other markers of M4 differentiation such as *ser-7b* and *flp-2*. Our work identifies a novel function for ZAG-1 in activating isthmus peristalsis of the M4 neuron and demonstrates that *zag-1* and *ceh-28* function in a hierarchy to regulate M4 differentiation.

4.3 Materials and Methods

4.3.1 Nematode handling, transformation and strains

C. elegans strains were grown under standard conditions (Lewis and Fleming, 1995). Germline transformations were performed using standard techniques with pRF4 (100 ng/µl) containing *rol-6(su1006)* as a transformation marker and 15 ng/ µl of gfp reporters (Mello and Fire, 1995).

The following strains were used in this study: NH2466 *ayIs4[egl-17::GFP dpy-20(+)] I; dpy-20(e1282ts) IV* (Burdine et al., 1998), OK0978 *ayIs4; ceh-28(cu11)*, OK0975 *cuEx793 [egl-17 M4 enhancer]*, OK0976 *ceh-28(cu11); cuEx793,* NY2049 *ynIs49[flp-5::gfp]* (Kim and Li, 2004), OK0979 *ynIs49 V; ceh-28(cu11) X*, NY2057 *nyIs47 III; him-5(e1490) V* (Kim and Li, 2004), OK0980 *ynIs57 III; ceh-28(cu11) X,* NY2080 *ynIs80[flp-21::gfp]* (Kim and Li, 2004), OK1013 *ynIs80; ceh-28(cu11) X,*
OP83 *unc-119(ed3) III; wgIs83[zag-1::TY1::EGFP::3xFLAG(92C12) + unc-119(+)]* (Sarov et al., 2012), OK0974 *unc-119(ed3)III; ceh-28(cu11) X; wgIs83, VH514 zag-1(hd16)/unc-17(ed113) dpy-14(e184) IV* (Wacker et al., 2003) (kindly provided by Dr. Harald Hutter, Simon Fraser University, Canada).

The following strains were used as markers to visualize M4 differentiation in *zag-1(hd16*) mutants. MT15672 *nIs177[ceh-28::4xNLS::gfp]* (Hirose et al., 2010) (kindly provided by Bob Horvitz, MIT), BW1946 *ctIs43[Pdbl-1::gfp]; unc-42(e270) V* (Suzuki et al., 1999) (kindly provided by Dr. Yo Suzuki, University of Colorado), NH2466, NY2049, OK516 *cuEx469[ser-*

7b::gfp], NY2057, NY2080, RM2258 *pha-1(e2132ts); mdIs18[unc-17::gfp]* (Alfonso et al., 1993).

To visualize the expression of *ser-7b::gfp* in *zag-1(hd16*) mutants, transgenic animals bearing the extra chromosomal array *cuEx469[ser-7b::gfp]* were mated with N2 males to generate an adequate number of rolling males. The rolling transgenic males were mated with *zag-1(hd16)/ unc-17(ed113) dpy-14(e184)* hermaphrodites and 25 cross progeny rolling hermaphrodites which were either heterozygous for *zag-1* and contained the *ser-7b* transgene (*zag-1/+* ; *cuEx469*) or heterozygous for *unc-17(ed113) dpy-14(e184)* and contained the *ser-7b* transgene (*unc-17(ed113) dpy-14(e184)/+* ; *cuEx469)* were cloned onto to individual plates and allowed to have progeny for 2 days at 25°C after which the mom was removed. Plates that segregated *zag-1(hd16)* homozygotes were identified and GFP expression was scored in *zag-1(hd16)* homozygotes and their siblings which were either heterozygous for *zag-1(hd16)* or wild-type and we refer to these animals as *zag-1(+)* animals.

To visualize the expression of various other M4 differentiation markers in *zag-1(hd16)* mutants, animals bearing the following integrated transgenes: *nIs177[ceh-28::gfp], ctIs43[dbl-1::gfp],], ayIs4[egl-17:gfp], ynIs49[flp-5::gfp], ynIs57[flp-2::gfp], ynIs80[flp-21::gfp], mdIs18[unc-17::gfp]* were crossed into N2 males to generate cross progeny males bearing the transgene of interest. The transgenic males were mated with *zag-1(hd16)*/ *unc-17(ed113) dpy-14(e184)* hermaphrodites and allowed to have progeny. 30 GFP expressing cross progeny hermaphrodites which are either double heterozygous for the transgene and *zag-1* or double heterozygous for the transgene and *unc-17* and *dpy-13* were cloned into individual plates and allowed to have progeny for 2 days at 25°C after which the mom was removed. Plates containing animals that segregated *zag-1(hd16)* homozygotes were identified and GFP expression was scored in *zag-1(hd16)* homozygotes and *zag-1(+)* animals. A maximum of 75% of all the progeny were expected to be transgenic.

4.3.2 General methods for nucleic acid manipulations and plasmid construction

Standard methods were used to manipulate all DNA sequences (Ausubel, 1990) and the sequences of all plasmids are available from the authors.

The *egl-17* M4 enhancer containing bp -2638 to -1709 of cosmid F38G1 was PCR amplified from N2 worm genomic DNA using primers PO1396 [AGCTCTAAGCTTCGAAATCACTGGAAGGCACT]
and PO1397 [AGCTCTGTCGACGCCATAACTGACCTCATCCAA] and digested with HindIII and SalI and cloned into the HindIII and SalI digested Δ*pes-10::gfp* plasmid PD95.67/pOK147.01 (provided by A. Fire, Stanford University) to generate pOK293.01.

4.3.3 Identification of candidate CEH-28 binding sites in potential targets

Candidate CEH-28 binding sites were identified by scanning the promoter sequences using the WormBase function Annotate Sequence Motif (www.wormbase.org) with the JASPAR position-frequency-matrix MA0264.1 (jaspar.cgb.ki.se) at a threshold of 0.82 (Berger et al., 2006).

4.3.4 Analysis of feeding behavior and drug studies

To record pumping and peristalsis in untreated animals, L1 animals from wild-type and *zag-1(hd16)* mutants were hatched in the absence of food by bleaching adult hermaphrodites from each genotype on an unseeded NGM plate. L1 larvae from each genotype were suspended in 5 µl of M9 buffer containing OP50 and imaged on a 2% agarose pad by placing a coverslip on the top.

To perform drug treatments, L1 animals from each genotype were identified from a mixed stage population and placed on an unseeded NGM plate for 20 min, following which animals of each genotype was soaked in 5 µl of 20 mM serotonin on a 2% agarose pad for 20

minutes. An additional 5 µl of 20 mM serotonin was added to keep the worms hydrated and a coverslip was placed on top before imaging them. At least 5 animals from each genotype was recorded and analyzed.

L1 larvae from wild-type and *zag-1(hd16)* mutants was treated with 5 mM arecoline using methods described previously (Ray et al., 2008) and feeding behavior was recorded and at least 5 animals of each genotype was analyzed.

4.3.5 **Microscopy**

Micrographs of wild-type and mutant animals were acquired using a Zeiss Axioskop microscope using an Axiocam MRm camera. Images were analyzed using AxioVision software and processed using Adobe Photoshop. Time lapse analysis of wild-type and *zag-1* mutants was performed in the L1 stage. Individual animals that pumped were recorded at 25 frames/sec for 2 min using a Zen Axiovert 200 microscope with an MRm camera and processed using ZEN Acquisition Software (2011). For each genotype, or drug treatment the feeding behavior was analyzed in at least 4 animals. Video frames and QuickTime movies of feeding behavior were exported and processed using ImageJ (developed at the US NIH and available at http://rsb.info.nih.gov/nih-image/) and quantifications were performed using Microsoft Excel 2010.

4.4 **Results**

4.4.1 **CEH-28 is necessary for *egl-17* and *flp-5* expression in M4**

CEH-28 is an NK-2 family homeodomain transcription factor that is expressed exclusively in the M4 pharyngeal neuron from mid-embryogenesis through adulthood, and it regulates M4 synapse assembly and signaling (Ray et al., 2008; Ramakrishnan et al., 2014). The only previously known transcriptional target of CEH-28 is *dbl-1*, which encodes a TGF-ß family growth factor secreted from M4 to affect the nearby g1 pharyngeal gland cells (Ramakrishnan et al., 2014). We sought to identify additional targets by comparing expression of *gfp* reporters regulated by the *egl-17*, *flp-5*, *flp-2* and *flp-21* promoters in wild-type animals and *ceh-28* mutants. These reporters are expressed in M4 (Burdine et al., 1998; Kim and Li, 2004), and some contain potential CEH-28 binding sites, suggesting they may be direct targets of CEH-28 regulation (Figure 22 A). *egl-17* encodes a fibroblast growth factor (FGF) that is expressed in M4 and vulval cells, while *flp-2*, *flp-5* and *flp-21* encode FMRFamide-like neuropeptides that are expressed in M4 and a variety of other neurons.

We found that *egl-17*, *flp-5* and *flp-2* are downstream targets of CEH-28. Expression of both *egl-17::gfp* and *flp-5::gfp* was completely lost in M4 in *ceh-28* mutants, but expression was normal in other cell types (Figure 23 A-B; F-G; Table V). In comparison, the frequency of *flp-2::gfp* expression in M4 was somewhat reduced in *ceh-28* mutants, but most animals retained expression (Figure 23 H,I; Table V). Finally, *flp-21::gfp* expression was unaffected in *ceh-28* mutants (Table V). Thus CEH-28 is necessary for expression of some markers of M4 differentiation, but others are expressed independently of CEH-28.

Activity of the *dbl-1* promoter in M4 and other neurons is mediated by separable sequences, and CEH-28 directly targets an M4-specific enhancer in *dbl-1 (Ramakrishnan et al., 2014)* . Previous studies suggest the *egl-17* promoter may have a similar organization

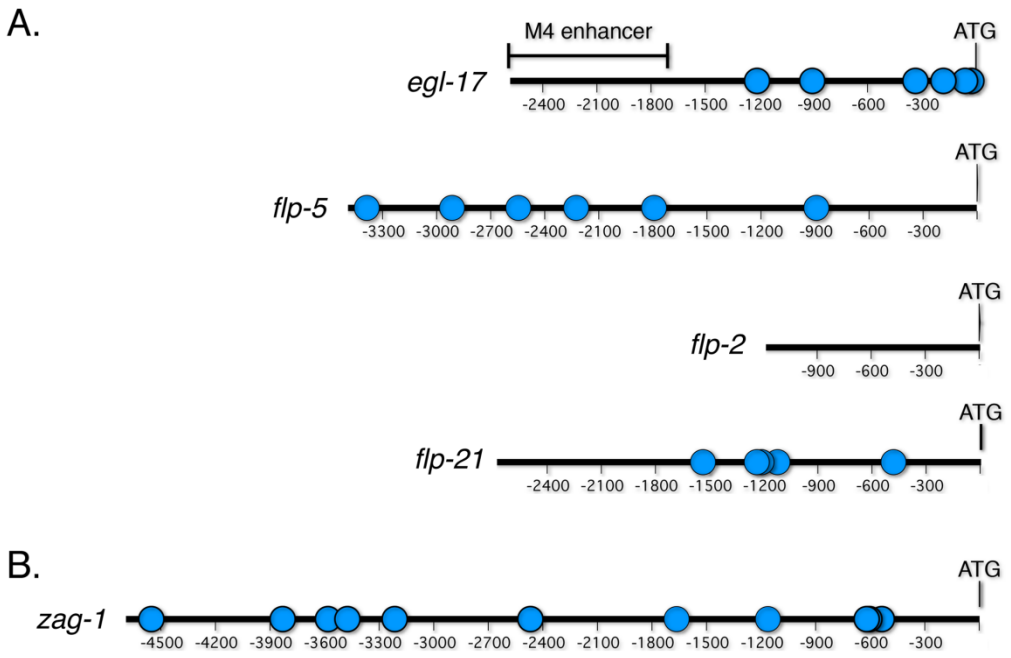

Figure 22 Promoters of potential CEH-28 target genes

(A) Schematic diagram of the indicated promoter fragments in *gfp* fusions used in this study (Burdine et al., 1998; Kim and Li, 2004). The translational start site (ATG) is numbered as bp 1. The location of an *egl-17* enhancer sufficient for expression in M4 is indicated by a bar, and potential CEH-28 binding sites are indicated as blue dots. The sites in *egl-17* are located at -1212, -906, -334, -179, -59, and -24. The sites in *flp-5* are located at -3387, -2914, -2546, -2225, -1793, and -892. The sites in *flp-21* are located at -1536, -1238,-1212, -1123, and -480 respectively.

(B) Schematic diagram of the *zag-1* promoter that is sufficient for normal *zag-1* expression (Wacker et al., 2003). Our studies used fosmid WRM063aA08 containing a *gfp* translational fusion (Sarov et al., 2012). The sites in *zag-1* are located at -4552, -3830, -3581, -3474, -3214, -2468, -1664, -1162, -619, -604, and -536 respectively.

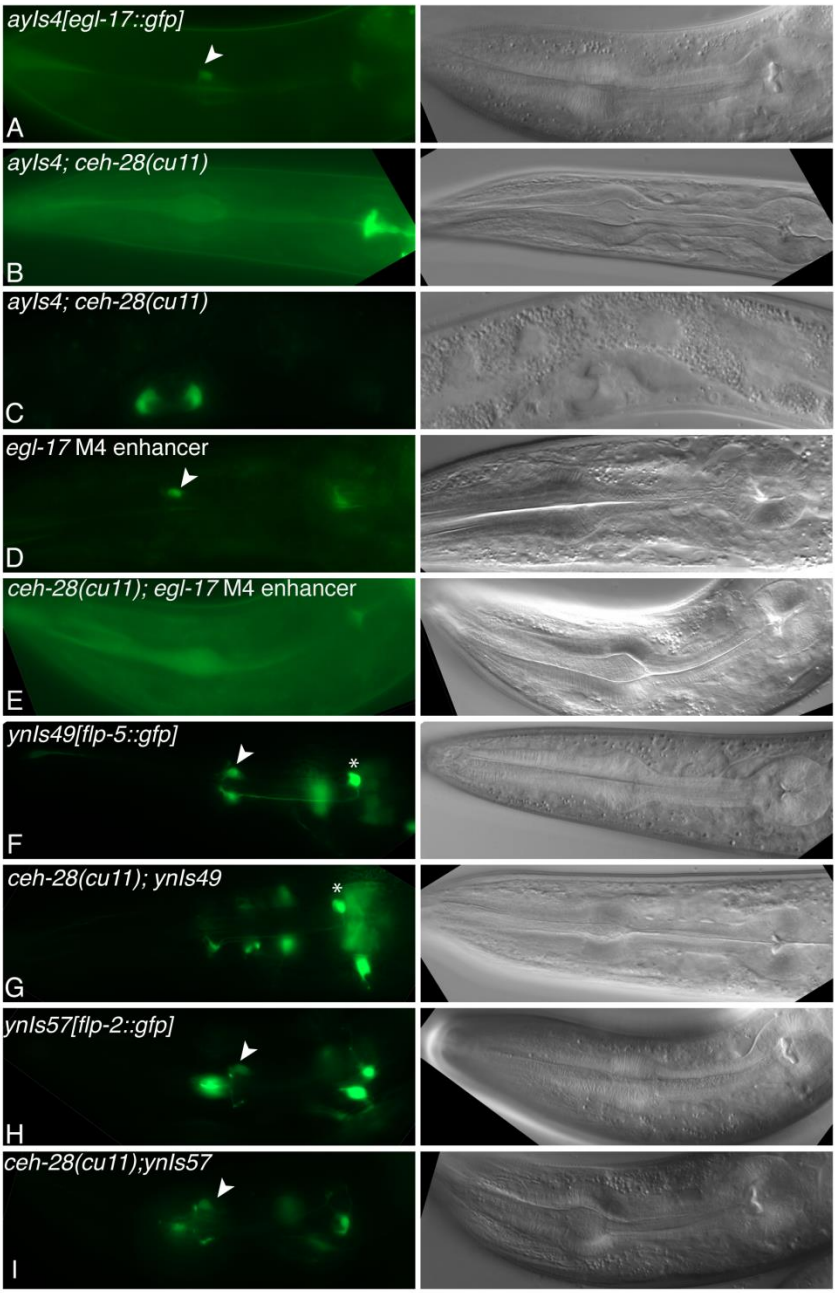

Figure 23 Analyzing M4 gene expression of the potential downstream targets of CEH-28

Fluorescence (left) and DIC (right) micrographs of L4 to adult animals of the indicated genotypes bearing *egl-17::gfp ayIs4* (A-C), the *egl-17* M4 enhancer*::*Δ*pes-10::gfp cuEx793* (D,E), the *flp-5::gfp ynIs49* (F,G), or the *flp-2::gfp ynIs57* (H,I). (A,B,D-I) Expression in the pharynx with M4 (arrowhead) or I4 (asterisk, F and G) indicated. (C) *egl-17::gfp* expression in the vulva, which is unaffected in *ceh-28* mutants.

Table V FREQUENCY OF ANIMALS EXPRESSING GFP IN M4 IN WILD-TYPE AND *ceh-28(cu11)* MUTANTS

Reporter	Percent animals expressing GFP in M4 in wild-type (n) [a]	Percent animals expressing GFP in M4 in *ceh-28(cu11)* (n) [b]	2 tailed P value Using Fisher's exact test
ayIs4[egl-17::gfp]	100 (35)	0 (40)	P<0.0001*
egl-17 M4 enhancer::gfp	80 (30)	0 (30)	P<0.0001*
ynIs49[flp-5::gfp]	100 (30)	0 (37)	P<0.0001*
ynIs57[flp-2::gfp]	100 (30)	80 (45)	P=0.0093**
ynIs80[flp-21::gfp]	100 (32)	100 (35)	
wgIs83[zag-1::gfp]	100 (40)	66 (45)	P<0.0001*

[a] Transgenic adults were scored for GFP expression in M4

[b] *ceh-28 (cu11)* homozygotes bearing the transgene were scored for GFP expression in M4

* Differences are extremely statistically significant

** Difference is statistically significant

(Cui and Han, 2003). This work identified a region from -2589 to -1756 bp upstream of the translational start site necessary for *egl-17::gfp* expression in M4, but it had no role in vulval cell expression. We asked whether this fragment was sufficient to enhance expression of the Δ*pes-10::gfp* reporter (Seydoux and Fire, 1994), and we found transgenic animals bearing this reporter expressed GFP exclusively in M4 (Figure 22A; Figure 23D). While this enhancer does not contain any recognizable CEH-28 binding sites, its activity was lost in *ceh-28* mutants, indicating that it functions downstream of CEH-28 (Figure 23E; Table V). We suggest either that this enhancer is directly activated by CEH-28 through non-consensus binding sites, or that it is activated indirectly by another CEH-28 dependent factor.

4.4.2 **ZAG-1 is essential for isthmus peristalsis**

ZAG-1 is a ZEB-family C_2H_2 zinc-finger/homeodomain transcription factor that regulates neuronal differentiation and axonal pathfinding in *C. elegans* (Clark and Chiu, 2003; Wacker et al., 2003). It is expressed in M4 and many other neurons, as well as in the intestinal and anal depressor muscles. Hypomorphic *zag-1* mutants are viable as homozygotes, but *zag-1(hd16)* null mutants arrest after hatching, and they exhibit a characteristic coiled phenotype and severe feeding defects that result in a partially stuffed pharynx (Wacker et al., 2003). Because a stuffed pharynx is also observed in *ceh-28* mutants, we were interested in characterizing the pharyngeal muscle contractions in *zag-1(hd16)* mutants.

Using time-lapse microscopy, we found that *zag-1(hd16)* mutants completely lack isthmus peristalses. These mutants still pump, although at a slower rate than wild-type L1s (Table VI). However, while wild-type L1s peristalse approximately after every 9th pump, *zag-1(hd16)* mutants never exhibited a peristalsis (Table VI). Both the slow pump rate and the absence of peristalses are observed in animals lacking M4 (Avery and Horvitz, 1987; Raizen et al., 1995), suggesting the M4 cell in *zag-1* mutants is non-functional.

We next examined pharyngeal muscle contractions in animals treated with compounds that stimulate either M4 or the pharyngeal muscles. Serotonin stimulates the MC and M4 neurons, and this leads to increased pumping and peristalsis, respectively (Song and Avery, 2012). We found that wild-type L1s treated with serotonin exhibited a moderate increase in the pump rate and frequency of peristalsis compared to untreated animals (Table VI). In comparison, *zag-1(hd16)* mutants treated with serotonin exhibited a strong increase in the pump rate compared to untreated animals, but they still failed to peristalse (Table VI). Arecoline is believed to directly stimulate mAChRs in the isthmus muscles ray (Raizen et al., 1995; Ray et al., 2008), and we found that arecoline treatment stimulated very frequent peristalses in both wild-type L1s and *zag-1(hd16)* mutants (Table VI). Together these results demonstrate that the isthmus muscle of *zag-1(hd16)* mutants can produce a peristaltic contraction, but the M4 cell in these animals cannot stimulate this contraction. While arecoline treated *zag-1* mutants did peristalse, these contractions were shorter than those in wild-type animals, suggesting the functional M4 in wild-type animals still affects peristalsis under these conditions (Table VI).

4.4.3 ***zag-1* mutants have broad defects in M4 differentiation**

zag-1 mutants exhibit differentiation defects in several neurons outside of the pharynx (Clark and Chiu, 2003; Wacker et al., 2003), and we were interested in asking if M4 differentiation is similarly affected in these mutants. To examine *gfp* reporter gene expression, *zag-1(hd16)/+* hermaphrodites that were heterozygous for chromosomally integrated reporters were generated, and we compared reporter expression in progeny *zag-1(hd16)*

Table VI SUMMARY OF FEEDING BEHAVIOR IN WILD-TYPE AND *zag-1* MUTANTS

Genotype	Pump Rate (pumps/ min)	Duration of Procorpus contractions (ms)	Duration of Posterior Bulb Contractions (ms)	Duration of Isthmus peristalsis (ms)	% Pumps followed by Isthmus Peristalsis
N2[a]	116±2	159±1	173±2	N.D	11%
zag-1(hd16)[b]	58±21	118±3	96±6	N.D	0%
N2+ serotonin [c]	177±39	N.D	N.D	N.D	30%
zag-1(hd16)+ serotonin [d]	158±41	N.D	N.D	N.D	0%
N2+ arecoline [e]	50±16	N.D	N.D	216±22	100%
zag-1(hd16)+ arecoline [f]	34±4	N.D	N.D	128±22	100%

[a] 4 N2 L1s were recorded for 35-40 s and a total of 213 pumps were analyzed

[b] 4 *zag-1(hd16)* L1s were recorded for 35-60 s and a total of 203 pumps were analyzed

[c] 4 N2 L1s were treated with 20mM serotonin and recorded for 15-20 s each and a total of 193 pumps were analyzed

[d] 5 *zag-1(hd16)* L1s were treated 20mM serotonin and recorded for 12-25 s each and a total of 222 pumps were analyzed

[e] 4 N2 L1s were treated with 5mM arecoline and recorded for 28-50 s each and a total of 115 pumps were analyzed

[f] 6 *zag-1(hd16)* L1s were treated with 5mMarecoline and recorded for 45-60 s each and a total of 166 pumps were analyzed

homozygotes and their viable wild-type or heterozygous *zag-1(hd16)/+* siblings. Thus, 75% of these animals will carry the *gfp* transgene.

We first examined expression of *ceh-28::gfp* and reporters for the CEH-28 targets *dbl-1*, *egl-17*, *flp-5* and *flp-2*. Both the frequency and intensity of *ceh-28::gfp* expression was strongly reduced in *zag-1(hd16)* homozygotes (Figure 24A; Table VII). Likewise, we also observed loss or reduced expression of the CEH-28 targets, strongly suggesting that expression of the endogenous *ceh-28* gene is reduced in *zag-1(hd16)* homozygotes (Figure 24 B-D; Table VII). The only CEH-28 target that retained some expression in *zag-1(hd16)* mutants was *flp-2::gfp*, and this expression was less frequent than in *zag-1(+)* animals. As *flp-2::gfp* expression was only partially affected in *ceh-28* mutants (Table V), we suggest that CEH-28 and other factors contribute to *flp-2* expression in M4.

We next examined reporters for the *ser-7b*, *flp-21*, and *unc-17* genes that are expressed in M4 independently of CEH-28 (Table V) (Ray et al., 2008). While *flp-21::gfp* and *unc-17::gfp* were expressed normally in *zag-1(hd16)* mutants, expression of *ser-7b::gfp* was completely lost (Figure 24E-G; Table VII). Loss of *ser-7b::gfp* expression is consistent with our observation that *zag-1(hd16)* mutants do not peristalse when treated with serotonin, and it strongly suggests that ZAG-1 is essential for expression of the endogenous *ser-7* gene in M4.

4.4.4 **CEH-28 activates *zag-1* expression in a positive feedback loop**

While ZAG-1 functions upstream to activate expression of *ceh-28*, we observed that the *zag-1* promoter also contains several potential CEH-28 binding sites (Figure 17B). To test if CEH-28 also regulates *zag-1* expression, we examined expression of a *zag-1::gfp* reporter in the M4 cell of wild-type animals and *ceh-28(cu11)* mutants at the young adult stage.

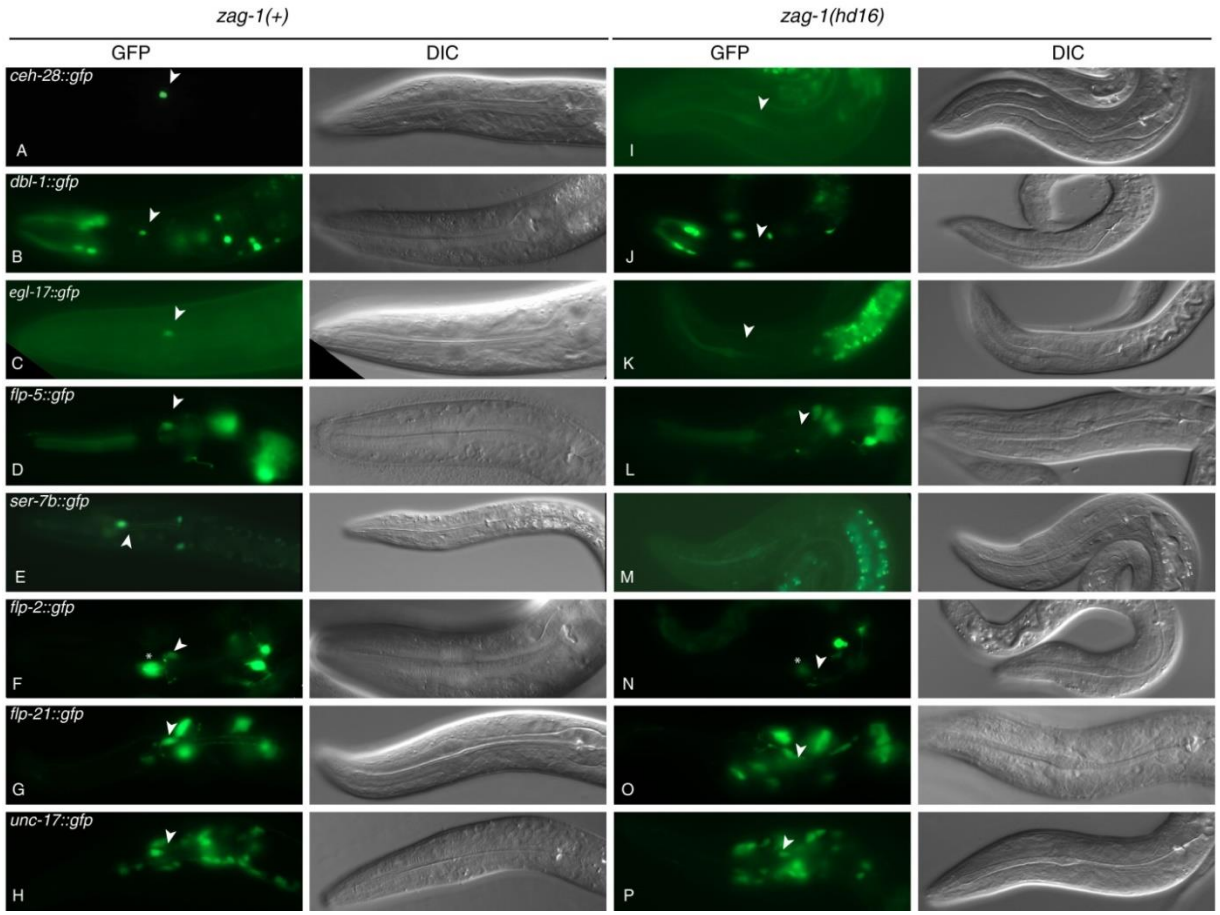
zag-1(+)
zag-1(hd16)
GFP
DIC
GFP
DIC
ceh-28::gfp
A
dbl-1::gfp
B
egl-17::gfp
C
flp-5::gfp
D
ser-7b::gfp
E
flp-2::gfp
F
flp-21::gfp
G
unc-17::gfp
H
I
J
K
L
M
N
O
P

Figure 24 Analysis of M4 differentiation defects in *zag-1(hd16)* mutants

(A-G) DIC and fluorescence micrographs of animals expressing *ceh-28::gfp,dbl-1::gfp, egl-17::gfp, flp-5::gfp,ser-7b::gfp, flp-2::gfp, flp-21::gfp, unc-17::gfp* respectively in a *zag-1(+)* background and (I-P) in *zag-1(hd16)* mutants (right) respectively. Arrowheads indicate the M4 cell body. Asterisk indicates the MC neuron cell body expressing *flp-2::gfp*.

Table VII EXPRESSION OF M4 DIFFERENTIATION MARKERS IN *zag-1(+)* AND *zag-1(hd16)* MUTANTS

Transgene	% animals expressing GFP in M4 in *zag-1(+)* (n) [a]	% animals expressing GFP in M4 in *zag-1(hd16)* (n) [b]	2 tailed P value using Fisher's exact test
nIs177[ceh-28::gfp] [a]	69 (54)	22 (58)	P<0.0001*
ctIs43[dbl-1::gfp] [c]	74 (43)	0 (32)	P<0.0001*
ayIs4[egl-17::gfp] [c]	74 (34)	0 (36)	P<0.0001*
ynIs49[flp-5::gfp] [c]	63 (40)	0 (40)	P<0.0001*
ynIs57[flp-2::gfp] [c]	67 (30)	38 (45)	P=0.0189**
cuEx469[ser-7b::gfp] [d]	63 (30)	0 (30)	P<0.0001*
ynIs80[flp-21::gfp] [c]	74 (34)	68 (25)	
mdIs18[unc-17::gfp] [c]	65 (40)	73 (30)	

[a] GFP expression was scored in the phenotypically wild-type +/+ or *zag-1(hd16)/+* progeny of *zag-1(hd16)/+* hermaphrodites and we refer to these as *zag-1(+)* animals

[b] GFP expression was scored in the *zag-1(hd16)* homozygous progeny of *zag-1(hd16)/+* hermaphrodites

[c] Chromosomally integrated transgene is expected to be present in 75% of the progeny of transgenic hermaphrodites

[d] *cuEx469* is an extra chromosomal transgene that is unlinked to any of the chromosomes

* Differences are extremely statistically significant

** Differences is statistically significant

zag-1::gfp was expressed in M4 in all wild-type animals, but the frequency of expression was moderately reduced in *ceh-28* mutants (Figure 25; Table V). Thus CEH-28 may function in a positive feedback loop to activate *zag-1* expression, perhaps to maintain stable expression of both *zag-1* and *ceh-28* after initial activation.

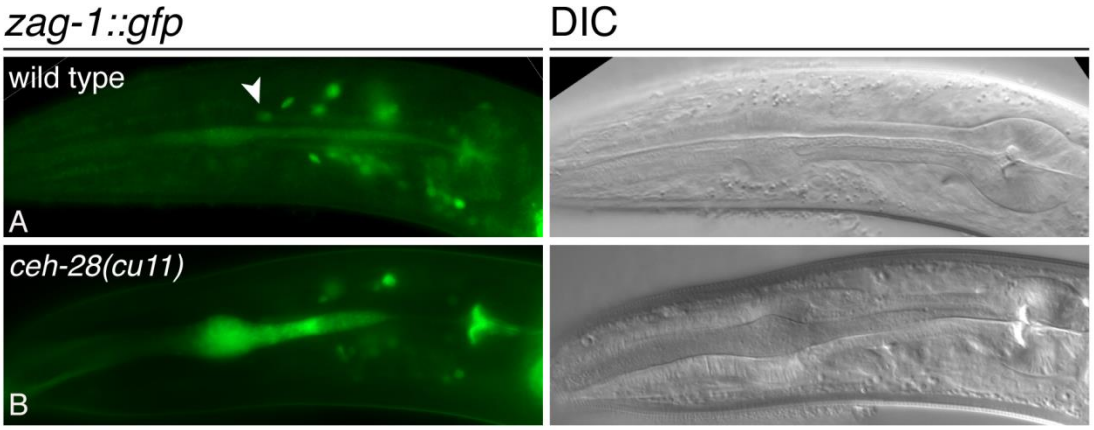

Figure 25 Expression of *zag-1::gfp* in wild-type and *ceh-28* mutants

(A) DIC (right) and fluorescence micrographs (left) of a wild-type animal expressing *zag-1::gfp* in wild-type and (B) in a *ceh-28(cu11)* mutant.

4.5 **Discussion**

Here we show that the transcription factors CEH-28 and ZAG-1 function in a hierarchy to regulate multiple aspects of M4 differentiation (Figure 26). We previously showed that *ceh-28* mutants lack expression of the TGF-ß family gene *dbl-1* in M4 (Ramakrishnan et al., 2014) , and here we find these mutants also lack or exhibit reduced expression of a subset of additional M4 differentiation markers, including *egl-17::gfp*, *flp-2::gfp* and *flp-5::gfp*. We also find that ZAG-1 functions upstream of CEH-28 and plays a broader role in M4 differentiation. *zag-1* mutants exhibit strongly reduced expression of both a *ceh-28::gfp* marker and reduced or eliminated expression of markers regulated by CEH-28. *zag-1* mutants also lack expression of a *ser-7b::gfp*, which is expressed normally in *ceh-28* mutants (Ray et al., 2008). We hypothesize that ZAG-1 is required for expression of the endogenous *ceh-28* gene and its downstream targets in M4, while it regulates promoters such as *ser-7b* independently of CEH-28. Despite this broader role for ZAG-1 in M4 differentiation, we find the M4 differentiation markers *unc-17::gfp* and *flp-21::gfp* are expressed normally in both *zag-1* and *ceh-28* mutants, indicating other mechanisms promote some aspects of M4 neuronal differentiation independently of ZAG-1 and CEH-28. Interestingly, ZAG-1::GFP expression is also reduced in *ceh-28* mutants, suggesting CEH-28 also contributes to *zag-1* expression through a positive feedback loop. We further show that defects in M4 differentiation in *zag-1* mutants result in an absence of peristaltic contractions in the pharyngeal isthmus muscles. This phenotype results from defects in the M4 neuron rather than in the muscle, because stimulating the isthmus muscles with arecoline stimulates isthmus peristalsis in *zag-1* mutants, whereas stimulating M4 with serotonin has no effect in these animals.

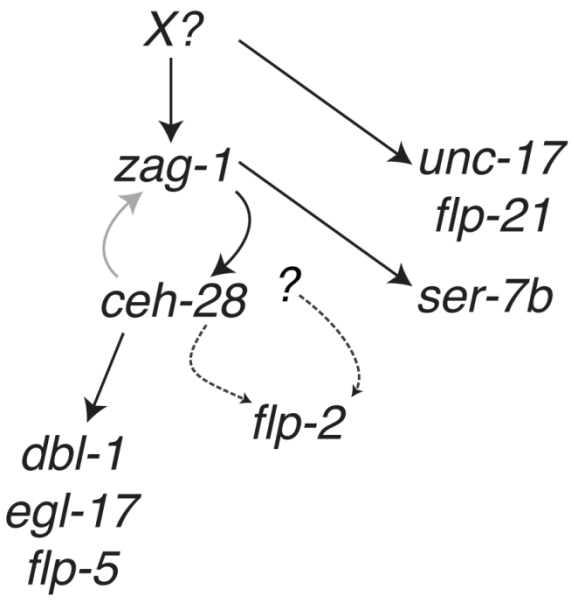

Figure 26 *zag-1* and *ceh-28* function in a hierarchy in the M4 neuron

In this hierarchy model, *zag-1* functions to activate the expression of *ceh-28* and its downstream targets *dbl-1*, *egl-17* and *flp-5* in M4 and other genes such as *ser-7b* and *flp-2* which are expressed normally in *ceh-28* mutants. *ceh-28* functions in a feedback loop to maintain expression of *zag-1* in M4 during later stages of development. An unknown upstream factor X, most likely activates the expression of *zag-1, flp-21* and *unc-17* in M4. Dotted arrows indicate that *flp-2* expression in M4 is activated partly by *ceh-28* ,and another unknown factor.

4.5.1 **CEH-28 regulates M4 signaling by activating growth factors and neuropeptides**

CEH-28 is not generally required for M4 neuronal differentiation; however, we previously found that *ceh-28* mutants fail to express *dbl-1* in M4 (Ray et al., 2008; Ramakrishnan et al., 2014). We now extend this work to show that *ceh-28* mutant also do not express *egl-17::gfp* and *flp-5::gfp* in M4, while expression of *flp-2::gfp* is reduced. Together, these results indicate CEH-28 regulates multiple neurosecretory functions of M4. Like *dbl-1*, *egl-17* and *flp-5* are also expressed in cells other than M4, and this expression is unaffected in *ceh-28* mutants. The *dbl-1* and *egl-17* promoters are complex, with separable regions controlling expression in M4 and other cells (Cui and Han, 2003; Reinke et al., 2013; Ramakrishnan et al., 2014), and we have identified M4 specific transcriptional enhancers in each of these promoters [(Ramakrishnan et al., 2014); this work]. CEH-28 directly targets the M4 enhancer in *dbl-1*, but the *egl-17* enhancer lacks high scoring consensus NK-2 factor binding sites, suggesting *egl-17* is indirectly activated by CEH-28.

DBL-1 secreted from M4 affects the morphology of the nearby pharyngeal g1 gland cells (Ramakrishnan et al., 2014), but the functions of the newly identified CEH-28 targets in M4 are unknown. EGL-17 has no known role in the pharynx, while exogenous FLP-5 and FLP-2 neuropeptides can excite pharyngeal pumping (Papaioannou et al., 2005). None of the mutants *egl-17(n1377), flp-5(gk3123)* or *flp-2(gk1039)* exhibit the stuffed pharynx phenotype found in *ceh-28* mutants, suggesting these secreted proteins are not necessary for normal feeding (data not shown). We cannot rule out however that the function of these genes is redundant with each other or with other signaling pathways, as has been observed for cholinergic and neuropeptide control of egg laying (Ringstad and Horvitz, 2008).

4.5.2 **ZAG-1 plays a crucial role in regulating M4 differentiation**

ZAG-1 is a conserved C_2H_2 zinc-finger/homeodomain transcription factor in *C. elegans* and is an ortholog of the vertebrate ZEB family of transcription factors and *Drosophila* Zfh1 (Clark and Chiu, 2003; Wacker et al., 2003). In vertebrates these proteins regulate epithelial to mesenchymal transitions during development and in cancer metastasis, and control differentiation of particular neuronal types (McKinsey et al., 2013; Vandewalle et al., 2009). Mutations affecting human ZEB proteins have been implicated in Mowat Wilson syndrome and corneal dystrophies ((Cacheux et al., 2001; Krafchak et al., 2005; Riazuddin et al., 2010; Wakamatsu et al., 2001). In *C. elegans* and *Drosophila*, ZEB family proteins function in axonal path finding, neuronal differentiation, and neuronal cell fate (Clark and Chiu, 2003; Layden et al., 2006; Smith et al., 2013; Wacker et al., 2003).

Our results indicate ZAG-1 is a key regulator of M4 differentiation. M4 is present and partially differentiated in *zag-1* mutants, but these mutants lack expression of several markers of M4 differentiation. Moreover *zag-1* mutants exhibit a complete loss of peristaltic contraction of the isthmus muscles. This contractile defect results from defects in M4 rather than the pharyngeal muscles themselves, because stimulation of mAChRs in the muscles with exogenous arecoline restores peristalses, while stimulation of M4 with serotonin has no effect. In wild-type animals the ability of serotonin to stimulate pharyngeal pumping and peristalses is mediated by the SER-7 receptor in the MC and M4 motor neurons, respectively (Song and Avery, 2012), and the failure of exogenous serotonin to simulate peristalsis in *zag-1* mutants indicates that expression of the endogenous *ser-7* gene is lost in M4 in these animals.

ZEB family proteins are often viewed as transcriptional repressors that interact with the CtBP co-repressor [reviewed in (Gheldof et al., 2012)]. However, ZEB-family factors can also activate transcription. Mammalian ZEB1 activates transcription of the ovalbumin gene in

response to estrogen signaling (Dillner and Sanders, 2004), as well as the MMP-1 matrix metalloproteinase 1 and CDK-4 genes (Hu et al., 2010; Hu et al., 2011). Likewise, Drosophila *zfh-1* can repress expression of *mef2* during muscle development (Postigo and Dean, 1999), while it activates expression of the FMRFa gene in neurons (Vogler and Urban, 2008). This ability of ZEB family factors to function either as activators or epressors may result from cell type specific cofactors, or post-translational modifications (Costantino et al., 2002; Long et al., 2005; Watanabe et al., 1993) or different DNA binding activities mediated through the multiple binding domains in these proteins (Ikeda and Kawakami, 1995).

Like its vertebrate and *Drosophila* orthologs, *C. elegans* ZAG-1 also functions as a repressor, where it negatively regulates its own expression and that of *unc-25* required for GABA synthesis (Clark and Chiu, 2003; Wacker et al., 2003). Our results now suggest ZAG-1 can also function as a transcriptional activator of the *ser-7b* and *ceh-28* promoters (Figure 5), although we do not know if this activation is direct. Current whole animal ChIP-seq analyses performed by the modENCODE consortium have not revealed significant ZAG-1 binding within these promoters (Gerstein et al., 2010), but this binding might be undetectable if it only occurs in M4 or a small number of other cells.

4.5.3 **A hierarchy of transcription factors control M4 differentiation**

In both invertebrates and vertebrates, ‘terminal selector’ transcription factors have been shown to be key activators of batteries of genes involved in terminal differentiation of specific neuronal types [reviewed in (Hobert, 2011)]. Such terminal selector genes are expressed in these specific neurons throughout development, and, after initial activation, they maintain their own expression through positive autoregulation. While mutants defective for terminal selector genes express markers of pan-neural differentiation, they fail to express markers of neuron type-specific differentiation. For example, *C. elegans* mutants defective in the Pitx-family

homeobox gene *unc-30* fail to express the GABAergic phenotype of type D motor neurons, while mouse mutants affecting the *Crx* homeobox gene fail to express many retinal photoreceptor genes.

While both *ceh-28* and *zag-1* are expressed in M4 throughout development, neither exhibits other characteristics of a terminal selector for the M4 phenotype. ZAG-1 represses its own promoter, rather than activating it (Clark and Chiu, 2003; Wacker et al., 2003), while CEH-28 does not regulate its own expression (Ray et al., 2008). More importantly, neither of these factors appears necessary for expression of batteries of genes for a specific aspect of M4 differentiation. For example, the *flp-5, flp-2*, and *flp-21* genes encoding FMRFamide-family neuropeptides all are regulated differently in M4 (Figure 26). Instead, our observations indicate ZAG-1 and CEH-28 function in a branched, hierarchical network to regulate M4 gene expression (Figure 26). CEH-28 activates expression of a subset of genes expressed in M4, while ZAG-1 functions upstream to activate expression of *ceh-28* and its downstream targets, as well as additional M4 expressed genes. Other genes are regulated independently of both CEH-28 and ZAG-1, indicating other transcription factors function upstream in this hierarchy for M4 differentiation. *zag-1* and *ceh-28* could themselves be activated by a terminal selector of M4 differentiation. Alternatively, different aspects of M4 differentiation might be independently regulated without a terminal selector transcription factor, perhaps resulting from the multifunctional nature of M4. More comprehensive analyses of M4 gene expression and the promoters of M4 expressed genes will distinguish between these possibilities.

.

5 Poly(A)- Binding protein based mRNA tagging method to perform M4 transcript profiling

5.1 Introduction

Investigating the transcript profiles of single neurons provides insights regarding how single neurons function within a fully developed nervous system. Neuron specific gene expression patterns define the biochemical and functional characteristics of individual neurons and address the molecular basis behind neuronal diversity. For example, mammalian olfactory sensory neurons express a unique olfactory receptor and respond to specific odorants (Malnic et al., 1999).

C. elegans is a great model for performing transcriptional analysis of single neurons, since it has a simple and well characterized nervous system (Albertson and Thomson, 1976; White et al., 1986a). The adult hermaphrodite consists of 302 neurons that can be further divided into the pharyngeal nervous system consisting of 20 neurons and the extra pharyngeal nervous system consisting of 282 neurons. The pharyngeal nervous system is separate from the extra pharyngeal nervous system.

The pharyngeal M4 motor neuron stimulates isthmus muscle contractions called peristalses which are essential for proper feeding (Avery and Horvitz, 1987). M4 extends two processes which travel posteriorly and forms synapses on the isthmus muscles to stimulate peristaltic contractions, required for normal feeding behavior (Albertson and Thomson, 1976).

We previously showed that the NK-2 homeodomain transcription factor CEH-28, functions exclusively in the M4 neuron to regulate M4 synapse assembly and morphology (Ray et al., 2008). *ceh-28* mutants have abnormal M4 synapses, and they hyperstimulate isthmus peristalsis, resulting in inefficient feeding. To understand how CEH-28 functions in regulating M4 synapse assembly, we were interested in identifying downstream targets of CEH-28.

We identified *dbl-1*, *egl-17*, *flp-5* and *flp-2* as downstream targets of CEH-28 (Ramakrishnan et al., 2014) (Ramakrishnan and Okkema unpublished). We find that *dbl-1* mutants have normal synapses and do not display any of the feeding defects associated with *ceh-28(cu11)* mutants. *egl-17(n1377), flp-5(gk3123)* or *flp-2(gk1039)* mutants also fail to exhibit stuffed pharynx phenotype typical of *ceh-28* mutants, suggesting these secreted proteins are not necessary for normal feeding. Since we were interested in understanding how CEH-28 regulates M4 synaptogenesis, we wanted to identify additional targets of CEH-28.

The mRNA tagging method has been successfully used in *C. elegans* to enrich for transcripts from single cells and less abundant cell types in *C. elegans* (Takayama et al., 2010; Von Stetina et al., 2007; Kunitomo et al., 2005). In this approach, FLAG tagged Poly(A)-binding protein (PABP) is expressed under the control of cell type specific promoters. PABP will bind the 3' end of Poly polyadenylated mRNA in the cell where it is expressed. This complex of mRNA bound by PABP can be immunoprecipitated using anti FLAG antibody. The isolated mRNA can then be further processed to perform RNA-seq or microarray analysis.

Here we describe the generation of transgenic lines which express functional FLAG tagged PABP in the M4 neuron of wild-type and *ceh-28* mutants. The M4 mRNA isolated from these strains by immunoprecipitation can be used to preform M4 transcript profiling by microarray or RNA-seq.

5.2 Nematode handing and transformation

5.2.1 Nematode handing and transformation

All strains were maintained using standard conditions (Lewis and Fleming 1995). Germline transformations were performed using micro particle bombardment with the PDS 1000/He particle Delivery system with a hepta adapter using protocols described for *C. elegans* using detailed methods described in section 2.2.2.1 adapted from detailed protocols described previously(Merritt and Seydoux, 2010) .

The following stains were used in this study: DP38 *unc-119(ed3) III*, OK0793 *unc-119(ed3); cuIs30 [ser-7b::3XFLAG::PABP],* OK0828 *ceh-28(cu11); cuIs30*, MT455 *lon-2(e678); unc-18(e81) X.* OK0793 was crossed into the mapping strain MT455 to ensure the *cuIs30* transgene was not integrated on the X chromosome and then crossed into *ceh-28(cu11)* mutants to generate OK0828. The linkage group of the *cuIs30* transgene is yet to be determined thus the exact integration site of this transgene is unknown.

The following extrachromosomal arrays expressing *ceh-28* promoter expressing FLAG tagged PABP were also generated by microparticle bombardment OK0767 *unc-119(ed3); cuEx614 ,* OK0768 *unc-119(ed3); cuEx615.*

5.2.2 Growing up worms for bombardment

The goal was to obtain forty large 15 cm diameter NEP plates containing lots of young adult hermaphrodites from the *unc-119(ed3)* strain which were then consolidated into two large (15 cm diameter) NEP plates for performing two bombardments. To maximize the chances of obtaining transgenic lines, typically each construct was bombarded twice on the same day.

Freshly starved *unc-119* worms from eight small (6 cm diameter) NGM plates were washed off using M9 and resuspended in 8 ml of M9. These worms were then plated onto eight

large NEP plates, and allowed to grow at 25° C for 5-6 days until they starved to form worm piles which contained large number of freshly starved L1s. The worms from these 8 plates were washed off and resuspended in a 50 ml conical tube with 45 ml of M9 and allowed to stand for 5 min. This allowed gravid adults to sink to the bottom of the tube and the L1-L4 stage animals to float in the supernatant. The supernatant containing the L1-L4 stage animals were plated onto 40 large NA22 bacteria seeded NEP plates by plating 1 ml of supernatant on each plate. These worms were allowed to grow for 3-5 days at 25°C until they become young adults. Worms were then washed off from the 40 large NEP plates into one 50 ml tube containing M9. Worms were spun at 1000 rpm and washed two more times to remove bacteria and the supernatant was discarded leaving behind 3-5 ml of a highly packed worm pellet. Using a Pasteur pipette, 1-2 ml of the worm pellet was spread onto 2 large NEP plates, allowed to dry for about 15 minutes to evaporate most of the liquid prior to bombardment.

The bombardment was performed using protocols described in section 2.2.2.1.

5.2.3 **Methods for manipulating plasmids and nucleic acids**

The following plasmids were used in this study: pDONR221[Gateway entry vector] (kindly provided by Dr. Susan Liebman, UIC), pSV41/pOK264.17 [gateway destination vector containing an N terminal FLAG tagged PABP and an *unc-119* rescue cassette] (kindly provided by Dr. David Miller, University of Vanderbilt), pOK271.13, pOK271.11, pOK271.09, pOK271.16

5.2.4 **Generating plasmids for expressing PABP in M4**

To generate the reporter construct pOK271.13 which contains the *ser-7b* promoter driving expression of FLAG tagged Poly(A) binding protein and pOK271.16 containing the *ceh-28* promoter driving expression of FLAG tagged Poly A binding protein, we used the Gateway cloning system (Life Technologies) and followed the manufacturers protocols. The *ser-7b* promoter and the *ceh-28* promoter were PCR amplified from worm genomic DNA and cloned

into an entry vector pDONR221 and recombined with the gateway destination vector pSV41/pOK264.17 containing FLAG tagged Poly A binding protein and an *unc-119* rescue cassette.

The *ser-7b* promoter was PCR amplified from 75 ng of N2 genomic DNA using primers PO1092 [GGGGACAAGTTTGTACAAAAAAGCAGGCTGCCTGCAGCAAACAGGTAG] and PO1093 [GGGGACCACTTTGTACAAGAAAGCTGGGTCCTCAGGCTGTGTCTGACTG] and the following PCR program was used: 94°C- 2 minutes, 94°C- 30 secs , 56°C- 45 secs, 72°C- 2.5 minutes , Goto 2- 6 times, 94°C - 30 secs, 72°C - 45 secs, 72°C - 2.5 min, Goto 6 -30 times, 12° C forever. The PCR product was visualized on a 1% agarose gel to ensure the presence of a 2.1 kb amplification product following which a PCR cleanup of the entire reaction was performed to remove enzymes and primer dimers.

The *ceh-28* promoter was amplified from N2 genomic DNA using primers: PO1090 [GGGGACAAGTTTGTACAAAAAAGCAGGCTTTGGTTGTCATGGTTGAAGC] and PO1091[GGGGACCACTTTGTACAAGAAAGCTGGGTTCTGATTTTGACTTGGAGAACC] using the following PCR program: 94°C - 2 min, 94°C - 30 secs, 54°C - 45°C secs, 72°C - 4 min, Goto 2- 6 times, 94°C - 30 secs, 72°C - 45 secs, 72°C - 4.5 min, Goto 6 - 30 times, 12°C - forever.

5.2.4.1 **Generating entry clones using the BP Gateway reaction**

The PCR amplified *ser-7b* promoter and the *ceh-28* promoter were initially cloned into the pDONR221 gateway entry vector to generate the entry clones pOK271.09 and pOK271.11 respectively by performing the BP gateway reaction according to the manufacturer's protocol. A 10 µl reaction containing 2 µl (150 ng) of the linearized entry vector (pDONR221) and 2 µl (150 ng) of the PCR amplified *ser-7b* promoter or *ceh-28* promoter insert were incubated with 2 µl of the BP Clonase enzyme and 4 µl of TE buffer at 25°C for overnight. The reaction was stopped by adding 1 µl of Proteinase K to the reaction mixture and incubated for 1 hour at 37°C. Following the Proteinase K treatment, the entire mixture was transformed into DH5 α *E coli* cells

and plated on kanamycin containing 2XTY plates. Single colonies were identified and inoculated in 2-3 ml of 2XTY growth media containing kanamycin and plasmids were isolated by miniprep. The correct clones were identified by performing restriction digest and later sequenced using M13F(-20) primer to verify the presence of the insert.

5.2.4.1.1.1 **Generating final expression clones using the LR gateway reaction**

The *ser-7b* promoter in pOK271.09 and the *ceh-28* promoter in pOK271.11 were cloned into the pSV41/pOK264.17 destination vector containing the FLAG tagged Poly(A) binding protein. The gateway LR reaction was performed by incubating a 10 µl final volume of a reaction mixture containing 2.5 µl of 150 ng of each entry clone (pOK271.09 and pOK271.11), 2 µl (150 ng) of the linearized destination vector (pSV41/pOK264.17), 2 µl of the LR Clonase enzyme and 3.5 µl of TE buffer at 25°C overnight. The reaction was stopped by adding 1 µl of Proteinase K to the reaction mixture and incubating for 1 hour at 37°C. Following the Proteinase K treatment, the entire mixture was transformed into DH5 α E coli cells and plated on ampicillin containing 2xTY plates. Single colonies were identified and inoculated in 2-3 ml of 2xTY growth media containing ampicillin and plasmids were isolated by miniprep. The right clones were identified by performing restriction digest and later sequenced using M13 Rev(-27) primer to verify the presence of the insert. Following confirmation, the clones were named pOK271.13 [*ser-7b* promoter driving expression of 3XFLAG::PABP] and pOK271.16 [*ceh-28* promoter driving expression of FLAG tagged PABP].

5.2.5 **PCR genotyping to verify transgenes obtained by bombardment**

Transformation of pOK271.13 into *unc-119(ed3)* animals by bombardment resulted in one integrated transgenic line which looked phenotypically wild-type and segregated 100% non unc animals. To confirm that the transformants contained the *cuIs30* [*ser-7b::3xflag::PABP]* transgene, these animals were subjected to single worm PCR genotyping using primers PO1203[GTAGACGGGAACATTGCGTT] and PO1204 [TGAAGATATTGCCAGCTCCC]

which specifically amplified a 631 bp sequence present only in the transgene. This amplified product spans the 3' end of the *ser-7b* promoter, the PABP and the N terminal sequences of the FLAG tag. The following PCR program was used: 95°C - 2 min, 95°C - 30 secs, 55°C - 45 secs, 72°C - 40 secs, Goto 2 - 35 times , 72°C - 5 min, 4°C forever. The plasmid pOK271.13 was used as positive control in these reactions.

The strains OK0767 and OK0768 containing the extrachromsomal arrays of the *ceh-28* promoter driving expression of FLAG tagged PABP were genotyped using primers PO1205 [TTTGGTGTGAAAATCCCTCCT] and PO1206 [GATTCTCATTGGTTTGCCGT] which amplified a 563 bp unique fragment from the transgene similar to the method described above. The plasmid pOK271.16 was used as a positive control. The following PCR program was used: 94°C - 2 min, 94°C - 30 secs, 55°C - 45 secs , 72°C – 1 min, Goto 2 - 5 times, 72°C - 5 min.

5.2.6 **Immunostaining using Anti FLAG antibody to confirm transgene function**

Worms from OK0793 *unc-119(ed3); cuIs30 [ser-7b::3XFLAG::PABP],* OK0828 *ceh-28(cu11)* , OK0767 *unc-119(ed3); cuEx614 ,* OK0768 *unc-119(ed3); cuEx615* were grown on 3-4 small NGM plates seeded with OP50 until a lot of young adults were present on the plate. The worms from each plate was washed with 1ml of M9 and transferred to an Eppendorf tubes and the antibody staining was performed according to the Finney-Ruvkun protocol (Finney and Ruvkun, 1990). Animals were fixed with freshly prepared formaldehyde and expression of Poly(A) binding protein in M4 was detected by staining with a FLAG antibody (Sigma) (1:1000 dilution) and a Texas Red labelled goat anti-mouse secondary antibody (1:250 dilution). Animals were also stained with DAPI (1mg/ml) (1:1000 dilution). Worms were mounted on a slide containing 2% agarose pad and a drop of slow fade component C was added. A cover slip was placed on top and sealed with nail polish. Worms were visualized on a Zeiss axioscope equipped for fluorescence microscopy and DIC. Images were captured with an MRm Axioskop camera and processed using Axiovision software and Adobe Photoshop.

5.3 Results and Discussion

Poly (A) binding protein is expressed in M4 in wild-type and *ceh-28* mutants

CEH-28 has been previously shown to affect M4 synaptogenesis. *ceh-28* mutants have abnormal and mispositioned M4 synapses which hyperstimulate isthmus muscle contractions and result in inefficient feeding (Ray et al., 2008). Based on this evidence, we hypothesized that CEH-28 potentially regulates genes involved in M4 synapse formation. To identify genes which are regulated by CEH-28 in M4, we wanted to compare the M4 transcript profile of wild-type animals to *ceh-28* mutants and identify genes regulating M4 synaptogenesis.

We generated transgenic lines which express the FLAG tagged Poly(A)-binding protein under the control of the *ser-7b* promoter in wild-type background and crossed this strain into *ceh-28* mutants. To verify the functionality of the transgene, we performed antibody staining on worms expressing the transgenes in the wild-type and *ceh-28* mutant backgrounds and found that FLAG tagged Poly (A)-binding protein expression was strongly detected in the M4 neuron when immunostained with the FLAG antibody in 100% of the animals (n=30) in both wild-type and *ceh-28* mutants (Figure 27 A, B). Outside of M4, expression of PABP expression was detectable in an additional cell, in the head of the animal in about 20% of the wild-type animals (n=35). In comparison, in *ceh-28* mutants, 60% of the animals (n=30) had detectable Poly(A) binding protein expression in an additional anterior cell besides M4. It is possible that the additional staining detected outside of M4 is due to experimental conditions which result in non-specific staining or it is also likely that the *ser-7b* promoter has an expanded expression pattern in *ceh-28* mutants.

We also generated extrachromosmal arrays strains containing *ceh-28* promoter driving expression of FLAG tagged Poly(A) Binding Protein using the bombardment protocol. We looked at Poly A binding protein expression in the M4 neuron of animals that express the

extrachromosomal array OK0767 *unc-119(ed3); cuEx614,* OK0768 *unc-119(ed3); cuEx615* (Figure 27C). The extrachromosomal array, OK0767 showed brighter antibody staining (Figure 24 C) compared to OK0768. These strains also differed in the frequency of Uncs that they segregated. The OK0767 strains segregated a higher percentage of Uncs (30-35%%) in comparison to the OK0768 strain, which segregated 10-15% of Uncs.

To characterize the M4 gene expression profiles of wild-type and *ceh-28* mutants, mRNA from M4 neurons of L1 stage larvae from both the wild-type and *ceh-28* mutants expressing FLAG-tagged PABP can be immunoprecipitated, using the mRNA tagging method and subjected to RNA-seq to analyze M4 gene expression and identify additional targets of *ceh-28*.

We previously identified genes which depend on *ceh-28* in M4 such as *dbl-1*, *egl-17* and *flp-5* and other genes, which are expressed independently of *ceh-28* such as *ser-7b*, *ceh-28* itself and *flp-21*. These genes can serve as controls to verify if the immunoprecipitation efficiently enriches for M4 RNA. By performing qPCR using the M4 RNA isolated from wild-type and *ceh-28* mutants and measuring the expression levels of the above listed genes we can determine the purity of the isolated M4 RNA.

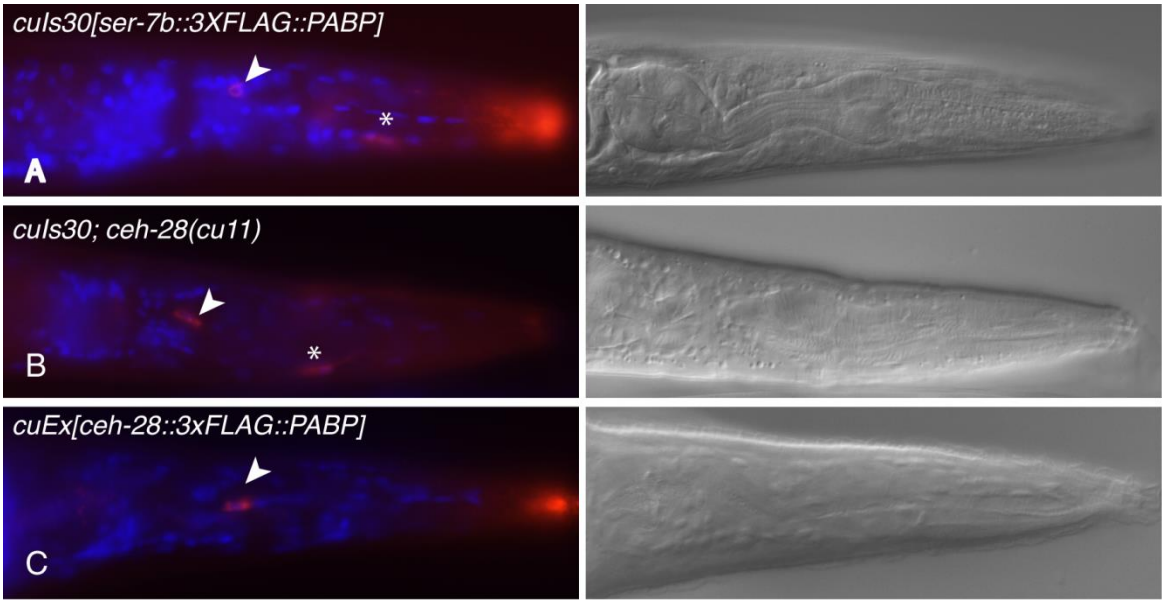

Figure 27 Detecting expression of PABP in M4 using anti-FLAG antibody

(A) PABP expression is detected in M4 neuron in a strain containing *culs30 [ser-b::3XFLAG::PABP]* in a wild-type background (A) and in a *ceh-28(cu11)* mutant in (B). (C) Expression of PABP in the M4 neuron is detected in an extrachromosomal array *cuEx614 [ceh-28::3XFLAG::PABP]*.

6 Discussion and Conclusions

6.1 Function of CEH-28 and ZAG-1 in the M4 neuron

The Nkx families of homeodomain transcription factors and the ZEB family proteins are predominantly expressed in neurons and muscles and they have important roles in development and disease. The mammalian Nkx families of homeodomain proteins regulate neuronal cell fate specification and differentiation (Briscoe et al., 2000; Briscoe et al., 1999; Sander et al., 2000). They also function in motor neurons to regulate specificity of target muscles (De Marco Garcia and Jessell, 2008). The ZEB family of Zinc finger homeodomain proteins are important regulators of embryonic development, neuronal differentiation, and promote epithelial to mesenchymal transitions (Sanchez-Tillo et al., 2011; Vandewalle et al., 2005). This thesis describes the functions of the *C. elegans* NK-2 family protein homeodomain transcription factor CEH-28 and the Zinc finger homeodomain transcription factor ZAG-1 in the M4 pharyngeal neuron. Using a *C. elegans* model, we describe the identification of the first direct target of CEH-28 and the discovery of a novel neuroendocrine function for the *C. elegans* M4 pharyngeal neuron (Ramakrishnan et al., 2014) . Another significant finding was the identification of ZAG-1 as an activator of M4 isthmus peristalsis, a feeding behavior required for the viability of the worm. In addition to activating peristalsis, ZAG-1 acts as an upstream activator of CEH-28 and its downstream targets, thereby regulating several aspects of M4 differentiation and signaling. Our results demonstrate that CEH-28 and ZAG-1 are two major regulators which function in a hierarchy and regulate differentiation and function of the M4 neuron. My results have identified a novel function for the M4 neuron and uncovered part of the complex gene regulatory network which exists in this single cell. Taken together my studies have extended our understanding regarding the mechanisms which regulate motor neuron differentiation.

6.2 Identifying additional targets of CEH-28

CEH-28 is an NK-2 family homeodomain transcription factor expressed in the M4 neuron where it regulates M4 synapse morphology and assembly. To understand how CEH-28 functions in M4, we wanted to identify downstream targets of CEH-28. We previously showed that *dbl-1* is a direct target of CEH-28 in M4 (Ramakrishnan et al., 2014). We also identified *egl-17*, *flp-5* and *flp-2* genes which are activated by CEH-28 in M4. However none of the downstream targets identified so far have any feeding or synaptic defects similar to *ceh-28* mutants. In order to understand how *ceh-28* regulates M4 synapse assembly, we need to identify additional targets of CEH-28.

Additional targets can be identified using the mRNA tagging method which has been successfully used in *C. elegans* previously (Kunitomo et al., 2005; Pauli et al., 2006; Von Stetina et al., 2007). We generated strains that express functional FLAG tagged Poly A binding protein (PABP) in the M4 neurons of wild-type and *ceh-28* mutants. PABP will bind to the 3' PolyA tail of mRNAs which are expressed in this cell and this complex can be isolated by immunorecipitating using anti FLAG antibody. The isolated M4 RNA from wild-type and *ceh-28* mutants can be isolated and RNA-Seq analysis can be performed to identify a list of differentially expressed M4 genes in *ceh-28* mutants. We expect to find the previously identified targets *dbl-1*, *egl-17* and *flp-5* in the list of differentially genes.

Since we hypothesize that CEH-28 plays an important role in regulating M4 synapse assembly, it is possible that *ceh-28(cu11)* misexpress genes involved in synaptogenesis such as *sad-1*, *syd-1* ,*rpm -1syg-1, syg-2* (Crump et al., 2001; Hallam et al., 2002; Zhen et al., 2000; Schaefer et al., 2000; Shen and Bargmann, 2003). It is also possible that we will identify other *flp* genes as potential targets of CEH-28 given that we find the expression of *flp-5* and *flp-*

2 depend on CEH-28. Other potential target genes could be netrin signaling pathway components which have roles in neuronal polarity (Colon-Ramos et al., 2007; Poon et al., 2008), TGF-β pathway components other than *dbl-1*, and Wnt signal pathway components (Klassen and Shen, 2007).

After arriving at a list of differentially expressed genes, we can further characterize these genes, by examining promoter::gfp fusions to verify if these genes are indeed expressed in the M4 neuron and ask if the expression is altered in *ceh-28* mutants. Existing mutants for these genes can be obtained from the knockout consortium and other *C. elegans* research labs or neuronal RNAi can be performed (Calixto et al., 2010) and the M4 synapses in these mutants can be visualized using a SNB-1::GFP. Promoters of these genes can be examined to screen for CEH-28 binding sites.

6.3 Exploring mechanisms by which ZAG-1 activates isthmus peristalsis

We find that the Zinc finger homeodomain transcription factor ZAG-1 activates M4 isthmus peristalsis in M4. We find that *zag-1(hd16)* null mutants completely lack peristaltic contractions, and therefore are unable to feed and hence arrest as larvae. Since *C. elegans zag-1* has been previously characterized to regulate axonal pathfinding,(Clark and Chiu, 2003; Wacker et al., 2003) it is possible that *zag-1(hd16)* mutants have misrouted or truncated M4 processes which fail to make synapses onto isthmus muscles. Due to unavailability of M4 specific markers which are active in a *zag-1(hd16)* mutant, we are currently unable to test this possibility. Results in chapter 4 show that the *flp-21* promoter is active in the M4 neuron of *zag-1(hd16)* mutants. We could characterize this promoter (2.5 kb) to identity if there are any M4 regulatory regions through a series of 5' deletions. Once an M4 specific regulatory region is identified, we could use this promoter to visualize the morphology of M4 synapses by fusing it to cytoplasmic gfp.

We found that the *ser-7b* promoter is not active in *zag-1* mutants and this is consistent with the finding that *zag-1* mutants cannot be stimulated with serotonin to produce isthmus peristalses. It will be interesting to ask if cell type specific rescue of this phenotype can be achieved by expressing SER-7under the control of the *flp-21* promoter in the M4 neuron. If we obtain rescue of isthmus peristalsis defects, it will suggest that *zag-1* activates the SER-7 signaling pathway in M4 to activate peristalsis. If no rescue is achieved, it is likely that ZAG-1 activates downstream genes in addition to serotonin to activate peristalsis. Another possibility is that, due to defective M4 morphology, which results in absence of M4 synapses, restoring serotonin signaling in M4 might still not have a functional effect in terms of restoring or activating M4 isthmus peristalsis.

6.4 Understanding the functions of *egl-17* and *flp-5* in M4

Based on the results in data in chapter IV, we found that expression of *egl-17* and *flp-5* in M4 completely depends on CEH-28. We found that the *egl-17* promoter contained separable regulatory elements controlling expression in M4 and other cells. We also found an M4 enhancer in the *egl-17* promoter that is activated by CEH-28. *egl-17* encodes a fibroblast growth factor family ligand (Burdine et al., 1997), and it is expressed in the M4 neuron and in the vulva. The function of *egl-17* in the vulva is well understood but its role in the M4 neuron and the pharynx are unknown. We did not observe any of the feeding defects in the *egl-17(n1377)* and *flp-5(gk3123)* observed in *ceh-28(cu11)* mutants.

It is possible that *egl-17* mutants and *flp-5* mutants contain gland cell defects similar to *dbl-1* and *ceh-28* mutants and this can be tested by visualizing gland cell morphology in these mutants using the *phat-1::yfp* or the *phat-3::yfp* gland cell reporters. Work by Ringstad and Horvitz has shown that FMRF peptides function redundantly with acetylcholine to inhibit egg laying (Ringstad and Horvitz, 2008). The authors showed that *flp-10* and *flp-17,* which are

expressed in neuronal tissues act as ligands for *egl-6* which functions in the HSNs to inhibit egg laying. Interestingly, the deletion mutants of *flp-10* and *flp-17* did not display any egg laying defects; however, these mutants were able to suppress the egg laying defects of *egl-6* mutants indicative of functional redundancy.

Based on these results it would be interesting to test whether *egl-17* and *flp-5* function redundantly in M4 to affect feeding. We can test this by examining an *egl-17; flp-5* double mutant and ask if the double mutant has any feeding defects similar to *ceh-28(cu11)* mutants. Alternatively, we could also test whether expressing *egl-17* and *flp-5* in the M4 neurons is able to rescue the feeding defects observed in *ceh-28* mutants.

7 APPENDICES

7.1 Appendix A: Site directed mutagenesis of the *dbl-1* promoter

Analysis of the full length *dbl-1* promoter in pOK205.01 indicated the presence of eight potential CEH-28 binding sites located at bp -2810, -2668, -2441, -2107, -2042, -835, -738, and -497 upstream of the *dbl-1* translational start site (Figure 28 B). Prior to the identification of an M4 regulatory region and the M4 enhancer, we mutated the sites at -2810 bp, -2107 bp, -2042 bp in the context of the full length *dbl-1* promoter as a template using oligos listed in Table VIII and we refer to these constructs *Pdbl-1*$^{-2810\ mut}$(pOK270.02), *Pdbl-1*$^{-2107\ mut}$ (pOK272.05), *Pdbl-1*$^{-2042\ mut}$ (pOK272.03) respectively. The sequences of the CEH-28 binding sites in the wild-type and the mutant constructs are shown in Figure 28 B.

We find that *dbl-1::gfp* is normally expressed in the M4 neuron in all the three constructs (Table IX) and that mutation of the sites at -2810 bp, -2107 bp and -2042 bp individually in the context of the full length *dbl-1* promoter had no effect on *dbl-1* expression in M4 (Figure 29A-C).

A.

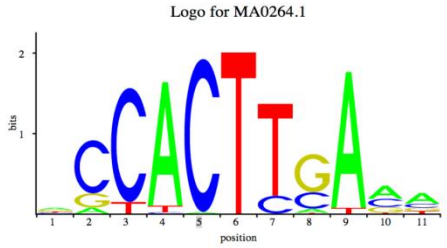


```
A  [33  8  0 93  1  0  0  7 95 46 51 ]
C  [15 71 89  1 97  0 16 27  0 29 20 ]
G  [31 19  0  0  0  0  0 63  0 20 15 ]
T  [19  0  9  5  0 99 83  1  4  3 12 ]
```

B.

		site directed mutagenesis
-2810	AACACTTCATC(+)	-2810 mut AACAgaTCATC
-2668	GTCACTTGAAG(-)	
-2441	ACTACTAGAAA(-)	
-2107	GCAACTTCAAA(-)	-2107 mut GCAAgaTCAAA
-2042	GCAACTTCAAG(-)	-2042 mut GCAAgaTCAAG
-835	CCCACTCGATG(+)	-835 mut CCCAgaCGATG(+)
-738	TGACAAGAGGC(+)	-738 mut TGACAtcAGGC(+)
-497	GAAACTTGAAA(-)	

C. CEH-22 binding sites in the *egl-17* promoter

```
-1212 TCCACTTTTAA(-)
-906  GCCAATTGAAC(-)
-334  ACAACTTCAAG(+)
-179  TGCAATTGAAA(-)
-59   TCCACTTGTTC(+)
-24   GGCACCTGAAA(-)
```

D. CEH-22 binding sites in the *flp-5* promoter

```
-3387 GCCAGTTCAAA(+)
-2914 TCCAATTGAAA(-)
-2546 CCCACTTGAAA(+)
-2225 AACTCTTCAGA(+)
-1793 AACACTTCAAT(+)
-892  ACCAATTCATA(-)
```

E. CEH-22 binding sites in the *flp-21* promoter

```
-1536 AAAACTTGAAA(-)
-1238 TGCTCTTCACA(+)
-1212 ACCACCTCAAA(-)
-1123 ACCACCTCAAA(-)
-480  GCCACCTCAAC(+)
```

F. CEH-22 binding sites in the *zag-1* promoter

```
-4552 GCAACTCCAAA(-)
-3830 CCTCTTGAAAT(-)
-3581 ACTTCTTCAAA(+)
-3474 AACTCTTGACA(+)
-3214 TCCATTTGAAA(-)
-2468 TCCATTTGAGC(+)
-1664 ACCACGTGAAC(-)
-1162 ACCACTTTACC(-)
-1123 AGCTCTTGAGG(-)
-604  AACTCTTGAGC(-)
-536  CCAACTTGACC(-)
```

Figure 28 CEH-28 Binding sites in target gene promoters

(A) CEH-22 consensus sequence and position weight matrix used to define the CEH-28 binding sites are shown (Berger et al., 2006). (B). The sequence of the CEH-28 binding sites present in the *dbl-1* promoter at bp -2810, -2668, -2441, -2107, -2042, -835, -738, and -497 bp upstream of the *dbl-1* translational start site are indicated on the left and the residues which were mutated are shown in lowercase in the resulting constructs indicated on the right. (C-F) The *ceh-28* binding sites present in the *egl-17, flp-5, flp-21* and *zag-1* promoters respectively are shown.

Table VIII SITE DIRECTED MUTAGENESIS OF THE *dbl-1* PROMOTER

Construct generated	Oligos used for site directed mutagenesis
Pdbl-1$^{-2810\ mut}$(pOK270.02)	PO1170[CCATTCAACTGTCCATTCTCTGTTTTAAACAGATCATCTCACTGACCTT PO1171[AAGGTCAGTGAGATGATCTGTTTAAAACAGAGAATGGACAGTTGAATGG]
Pdbl-1$^{-2107\ mut}$ (pOK272.05),	PO1174[ACACAATTGTTAGTTATCGTTTGATCTTGCCGCCGTCTCCG] PO1175[CGGAGACGGCGGCAAGATCAAACGATAACTAACAATTGTGT]
Pdbl-1$^{-2042\ mut}$ (pOK272.03)	PO1176[ATATGAGAAGAAAACATTCTTGATCTTGCGAGCAACTTCTTGCTGTC] PO1177[GACAGCAAGAAGTTGCTCGCAAGATCAAGAATGTTTTCTTCTCATAT]
-3061Δ $^{-825\ mut}$ pOK264.01	PO1248[TGGAGCTATTGTTTTTCACACCCAGACGATGAATCTGGTGGG] P01249[CCCACCAGATTCATCGTCTGGGTGTGAAAAACAATAGCTCCA]

Based on the data obtained from the 5' deletions of the *dbl-1* promoter fused to gfp, we found that the -3061 Δ/ pOK264.01 promoter had normal *dbl-1* expression in the M4 neuron, but reduced *dbl-1* expression in the other head neurons (Ramakrishnan et al., 2014). Hence we mutated the conserved site at -825 bp in the context of -3061 Δ/ pOK264.01 promoter and we refer to this as -*3061Δ* $^{-825\ mut}$. We observed a moderate decrease in intensity of *dbl-1* expression in M4 in the -*3061Δ* $^{-825\ mut}$ animals (20%, n=30, Figure 29 D). We also previously showed that when the conserved CEH-28 binding site -825 bp is mutated in the context of the *dbl-1* M4 enhancer, we see a reduction in intensity as well as frequency of M4 expression (Ramakrishnan et al., 2014). Hence our results indicate that the conserved CEH-28 binding site at -825 bp affects *dbl-1* expression in M4 in the context of the *dbl-1* promoter as well the enhancer.

Table IX FREQUENCY OF *Pdbp-1::gfp* EXPRESSION IN THE M4 NEURON IN THE SINGLE MUTANTS

Pdbl-1::gfp mut	Frequency of M4 expression (n)[a]
Pdbl-1 $^{-2810\ mut}$	100% (35)
Pdbl-1 $^{-2107\ mut}$	100% (42)
Pdbl-1 $^{-2042\ mut}$	100% (32)
-3061Δ $^{-825\ mut}$	80% (43)

[b] GFP expression in M4 was scored in young adults

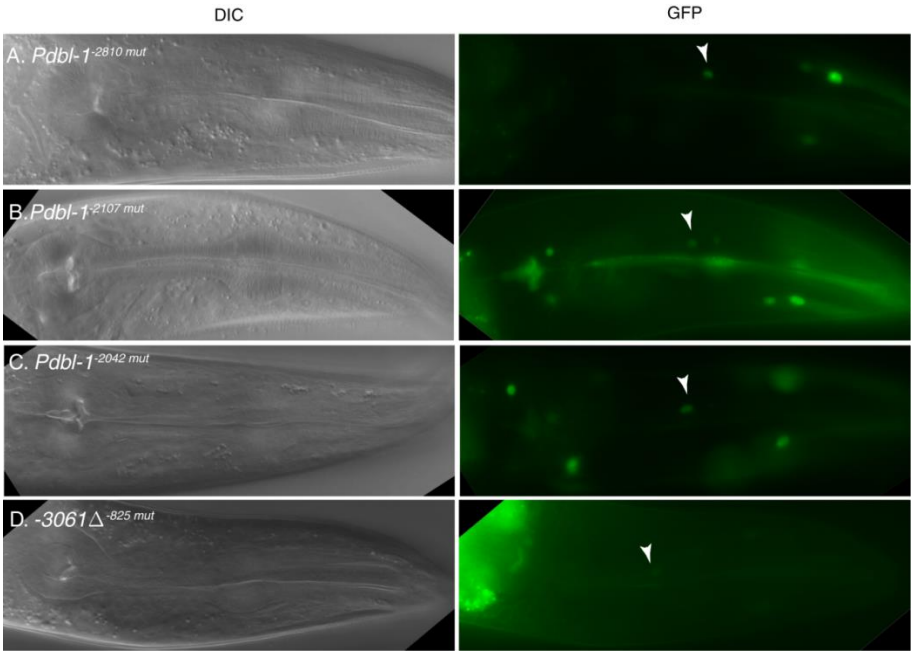

Figure 29 Site directed mutagenesis of the *dbl-1* promoter

DIC (right) and GFP (left) micrographs of young adults expressing *dbl-1::gfp* in the M4 neuron (arrowheads). (A-C) Constructs expressing the full length *dbl-1* promoter (4658 bp) fused to gfp in which the CEH-28 binding sites at -2810 bp in (A), -2107 bp in (B) and -2042 bp respectively are mutated. (D).The CEH-28 binding site at -825 bp is mutated in the context of the -3061Δ *dbl-1* promoter.

7.2 Appendix B: Isolation of GFP tagged M4 neurons from L1 larvae using larval cell isolation protocol and flow cytometry

C. elegans is a great developmental model system and a resource to perform genetic studies. It offers several advantages such as the invariant cell linage (Sulston and Horvitz, 1977) completely sequenced genome and availability of viable loss of function mutants. However, isolating individual cell types and performing cell culture has been a challenge and this technique was limited to the embryonic stages of development (Bianchi and Driscoll, 2006; Christensen et al., 2002; Strange et al., 2007) until recently. Protocols to perform isolation and culture of *C. elegans* cells from larval stage animals were developed recently. (Zhang et al., 2011) The cells isolated using these methods can be used for many potential downstream applications such as cell sorting, electrophysiology and transcriptional profiling.

We were interested in using this protocol to isolate M4 neurons from wild-type and *ceh-28* mutants to isolate M4 RNA and perform transcriptional profiling using RNA-Seq. We previously identified downstream targets of CEH-28 including *dbl-1* (Ramakrishnan et al., 2014), *egl-17* and *flp-5* (Ramakrishnan and Okkema, unpublished). We wanted to identify additional downstream targets of CEH-28, by comparing the wild-type M4 transcriptome to that of *ceh-28* mutants using RNA-Seq.

We isolated GFP tagged M4 neurons from L1 stage wild-type and *ceh-28* mutants using a modified version of the larval cell isolation protocol described in section 2.9.3 and sorted cells using flow cytometry in collaboration with the RRC facility at UIC using methods described in section 2.9.4

We performed multiple independent trials of the larval cell isolation and the cell sorting experiments to successfully obtain M4 cells from wild-type and *ceh-28* mutants (Table X) using N2 cells as a negative control or GFP positive cells from the NW1229 strain as a positive control. The control cell populations were used to determine the optimum gating parameters

(Figure 30) prior to the sort. The same gating conditions used in the controls were then applied to sort the GFP positive M4 cells from the experimental cell population (Figure 31).

We find that the efficiency of isolating M4 neurons from intact L1 larvae is very low given that we were able to only obtain a few thousand M4 neurons, starting from a large population of 500,000- 800,000 L1 animals (Table X). We find that the L1 larvae in particular are resistant to Protease digestion and this finding is consistent with the detailed methods for larval cell isolation protocols described by the authors in Wormbook (Zhang and Kuhn, 2013). Since the M4 neuron is a single cell, isolating one neuron among five hundred fifty other larval cells, is another additional challenge.

To verify the purity of the isolated M4 cell population, RNA from these M4 cells can be isolated and the expression levels of M4 expressed genes such *dbl-1*, *egl-17* and *ser-7* can be assayed from each independent population of cells using q PCR.

Table X SUMMARY OF GFP POSITIVE M4 CELLS OBTAINED FROM WILD-TYPE AND *ceh-28(cu11)* MUTANTS USING FLOURESCENCE ACTIVATED CELL SORTING

Experiment Number	Number of M4 cells obtained from wild-type[(a)]	Number of M4 cells obtained from *ceh-28* mutants[(b)]	Strains used in the control sort [(c,d)]
1	784	N/A	N2 cells [c]
2	13567	N/A	N2 [c]
3	5865	N/A	N2 [c]
4	1500	N/A	NW1229 [d]
5	N/A	6500	NW1229 [d]

[a] To isolate M4 cells from wild-type animals, the MT15672 strain expressing an integrated *nIs177[pceh-28::4xNLS::gfp; lin-15AB(+)]* was used.

[b] To isolate M4 cells from *ceh-28* mutants, the OK0944 strain expressing the *nIs177* transgene in a *ceh-28(cu11)* background was used

[c] As a negative control for cell sorting, cells isolated from N2 animals were used

[d] As a positive control for cell sorting, cells isolated from the NW1229 strain expressing the pan neuronal transgene *evIs111[[PF25B3.3::GFP]* were used

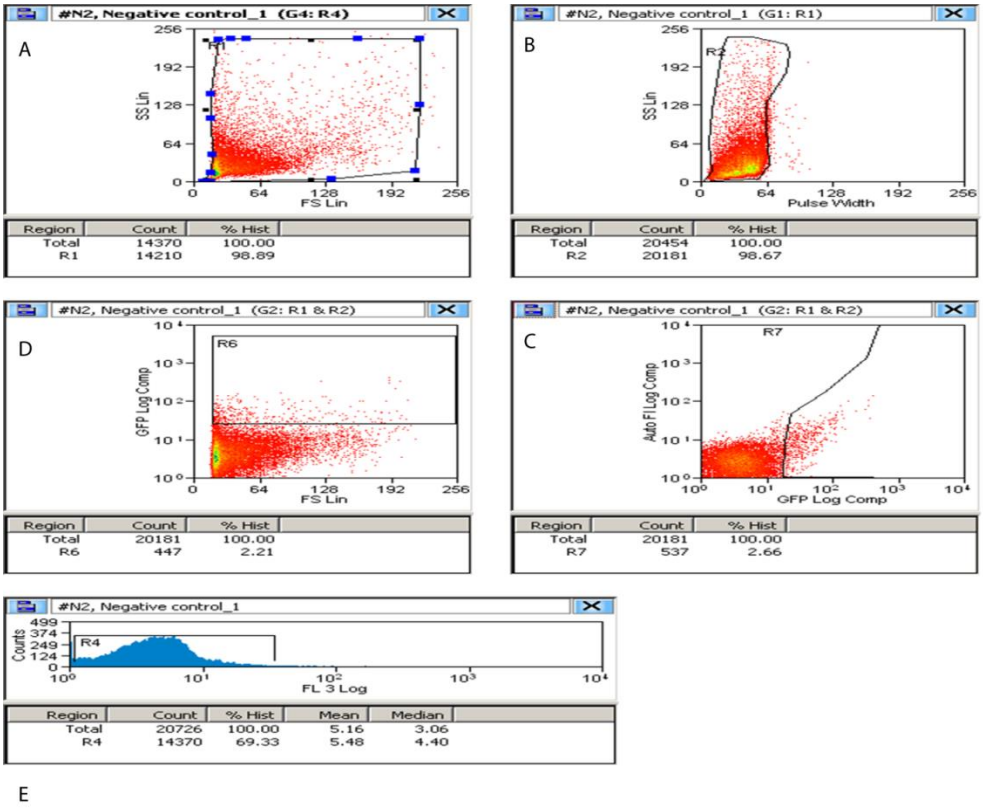

Figure 30 Flow Cytometry scatter plots for determining gating parameters using N2 cells as a negative control

Screenshots from the Experiment 2 in Table X are shown. (A) Linear function of Side Scatter (SS Lin) on Y-axis versus Linear Function of Forward Scatter (FS Lin) on X- axis versus for N2 cells. FS Lin provides information about the relative size of the cells and SS Lin is used to determine granularity. Individual events are pseudo colored in red. (B) SS Lin on Y-axis versus Pulse Width on X-axis. Pulse width function specifies sizes of individual particles. (C) Log function of Auto fluorescence compensation on Y- axis versus Log function of GFP compensation on X-axis. This compensation parameter is applied to mathematically account for background signal that is usually caused due to GFP bleed through. (D) Log function of GFP compensation on Y-axis versus FS Lin on X- axis scatter performs background subtraction and determines the population of GFP positive cells. (E) Histogram showing the count of live cell population which are negative for Propidium Iodide staining.

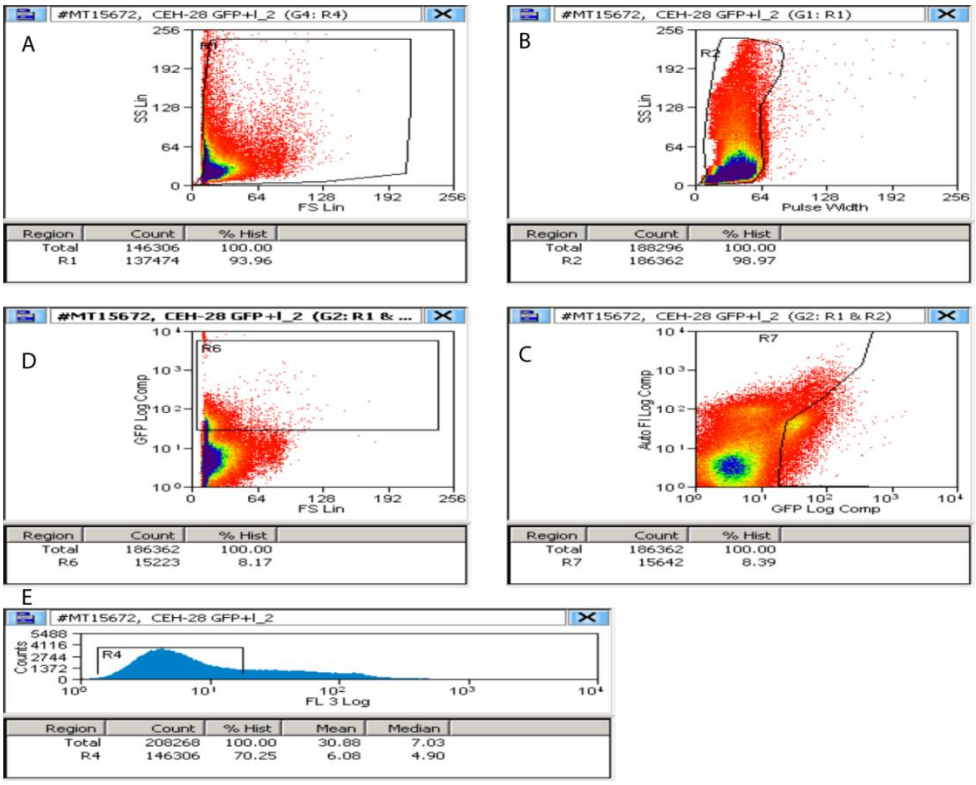

Figure 31 Isolating GFP positive M4 cells from wild-type animals

Screenshots from the Experiment 2 in Table X. The gating parameters which were determined using the cells from the N2 strain in experiment 2 (Figure 23) were applied to the experimental sample to sort the M4 cells from the MT1562 strain. (A) Size and granularity of the experimental cells are determined by plotting the Linear Function of Forward Scatter (FS Lin) on X-axis versus Linear function of Side Scatter (SS Lin) on Y-axis. Individual events are pseudo colored in red and double events are pseudo colored in yellow. (B) Scatter plot depicting Pulse width on X-axis versus SS Lin on Y-axis. (C) The amount of autofluorescence in the sample is determined by determined by plotting Log function of Log function of GFP compensation on X-axis versus Log function of Auto fluorescence compensation on Y-axis. D) Background subtraction for the experimental cells is determined by plotting FS Lin on X-axis versus Log function of GFP compensation on Y- axis. (E) Histogram showing the count of live cell populations which are negative for Propidium Iodide staining.

7.3 Appendix C: Quantitative PCR to analyze *dbl-1* gene expression in M4

We previously showed that *dbl-1::gfp* is not expressed specifically in the M4 neuron of *ceh-28(cu11)* mutants (Ramakrishnan et al., 2014) . However, the levels of *ser-7* and *ceh-28* itself are unaffected in *ceh-28* mutants (Ray et al., 2008). We also found that the expression of an integrated transgene *nIs177[ceh-28::4xnls:gfp]* (Hirose et al., 2010) was normal in *ceh-28* mutants.

We asked if the endogenous level of *dbl-1* was down regulated in a *ceh-28* mutant by performing quantitative RT- PCR on whole worm L1 RNA isolated from wild-type and *ceh-28* mutants bearing an integrated *ceh-28::4XNLS::gfp* transgene which marks the M4 neuron. To obtain a synchronous population of L1 animals from wild-type and *ceh-28(cu11)* mutants, 5-6 10 cm NEP plates containing lots of young adults were bleached and hatched in M9 using methods described in section 2.9.2. Total whole worm L1 RNA was isolated from wild-type and *ceh-28(cu11)* mutants using the TRIzol method described in section 2.10. The RNA isolation was performed two times in both *wild-type* and *ceh-28* mutants to obtain two biological replicates. We used *ser-7*, *gfp* and *ama-1* as controls since these genes are expressed normally in the M4 neuron of *ceh-28* mutants. The primer pairs for each gene are listed in Table XI.
Every q PCR reaction was set up as a triplicate to minimize variations and errors due to pipetting.

We calculated the expression of *dbl-1* relative to *ser-7*, *gfp* and *ama-1* in a wild-type background and compared these ratios in a *ceh-28* mutant to ask if these ratios are decreased in a *ceh-28* mutant since *dbl-1* expression is lost specifically in M4. We used the 2^-ΔΔCt method (Livak and Schmittgen, 2001) to compare fold change in the *dbl-1* levels. We find an inconsistent trend in *dbl-1* expression ratio in *ceh-28* mutants when compared to wild-type between biological replicates (Table XII). This inconsistency was primarily caused due to the large amount of variation between the biological replicates of RNA isolated from *ceh-28*

mutants. One of the factors causing the variation in the biological replicates could be potentially attributed to the inability to produce high yields of pure total L1 RNA from *ceh-28* mutants. Despite multiple optimizations and trials, obtaining high yields of pure L1 RNA from *ceh-28* mutants was a challenge. To obtain pure samples, the RNA had to be purified using an RNeasy clean up column (Qiagen). This purification step greatly affected the yield of the isolated RNA.

The total L1 RNA isolation needs to be further optimized to yield comparable results between biological replicates. Once that is achieved, the fold differences can be calculated and the statistical significance of this value can be determined. It is likely, that we might be unable to detect differences in *dbl-1* expression levels between wild-type and *ceh-28* mutants, in total L1 RNA samples, given that M4 is a single cell among five hundred fifty other cells in the L1 larval stages. Hence it is possible that the differences of *dbl-1* expression in the M4 neuron might not be accurately or significantly detected while using total L1 RNA.

An alternative approach would be to use M4 RNA which can be isolated from M4 cells isolated from wild-type and *ceh-28* mutants (Appendix B, Table X) using larval cell isolation and cell sorting using methods described in section 2.9.4 since this is population is more likely to be enriched for M4 cells. By performing a q-PCR on the M4 RNA, we can more accurately, measure the differences in the endogenous levels of *dbl-1* expression between wild-type and *ceh-28* mutants in the M4 neuron.

Table XI OLIGOS FOR PERFROMING QUANTITATIVE PCR

Gene	Primer pairs	Size of the amplicon in bp
ama-1	PO1061[AGGCGAAGGATGTGTTGTG] PO1062[TCACCGTGTTCTTTGGGTC]	120
dbl-1	PO1317 [AAGCATCATAACACCGAGGC] PO1318 [ACTGAGCTGGCATTGGATTT]	157
gfp	PO1399[ACTTTTCACTGGAGTTGTCCCA] PO1400[GGTAGTTTTCCAGTAGTGCA]	144
ser-7	PO1401[CTTTTTCGTGGGGCTCGTTG PO1402[GTGCATAGCGTTAGGTCGGA	174
ceh-28	PO1315 [GCCCAGGACAGAACCTTACA] P01316[ATGGTGCAGTTCCAAAGCTG]	97

Table XII QUANTIFYING RELATIVE FOLD CHANGE OF *dbl-1* LEVELS IN WILD-TYPE AND *ceh-28(cu11)* MUTANTS USING THE 2^-ΔΔCt METHOD

Template RNA	Fold difference of *dbl-1* relative to *gfp*	Fold difference of *dbl-1* relative to *ser-7*	Fold difference of *dbl-1* relative to *ama-1*
Wild-type L1 RNA A	1 (0.7-1.4)	1 (0.54-1.85)	1 (0.83 -1.2)
ceh-28 (cu11) L1 RNA A	0.356 (0.22-0.59)	0.309 (0.15-0.63)	0.3 (0.24-0.33)
Wild-type L1 RNA B	1 (0.7-1.4)	1 (0.32-3.2)	1 (0.76-1.3)
ceh-28(cu11) L1 RNA B	1.5279 (0.7-3.6)	2.54 (0.98-6)	1.12± (0.5-2.7)

The expression levels of *dbl-1* relative to *gfp*, *ser-7* and *ama-1* were calculated in a wild-type background and compared to *ceh-28* mutants using the 2^-ΔΔCt method.

7.4 Appendix D: RNAi screen to identify genes regulated by *tbx-2*

TBX-2 is a T-box transcription factor for pharyngeal muscle development (Roy Chowdhuri et al., 2006). Lynn Clary previously compared mRNA expression levels in wild-type and *tbx-2(bx59)* embryos (Huber et al., 2013). We wanted to identify downstream targets and developmental regulators of TBX-2 from the list of differentially expressed genes in the microarray data generated by Lynn Clary. To initially screen for targets, we searched for genes which overlapped both Susan Mango's microarray (Gaudet and Mango, 2002) data identifying genes expressed in the embryonic pharynx and our microarray data (Huber et al., 2013) and asked if these gene promoters contain a brachury T-box binding site at a cut off frequency of 75% or greater when searched using the JASPAR database. Additionally we also searched these genes on NEXTDB to ask if there was in situ hybridization data suggesting evidence of pharyngeal gene expression. Based on this criteria we initially identified 5 genes namely, *cdr-4, C53C9.2, Y73F4A.2 and fat-5* and *nspb-12*. We wanted to test if knockdown these genes by feeding RNAi resulted in pharyngeal defects similar to *tbx-2* mutants.

We used the clones from the feeding RNAi library (Kamath and Ahringer, 2003) to perform RNAi by feeding. Prior to performing RNAi, we verified for the presence of the right clones using colony PCR and sequence verified the clones using methods described in section 2.12. RNAi was performed using methods described previously (Kamath and Ahringer, 2003; Milton et al., 2013).

We find that knockdown of these five candidates in the N2 background, by feeding RNAi did not result in any pharyngeal defects or phenotypes (Table XIII).

To screen for additional targets, we identified genes which encode transcription factors among the differentially expressed genes in the microarray and performed RNAi on these candidates in a strain containing an integrated *ceh-22::gfp* reporter, which marks pharyngeal muscle nuclei (Okkema and Fire, 1994).

We find that *nhr-50(RNAi)* and *nhr-3 (RNAi)* animals exhibited a low penetrance of the Pharynx unattached (Pun) phenotype and Embryonic arrest (Emb) phenotype (Figure 32, Table XIII). We also find varying levels of embryonic lethality caused in *mxl-3 (RNAi), T15H9.6(RNAi), his-5(RNAi)* and *daf-18(RNAi)* animals (Table XIII).

To further investigate the phenotypes observed in *nhr-50(RNAi)* and *nhr-3 (RNAi)* animals, we examined the *nhr-50 (ok671)* and *nhr-3(gk258*) and *mxl-3(ok1947)* mutants and did not observe any pharyngeal defects in these mutants. Hence we conclude that the low penetrance pharyngeal defects observed in the *nhr-3(RNAi)* and *nhr-50(RNAi)* might have resulted due to non-specific and off target effects of the RNAi technique.

Table XIII QUANTIFICATION OF FEEDING RNAi PEHNOTYPES OBSERVED IN POTENTIAL TARGETS OF TBX-2

Gene	RNAi clone name	RNAi phenotype in N2 background (n) [a,b]	RNAi phenotype in *ceh-22::gfp* background (n) [a,b]
cdr-4 [c]	KOD12.1	None (45)[b]	Emb 28% (40)[a]
C53C9.2 [c]	C53C9.2	None (30)[b]	None (45)[b]
Y73F4A.2 [c]	Y73F4A.2	None (40)[b]	N.D
fat-5 [d]	W06D12.3	None (30)[b]	N.D
nspb-12[c]	F09F7.1	None (37)[b]	N.D
nhr-50 [d]	C06C6.5	N.D	Emb 37% (30)[a] Pun 13% (24)[b]
nhr-3 [d]	H01A20.1	N.D	Emb 10% (65)[a] Pun 15% (20)[b]
mxl-3 [d]	F46G10.6	N.D	Emb 37% (38)[a]
T15H9.6 [d]	T15H9.6	N.D	Emb 35% (48)[a]
fos-1 [d]	F29G9.4	Muv 20%(30)[a] , Emb 80% (30)[b]	N.D
his-5 [d]	F45F2.3	N.D	Emb 34% (35)[a]
daf-18 [d]	R13H8.1	N.D	Emb 38% (80)[a]
cbp-1 [d]	C40H1.1	N.D	None (38)[a]
egl-27 [d]	C04A2.3	N.D	None (50)[a]
F48B9.5 [d]	F48B9.5	N.D	None (32)[b]
M01E5.6 [d]	M01E5.6	N.D	None (40)[b]
nhr-11 [d]	ZC410.1	N.D	None (25)[b]

nhr-115 [d]	T27B7.4	N.D	None (30)[b]
nhr-157 [d]	C17E7.5	N.D	None (40)[b]
nhr-249 [d]	ZK381.3	N.D	None (35)[b]
nhr-264 [d]	F14A5.1	N.D	None (33)[b]
T27F2.4 [d]	T27F2.4	N.D	None (44)[b]
zip-2 [d]	K02F3.4	N.D	None (30)[b]
zip-5 [d]	C34D1.5	N.D	None (42)[b]

[a] number of embryos quantified after RNAi by feeding

[b] number of animals quantified in the L1-L4 stage after RNAi by feeding

[c] genes misregulated in *tbx-2(bx59)* mutants and reported as expressed in the pharynx(Gaudet and Mango, 2002; Huber et al., 2013)

Emb - Embryonic arrest phenotype

Muv - Multivulva phenotype

Pun - Pharynx unattached phenotype

N.D - Not defined; experiment was not performed in the respective cases

None - No RNAi phenotypes were observed

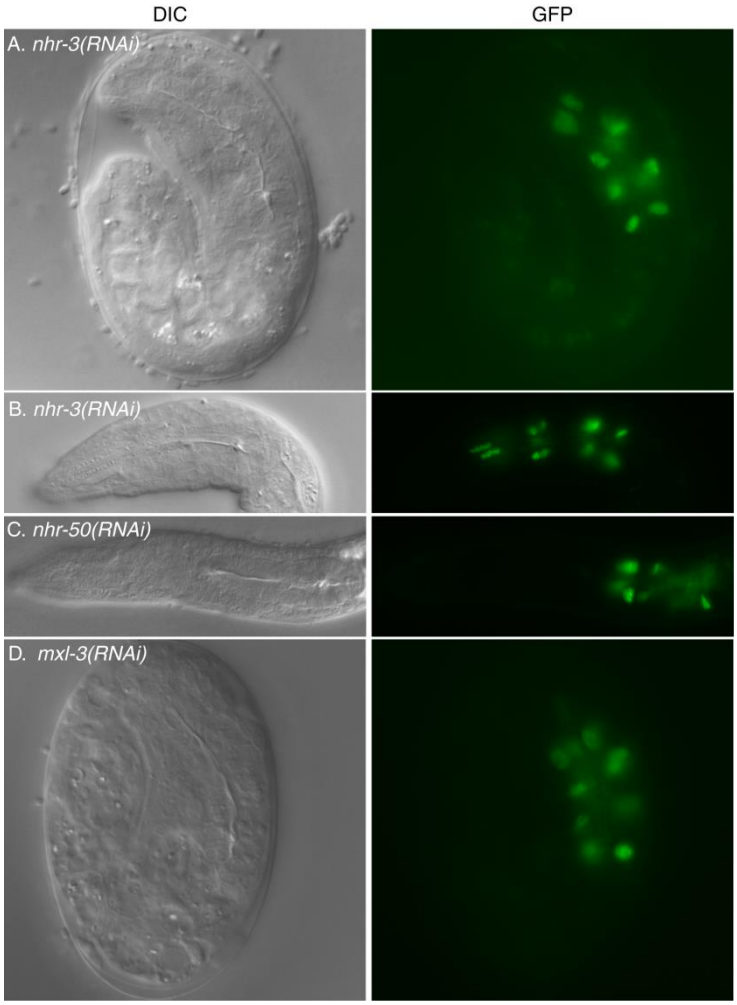

Figure 32 : Embryonic and pharyngeal phenotypes observed in *nhr-3(RNAi), nhr-50(RNAi)* and *mxl-3(RNAi)* animals

DIC (left) and GFP (right) micrographs of an *nhr-3 (RNAi)* animal displaying an Embryonic arrest phenotype in (A) and a pharyngeal defect in (B). (C) DIC (left) and GFP (right) of an *nhr-50(RNAi)* animal displaying the Pharynx unattached phenotype. (D) DIC (right) and GFP (left) of an *mxl-3 (RNAi)* embryo displaying defects in pharyngeal development.

7.5 **Appendix E: List of Plasmids**

Table XIV: LIST OF PLASMIDS

Plasmid	Description	Chapter
pDONR221	Gateway entry vector. Suitable for propagation in DB3.1 bacteria	5
pOK147.01	contains a *Δpes-10::gfp ba*sal promoter which is sensitive to upstream transcriptional enhancers	3
pOK197.03	*Pser-7b::gfp* Obtained from Richard Komuniecki	2,3,5
pOK205.01	Full length dbl-1 promoter (a.k.a pMY+NLS) containing bp 11,900-16,530 of T25F10 cosmid fused to gfp. Obtained from Bills Woods lab	2,3
pOK210.01	*phat-3::yfp*. Obtained from Jeb Gaudet	2,3
pOK230.01	*ser-7b* promoter driving expression of *dbl-1 cDNA*. *dbl-1 cDNA* was PCR amplified from pOK227.02 using primers PO801 and PO803 and cloned into KpnI to EcoRI digested pOK197.03	3
pOK264.01,pOK264.02	A 3061 bp *dbl-1* promoter fused to gfp generated by digesting the full length *dbl-1* promoter (pOK205.01) with Pst1 and Nhe1 and recircularizing the digested DNA. Also known as -3061Δ	2,3
pOK264.03, pOK264.04	A 2472 bp *dbl-1* promoter fused to gfp. Generated by digesting pOK205.01 with PstI and DraIII and recircularizing the digested DNA. Also known as -2472Δ	2,3

APPENDIX E: TABLE XIV: LIST OF PLASMIDS (continued)

pOK264.05, pOK264.06	A 646 bp *dbl-1* promoter fused to gfp. Generated by digesting pOK205.01 with XbaI and recircularizing the digested DNA. Also known as -646Δ	2,3
pOK264.07, pOK264.08	Generated by digesting pOK205.01 with HindIII and recircularizing the digested DNA. Also known as -1278Δ	2,3
pOK264.09, pOK264.10	Generated by digesting pOK205.01 with SphI and recircularizing the digested DNA. Also known as - 3764Δ	2,3
pOK264.17	Gateway expression vector containing FLAG tagged Poly A binding protein and an *unc-119* rescue cassette. Suitable for propagation in DB3.1 bacteria. Obtained from David Miler's lab. Also known as pSV41	5
pOK270.02	4.6 kb *dbl-1* promoter in which the CEH-28 binding site at -2810 bp was mutated using primers PO1170/PO1171 by site directed mutagenesis	Appendix A
pOK271.09	*ser-7b* promoter PCR amplified from pOK197.03 using primers pairs PO1092 ,PO1093 and cloned into pDONR221 by Gateway cloning	5
pOK271.11	*ceh-28* promoter PCR amplified from pOK176.09 using primer pairs PO1090, PO1091 and cloned into pDONR221 by Gateway cloning	5
pOK271.13	*Pser-7b ::3XFLAG::PABP*. *ser-7b* promoter driving expression of FLAG tagged Poly A Binding protein. This construct was generated by cloning *ser-7b* promoter	5

APPENDIX E: TABLE XIV: LIST OF PLASMIDS (continued)

	from pOK271.09 into the gateway destination vector pOK264.17/pSV41 by gateway cloning	
pOK271.16	*Pceh-28::3XFLAG::PABP*. This construct was generated by cloning the *ceh-28* promoter from pOK271.11 into the pOK264.17/pSV41 gateway destination vector.	5
pOK272.03	4.6 kb *dbl-1* promoter in which the site at -2042 bp was mutated using primers PO1176/PO1177 by site directed mutagenesis	Appendix A
pOK272.04	4.6 kb *dbl-1* promoter in which the site at -738 bp was mutated using primers by PO1178/1179 by site directed mutagenesis	Appendix A
pOK272.05	4.6 kb *dbl-1* promoter in which the site at -2107 bp was mutated using primers PO1174/PO1175 by site directed mutagenesis	Appendix A
pOK272.06	*dbl-1* M4 enhancer was PCR amplified from pOK205.01 using primers PO1244/PO1249 , cut with Hind III and XbaI and cloned into the HindIII-XbaI sites of pOK147.01	2, 3
pOK274.19	The HindIII- NheI fragment of the *dbl-1* promoter containing bp 13,502-15,284 of cosmid T25F10 was amplified and inserted upstream of *Δpes-10::gfp* to generate pOK274.19	3
pOK275.01	3061 bp *dbl-1* promoter in which the site at -825 b is mutated using primers	Appendix A

APPENDIX E: TABLE XIV: LIST OF PLASMIDS (continued)

	PO1248/PO1249 by site directed mutagenesis.	
pOK277.01	*dbl-1* M4 enhancer in which the CEH-28 binding site at -835 bp is mutated . Generated by site directed mutagenesis of pOK272.06 with primer PO1248	3
pOK277.03	*dbl-1* M4 enhancer in which the CEH-28 binding site at -738 bp is mutated . pOK277.03 was generated by mutating pOK272.06 with PO1178 primer by site directed mutagenesis	2,3
pOK277.05	*dbl-1* M4 enhancer in which the CEH-28 binding site at -825 bp and -738 bp were mutated . pOK277.05 was generated by mutating pOK277.01 with primer PO1178 by site directed mutagenesis	2,3
pOK291.06	*egl-17* promoter necessary for M4 expression (Burdine et al 1998) amplified from N2 genomic DNA using PO1396 and PO1397 and cloned into the HindIII and SalI sites of pOK147.01	4
pOK293.01	*egl-17* M4 enhancer fragment amplified from N2 genomic DNA using PO1396 and PO1398 and cloned into the HindIII and SalI sites of pOK147.01. This fragment shows M4 enhancer activity	4

7.6 Appendix F: List of Oligos

Table XV: LIST OF OLIGOS

Oligo	Sequence 5-3’	Description
FLP109	CTGTGTTCACTCTACCAGG	Reverse PCR primer to amplify *flp-2* promoter. Sequences obtained from Chris Li
FLP21(f)	AACTAGGTCCAGTGACCGAAAGTG	Forward PCR primer to amplify *flp-2*1promoter. Sequences obtained from Chris Li
FLP353	ACAGCCGCAACGTCTGAAAATGAC	Reverse PCR primer to amplify *flp-2*1promoter. Sequences obtained from Chris Li
FLP55	TTGCGTGGTTTGCGACAATTGG	Forward PCR primer to amplify *flp-2* promoter. Sequences obtained from Chris Li
M13F-20	GTAAAACGACGGCCAGT	Standard sequencing primer to sequence inserts
M13R -27	AACAGCTATGACCATG	Standard sequencing primer to sequence inserts
PO640	CCCAATGCAATCTACGCAG	Forward primer for genotyping *ceh-28(cu11)* mutants
PO641	GAATCAAACCGCCAACCAG	Forward primer for genotyping *ceh-28(cu11)* mutants
PO642	CCCAGCGTGTCATACATGG	Reverse primer for genotyping *ceh-28(cu11)* mutants

APPENDIX F: TABLE XV: LIST OF OLIGOS (continued)

PO801	CAGGTACCAAAATGAACGACTCTGTGCGGAC	Upstream primer for amplifying *dbl-1* orf with KpnI linker
PO802	CATCTAGAAAAATGAACGACTCTGTGCGGAC	Downstream primer for amplifying *dbl-1* orf with XbaI linker
PO1061	AGGCGAAGGATGTGTTGTG	Forward primer for amplifying *ama-1* exons by q RT-PCR
PO1062	TCACCGTGTTCTTTGGGTC	Reverse primer for amplifying *ama-1* exons by q RT-PCR
PO1090	GGGGACAAGTTTGTACAAAAAAGCAGGCTTTGGTTGTCATGGTTGAAGC	Forward PCR primer for amplifying *ceh-28* promoter. Contains the att B1 adaptor sequences necessary for Gateway cloning
PO1091	GGGGACCACTTTGTACAAGAAAGCTGGGTTCTGATTTTGACTTGGAGAACC	Reverse PCR primer for amplifying *ceh-28* promoter. Contains the attB2 adaptor sequences necessary for Gateway cloning
PO1092	GGGGACAAGTTTGTACAAAAAAGCAGGCTGCCTGCAGCAAACAGGTAG	Forward PCR primer for amplifying the ser-7b promoter. Contains the att B1 adaptor sequences necessary to perform Gateway cloning
PO1093	GGGGACCACTTTGTACAAGAAAGCTGGGTCCTCAGGCTGTGTCTGACTG	Reverse PCR primer for amplifying *ser-7b* promoter. Contains att B2 adaptor sequences necessary for Gateway cloning
PO1170	CCATTCAACTGTCCATTCTCTGTTTTAAACAGATCATCTCACTGACCTT	Forward primer for mutating the CEH-28 binding site at - 2810 bp in the *dbl-1* promoter

APPENDIX F: TABLE XV: LIST OF OLIGOS (continued)

PO1171	AAGGTCAGTGAGATGATCTGTTTAAAACA GAGAATGGACAGTTGAATGG	Reverse primer for mutating the CEH-28 binding site at - 2810 bp in the *dbl-1* promoter
PO1174	ACACAATTGTTAGTTATCGTTTGATCTTGC CGCCGTCTCCG	Forward primer for mutating the CEH-28 binding site -2107 bp in the full length *dbl-1* promoter (pOK205.01)
PO1175	CGGAGACGGCGGCAAGATCAAACGATAA CTAACAATTGTGT	Reverse primer for mutating the CEH-28 binding site -2107 bp in the full length *dbl-1* promoter (pOK205.01)
PO1176	ATATGAGAAGAAAACATTCTTGATCTTGC GAGCAACTTCTTGCTGTC	Forward primer for mutating CEH-28 binding site at -2042 in the full length *dbl-1* promoter (pOK205.01)
PO1177	GACAGCAAGAAGTTGCTCGCAAGATCAAG AATGTTTTCTTCTCATAT	Reverse primer for mutating CEH-28 binding site at -2042 in the *dbl-1* promoter (pOK205.01)
PO1178	TTTTAAGCAACAGTGGTAGTAAGTTGACA TCAGGCATTTCGAAAACC	Forward primer for mutating the CEH-28 binding site at -738 bp in pOK205.01 and pOK272.06
PO1179	GGTTTTCGAAATGCCTGATGTCAACTTAC TACCACTGTTGCTTAAAA	Reverse primer for mutating the CEH-28 binding site at -738 bp in pOK205.01 and pOK272.06
PO1180	TGAAAGAACATTGATGGG	Sequencing primer for sequencing 5' end of inserts cloned in pSV41/pOK264.17 (PABP gateway) vector
PO1181	TCTCGAACAGGATCGACTCG	Sequencing primer for sequencing 3' end of inserts cloned in

APPENDIX F: TABLE XV: LIST OF OLIGOS (continued)

		pSV41/pOK264.17 (PABP gateway expression vector)
PO1203	GTAGACGGGAACATTGCGT	Forward PCR primer for genotyping integrated *Pser7b::3XFLAG::PABP* (cuIs30) transgene generated by microparticle bombardment
PO1204	TGAAGATATTGCCAGCTCCC	Reverse PCR primer for genotyping integrated Pser7b::3XFLAG::PABP (cuIs30) transgene generated by microparticle bombardment
PO1205	TTTGGTGTGAAAATCCCTCCT	Forward PCR primer for genotyping strains expressing the *Pceh-28::3XFLAG::PABP* transgene
PO1206	GATTCTCATTGGTTTGCCGT	Reverse PCR Primer for genotyping strains expressing the ceh-8::3XFLAG::PABP transgene
PO1242	GTTTTAAAAGCAACCCTGCG	Forward primer to amplify (Hind III-Nhe I)*dbl-1* promoter fragment containing bp 13,502-15,284 of *dbl-1* cosmid T25F10
PO1243	TGATAAGTTTTGCGCTGCTG	Reverse primer to amplify (Hind III-Nhe I) *dbl-1* promoter fragment containing bp 13,502-15,284 of *dbl-1* cosmid T25F10
PO1244	TAATGTCCGTCTTTGGGGTC	Forward primer for amplifying the *dbl-1* M4 enhancer from pOK205.01

APPENDIX F: TABLE XV: LIST OF OLIGOS (continued)

PO1245	CCAAGAACTGCGTTCAGACA	Reverse primer for amplifying the *dbl-1* M4 enhancer from pOK205.01
PO1248	TGGAGCTATTGTTTTTCACACCCAGACGA TGAATCTGGTGGG	Forward primer for mutating the CEH-28 binding site at -825bp in the *dbl-1* promoter (pOK205.01) and the *dbl-1* enhancer (pOK272.06)
PO1249	CCCACCAGATTCATCGTCTGGGTGTGAAA AACAATAGCTCCA	Reverse primer for mutating the CEH-28 binding site at -825 bp in the *dbl-1* promoter (pOK205.01) and the *dbl-1* enhancer (pOK272.06)
PO1313	ATCTTCTGAACGACGGCACT	Forward primer for amplifying *ser-7* exons by q RT-PCR.
PO1314	ACCTGTCTTGAGCTGCCAAT	Reverse primer for amplifying *ser-7* exons by q RT-PCR
PO1315	GCCCAGGACAGAACCTTACA	Forward primer for amplifying *ceh-28* exons by q RT-PCR.
PO1316	ATGGTGCAGTTCCAAAGCTG	Reverse primer for amplifying *ceh-28* exons by q RT-PCR
PO1317	AAGCATCATAACACCGAGGC	Forward primer for amplifying *dbl-1* exons using q RT-PCR
PO1318	ACTGAGCTGGCATTGGATTT	Reverse Primer for amplifying *dbl-1* exons using q RT-PCR
PO1396	AGCTCTAAGCTTCGAAATCACTGGAAGGC ACT	Forward PCR primer to amplify *egl-17* M4 enhancer and the fragment described previously (Cui and Han, 2003) to be necessary

APPENDIX F: TABLE XV: LIST OF OLIGOS (continued)

		for M4 expression. Includes HindIII linker
PO1397	AGCTCTGTCGACGCCATAACTGACCTCATCCAA	Reverse PCR primer for amplifying region necessary for M4 expression described previously (Cui and Han, 2003). Includes SalI linker
PO1398	AGCTCTGTCGACGAGCGCTATTGGTTTTGTAC	Reverse PCR primer to amplify *egl-17* M4 enhancer, contains SalI restriction site
PO1399	ACTTTTCACTGGAGTTGTCCCA	Forward primer to amplify GFP orf by q RT-PCR
PO1400	GGTAGTTTTCCAGTAGTGCA	Reverse primer to amplify GFP orf by q RT-PCR
PO1401	PO1401[CTTTTTCGTGGGGCTCGTTG	Forward primer used to amplify SER-7 orf by q RT-PCR
PO1402	PO1402[GTGCATAGCGTTAGGTCGGA	Reverse primer used to amplify SER-7 orf by q RT-PCR

7.7 **Appendix G: List of Strains**

Table XVI: LIST OF STRAINS

Strain	Description	Chapter
BW1806	*dbl-1(ev580) V dbl-1* mutant obtained from Bill Wood's lab	3
BW1946	*ctIs43[Pdbl-1::gfp]; unc-42(e270) V dbl-1::gfp* obtained from Bill Wood's lab	3
CB928	*unc-31(e928) IV unc-31* mutants defective in dense core vesicle release. Strain obtained from Janet Richmond	3
GD273	*sma-2(e502) III; ivls12 II sma-2* mutants containing the *phat-1::yfp* gland cell reporter. Strain obtained from Jeb Gaudet	3
GD274	*sma-3 (e491) III; ivls12 II*, *sma-3* mutants containing the *phat-1::yfp* gland cell reporter. Strain obtained from Jeb Gaudet	3
MT15672	*nls177 I [pceh-28::4xNLS::gfp; lin-15AB(+)]* Strain expressing an integrated *ceh-28::4xNLS::gfp* Obtained from Bob Horvitz	4. Appendix C
NH2466	*ayIs4[egl-17::GFP dpy-20(+)] I; dpy-20(e1282ts) IV*	4
NW1229	*dpy-20(e1362) IV; evIs111[Prgef-1::gfp]*	Appendix B
NY2049	*ynIs49V [flp-5::gfp]* Integrated transgenic strain expressing *Pflp-5::gfp* reporter. Obtained from Caenorhabditis Genetics Center (CGC).	4

APPENDIX G: TABLE XVI: LIST OF STRAINS (continued)

NY2057	*ynIs57 III; him-5(e1490) V* Integrated transgenic strain expressing *Pflp-2::gfp* Obtained from CGC.	4
NY2080	*ynIs80[Pflp-21::gfp]* Integrated strain expressing *Pflp-21::gfp*. Obtained from CGC	4
OK0516	*cuEx469* Extra chromosomal array carrying *ser-7b*::*gfp* (pOK 197.03) and100 ng/µl of pRF4	4
OK0762	*cuEx611* Extra chromosomal array containing 10 ng/ µl of pOK210.01 (*phat-3::yfp*) and 15 ng/µl of pOK230.01(*ser7b* promoter driving *dbl-1c DNA*) and 100 ng/µl of pRF4	2
OK0763	*dbl-1(ev580); cuEx611 dbl-1 m*utants carrying the *cuEx611* extrachromosomal array	2
OK0764	*cuEx612* Extrachromosomal array containing 10 ng/µl of pOK272.06 [*dbl-1 M4* enhancer] and 100 ng/µl of pRF4	2
OK0765	*cuEx613* Extrachromosomal array containing 10 ng/µl of pOK272.06 [*dbl-1 M4* enhancer] and 100 ng/µl of pRF4	2,3
OK0766	*ceh-28(cu11); cuEx613 ceh-28(cu11)* mutants carrying the *cuEx613[dbl-1 M4 enhancer]* extrachromosomal array	2,3
OK0767	*unc-119(ed3); cuEx614* Extrachromosomal array obtained by transforming *unc-119* worms with pOK271.16 *[Pceh-28::3X FLAG::PABP]* using micro particle bombardment	5
OK0768	*unc-119(ed3); cuEx615* Extra chromosomal array generated by transforming *unc-119* worms with pOK 271.16 *[Pceh-28::3X FLAG::PABP]* using micro particle bombardment	5

APPENDIX G: TABLE XVI: LIST OF STRAINS (continued)

OK0768	*unc-119(ed3);* cuEx616 Extrachromosomal array generated by transforming *unc-119* worms with pOK 271.*16 [pceh-28::3X FLAG::PABP*] using micro particle bombardment	5
OK0770	*cuEx617* Extrachromosomal array containing 10 ng/µl of pOK272.06 *[dbl-1 M4* enhancer*]* and 100 ng/µl of pRF4	3
OK0771	*cuEx618* Extrachromosomal array containing 10 ng/µl of pOK274.19 (HindIII-NheI fragment of the *dbl-1* promoter containing bp 13,502-15,284 of cosmid T25f10) and100ng/µl ofpRF4	3
OK0772	*cuEx619* Extrachromosomal array containing 10 ng/ µl of pOK277.01(M4 enhancer -$^{825\ mut}$) and 100 ng/µl of pRF4	2,3
OK0773	*cuEx620* Extrachromosomal array containing 10 ng/ µl of pOK277.01(M4 enhancer -$^{825\ mut}$) and 100 ng/µl of pRF4	2
OK0774	*cuEx623* Extrachromosomal array containing 10 ng/µl of pOK277.03 (M4 enhancer -$^{738\ mut}$) and 100 ng/ µl of pRF4	2,3
OK0775	*cuEx623* Extrachromosomal array containing 10 ng/µl of pOK277.03 (M4 enhancer -$^{738\ mut}$) and 100 ng/µl of pRF4	2
OK0776	*cuEx623* Extrachromosomal array containing 10 ng/µl of pOK277.03 (M4 enhancer -$^{738\ mut}$) and 100 ng/µl of pRF4	2
OK0777	*cuEx624* Extrachromosomal array containing 10 ng/µl of pOK277.03 (M4 enhancer -$^{738\ mut}$) and	2

APPENDIX G: TABLE XVI: LIST OF STRAINS (continued)

	100 ng/µl of pRF4	
OK0778	*cuEx625* Extrachromosomal array containing 10 ng/µl of pOK277.05 (M4 enhancer $^{\text{double mut)}}$and 100 ng/µl of pRF4	2
OK0779	*cuEx626* Extrachromosomal array containing 10 ng/µl of pOK277.05 (M4 enhancer $^{\text{double mut)}}$and 100 ng/µl of pRF4	2
OK0780	*cuEx628* Extrachromosomal array containing 10 ng/µl of pOK277.05 (M4 enhancer $^{\text{double mut)}}$and 100 ng/µl of pRF4	2,3
OK0782	*cuEx629* Extrachromosomal array containing 10 ng/µl of pOK275.01(the CEH-28 binding site at -738 bp is mutated in the -3061Δ *dbl-1* promoter) and 100ng/µl of pRF4	Appendix A
OK0783	*cuEx630* Extrachromosomal array containing 10 ng/µl of pOK272.04(full length *dbl-1* promoter in which the CEH-28 site at -825 is mutated) and 100ng/µl of pRF4	Appendix A
OK0792	*dbl-1(ev580); Ex[C49G7.4::YFP] dbl-1* mutants expressing the gland cell reporter *phat-1::yfp*	2,3
OK0793	*unc-119(ed3); cuIs30[ser7b::3XFLAG::PABP] unc-119(ed3)* worms carrying pOK271.13 (*ser-7b* promoter driving expression of FLAG tagged PolyA Binding Protein (PABP) obtained by micro particle bombardment)	5
OK0828	*cuIs30; ceh-28(cu11) X ceh-28(cu11)* mutants expressing the *cuIs30* transgene. Obtained by crossing *ceh-28* mutants with the *cuIs30* transgenic worms.	5

APPENDIX G: TABLE XVI: LIST OF STRAINS (continued)

OK0829	*cuEx658* Extrachromosomal array containing 5 ng/ µl pOK264.09 (-3764Δ) and 100 ng/ µl of pRF4.	2
OK0830	*cuEx659* Extrachromosomal array containing 5 ng/ µl pOK264.09 (-3764Δ) and 100 ng/ µl of pRF4.	2,3
OK0831	*cuEx660* Extrachromosomal array containing 5 ng/ µl pOK264.09 (-3764Δ) and 100 ng/ µl of pRF4.	2
OK0832	*cuEx661* Extrachromosomal array containing 5 ng/ µl pOK264.09 (-3764Δ) and 100 ng/ µl of pRF4.	2
OK0833	*cuEx662* Extrachromosomal array containing 5 ng/ µl pOK264.01 (-3061 Δ) and 100ng/ µl of pRF4.	2,3
OK0834	*cuEx663* Extrachromosomal array containing 5 ng/ µl pOK264.01 (-3061 Δ) and 100ng/ µl of pRF4	2
OK0835	*cuEx664* Extrachromosomal array containing 5ng/ µl pOK264.01 (-3061 Δ) and 100ng/ µl of pRF4	2
OK0836	*cuEx665* Extrachromosomal array containing 5ng/ µl pOK264.03 (-2472 Δ) and 100ng/ µl of pRF4	2
OK0837	*cuEx666* Extrachromosomal array containing 5ng/ µl pOK264.03 (-2472 Δ deletion) and 100ng/ µl of pRF4	2,3
OK0838	*cuEx667* Extrachromosomal array containing 5ng/ µl pOK264.07(-1278 Δ) and 100ng/ µl of pRF4	2

APPENDIX G: TABLE XVI: LIST OF STRAINS (continued)

OK0839	*cuEx668* Extrachromosomal array containing 5ng/ µl pOK264.07 (-1278 Δ) and 100ng/ µl of pRF4	2.3
OK0840	*cuEx669* Extrachromosomal array containing 5ng/ µl pOK264.07(-1278 Δ) and 100ng/ µl of pRF4	2
OK0842	*cuEx671* Extrachromosomal array containing 5ng/ µl pOK264.05 (-646 Δ) and 100ng/ µl of pRF4	2,3
OK0859	*ceh-28(cu11); cuEx611* ceh-28(cu11) mutant worms carrying the *cuEx611[ser-7b::dbl-1;phat-3::yfp]* array.	2,3
OK0944	*nIs177 I; ceh-28(cu11) ceh-28(cu11)* mutants carrying the *ceh-28::4XNLS*::*gfp* marker	Appendix B, C
OK0973	*unc-31(e928); ivIs12 unc-31(e928)* mutants expressing the *phat-1::yfp* gland cell reporter	2,3
OK0974	*wgIs83; ceh-28(cu11) ceh-28 (cu11)* mutants expressing *zag-1:* gfp	4
OK0975	*cuEx793[egl-17 M4 enhancer].* Strain constructed by injecting 10 ng/µl of pOK293.01 and 100 ng/µl of pRF4. This strain shows enhancer activity in M4	4
OK0976	*ceh-28(cu11)*; *cuEx793* Strain constructed by crossing the *cuEx793[egl-17 M4 enhancer]* into *ceh-28(cu11)* mutants.	4
OK0977	*ivIs12 [phat-1::yfp ;elt-2::gfp; rol-6(su1006)]* Integrated rolling array expressing *phat-1::yfp* in a wild-type background.	3
OK0978	*ayIs4; ceh-28(cu11) ceh-28(cu11)* mutants expressing the *ayIs4[egl-17::gfp]* transgene.	4
OK0979	*ynIs49 V; ceh-28(cu11) X* Strain constructed by crossing *Pflp-5::gfp* into *ceh-28(cu11)* mutants.	4

APPENDIX G: TABLE XVI: LIST OF STRAINS (continued)

OK0980	*ynIs57 III; ceh-28(cu11) X* Strain constructed by crossing *flp-2::gfp* into *ceh-28(cu11)* mutants	4
OK1013	*ynIs80/+; ceh-28(cu11) ceh-28(cu11)* worms carrying the *ynIs80[flp-21::gfp]* transgene. Worms are heterozygous for *flp-21*. Pick transgenic worms by examining them under dissecting scope	4
OK1014	*daf-8(e1393) I; ivIs12 II* /+ daf-8 mutants expressing the *phat-1::yfp* gland cell reporter. Passage rollers and maintain at 16°C. Dauer constitutive at 25°C. Strain is heterozygous for *ivIs12.*	3
OK1015	*daf-14(m77) IV; ivIs12 II/+ daf-14* mutants expressing the *phat-1::yfp* gland cell reporter. Passage rollers and maintain at 16C. Dauer constitutive at 25°C. Strain is heterozygous for *ivIs12*	3
OK1016	*daf-3(mg90) X; ivEx[phat-3::yfp]*	3
OK1017	*sma-4(e729) III; ivIs12 II*	3
OP83	*unc-119(ed3) III; wgIs83[zag-1::TY1::EGFP::3xFLAG(92C12) + unc-119(+)]* Strain expressing *zag-1::gfp* fosmid. Obtained from Caenorhabditis Genetics Center	4
RB1588	*mxl-3(ok1947) X mxl-3* mutant obtained from the Caenorhabditis Genetics Center	Appendix D
RB844	*CO6C6.5(ok671) V nhr-50* mutant obtained from the Caenorhabditis Genetics Center	Appendix D
VC2490	*WO7E11.1; flp-2(gk1039) X flp-2* mutant obtained from CGC. This strain grows normally and does not have any gross feeding defects	4

APPENDIX G: TABLE XVI: LIST OF STRAINS (continued)

VC3280	*F15A4.5(gk3259) II; flp-5(gk3123) X flp-5* mutant obtained from the CGC. Strain grows and feeds normally	4
VC496	*nhr-3(gk258) X* nhr-3 mutant obtained from the Caenorhabditis Genetics Center	Appendix D
VH514	*zag-1(hd16)/ unc-17(e113) dpy-13(e184) IV zag-1(hd16*) mutants balanced over *unc-17(e113) dpy-13(e184)*. Strain obtained from Dr. Harald Hutter's lab. *zag-1(hd16)* homozygotes arrest as L1 larvae. They have a stuffed pharynx and are severely uncoordinated in motion. They also completely lack isthmus peristalsis.	4

7.8 **Appendix H Copyright**

ELSEVIER LICENSE
TERMS AND CONDITIONS

May 24, 2014

This is a License Agreement between Kalpana Ramakrishnan ("You") and Elsevier ("Elsevier") provided by Copyright Clearance Center ("CCC"). The license consists of your order details, the terms and conditions provided by Elsevier, and the payment terms and conditions.

All payments must be made in full to CCC. For payment instructions, please see information listed at the bottom of this form.

Supplier	Elsevier Limited The Boulevard,Langford Lane Kidlington,Oxford,OX5 1GB,UK
Registered Company Number	1982084
Customer name	Kalpana Ramakrishnan
Customer address	900 S Ashland Avenue, CHICAGO, IL 60612
License number	3395511409532
License date	May 24, 2014
Licensed content publisher	Elsevier
Licensed content publication	Developmental Biology
Licensed content title	CEH-28 activates*dbl-1*expression and TGF-β signaling in the*C. elegans*M4 neuron
Licensed content author	Kalpana Ramakrishnan,Paramita Ray,Peter G. Okkema
Licensed content date	15 June 2014
Licensed content volume number	390
Licensed content issue number	2
Number of pages	11
Start Page	149
End Page	159
Type of Use	reuse in a thesis/dissertation
Intended publisher of new work	other

APPENDIX H: COPYRIGHT (Continued)

Portion	figures/tables/illustrations
Number of figures/tables/illustrations	All
Actual number of figures/tables/illustrations	11
Format	both print and electronic
Are you the author of this Elsevier article?	Yes
Will you be translating?	No
Title of your thesis/dissertation	CEH-28 and ZAG-1 function in regulating differentiation of the *C. elegans* M4 pharyngeal neuron
Expected completion date	May 2014
Estimated size (number of pages)	250
Elsevier VAT number	GB 494 6272 12
Permissions price	0.00 USD
VAT/Local Sales Tax	0.00 USD / 0.00 GBP
Total	0.00 USD

Terms and Conditions

INTRODUCTION

1. The publisher for this copyrighted material is Elsevier. By clicking "accept" in connection with completing this licensing transaction, you agree that the following terms and conditions apply to this transaction (along with the Billing and Payment terms and conditions established by Copyright Clearance Center, Inc. ("CCC"), at the time that you opened your Rightslink account and that are available at any time at http://myaccount.copyright.com).

GENERAL TERMS

2. Elsevier hereby grants you permission to reproduce the aforementioned material subject to the terms and conditions indicated.

3. Acknowledgement: If any part of the material to be used (for example, figures) has appeared in our publication with credit or acknowledgement to another source, permission must also be sought from that source. If such permission is not obtained then that material may not be included in your publication/copies. Suitable acknowledgement to the source must be made, either as a footnote or in a reference list at the end of your publication, as follows:

“Reprinted from Publication title, Vol /edition number, Author(s), Title of article / title of chapter, Pages No., Copyright (Year), with permission from Elsevier [OR APPLICABLE SOCIETY COPYRIGHT OWNER].” Also Lancet special credit - “Reprinted from The

APPENDIX H: COPYRIGHT (Continued)

Lancet, Vol. number, Author(s), Title of article, Pages No., Copyright (Year), with permission from Elsevier."

4. Reproduction of this material is confined to the purpose and/or media for which permission is hereby given.

5. Altering/Modifying Material: Not Permitted. However figures and illustrations may be altered/adapted minimally to serve your work. Any other abbreviations, additions, deletions and/or any other alterations shall be made only with prior written authorization of Elsevier Ltd. (Please contact Elsevier at permissions@elsevier.com)

6. If the permission fee for the requested use of our material is waived in this instance, please be advised that your future requests for Elsevier materials may attract a fee.

7. Reservation of Rights: Publisher reserves all rights not specifically granted in the combination of (i) the license details provided by you and accepted in the course of this licensing transaction, (ii) these terms and conditions and (iii) CCC's Billing and Payment terms and conditions.

8. License Contingent Upon Payment: While you may exercise the rights licensed immediately upon issuance of the license at the end of the licensing process for the transaction, provided that you have disclosed complete and accurate details of your proposed use, no license is finally effective unless and until full payment is received from you (either by publisher or by CCC) as provided in CCC's Billing and Payment terms and conditions. If full payment is not received on a timely basis, then any license preliminarily granted shall be deemed automatically revoked and shall be void as if never granted. Further, in the event that you breach any of these terms and conditions or any of CCC's Billing and Payment terms and conditions, the license is automatically revoked and shall be void as if never granted. Use of materials as described in a revoked license, as well as any use of the materials beyond the scope of an unrevoked license, may constitute copyright infringement and publisher reserves the right to take any and all action to protect its copyright in the materials.

9. Warranties: Publisher makes no representations or warranties with respect to the licensed material.

10. Indemnity: You hereby indemnify and agree to hold harmless publisher and CCC, and their respective officers, directors, employees and agents, from and against any and all claims arising out of your use of the licensed material other than as specifically authorized pursuant to this license.

11. No Transfer of License: This license is personal to you and may not be sublicensed, assigned, or transferred by you to any other person without publisher's written permission.

12. No Amendment Except in Writing: This license may not be amended except in a writing signed by both parties (or, in the case of publisher, by CCC on publisher's behalf).

13. Objection to Contrary Terms: Publisher hereby objects to any terms contained in any purchase order, acknowledgment, check endorsement or other writing prepared by you,

APPENDIX H: COPYRIGHT (Continued)

which terms are inconsistent with these terms and conditions or CCC's Billing and Payment terms and conditions. These terms and conditions, together with CCC's Billing and Payment terms and conditions (which are incorporated herein), comprise the entire agreement between you and publisher (and CCC) concerning this licensing transaction. In the event of any conflict between your obligations established by these terms and conditions and those established by CCC's Billing and Payment terms and conditions, these terms and conditions shall control.

14. Revocation: Elsevier or Copyright Clearance Center may deny the permissions described in this License at their sole discretion, for any reason or no reason, with a full refund payable to you. Notice of such denial will be made using the contact information provided by you. Failure to receive such notice will not alter or invalidate the denial. In no event will Elsevier or Copyright Clearance Center be responsible or liable for any costs, expenses or damage incurred by you as a result of a denial of your permission request, other than a refund of the amount(s) paid by you to Elsevier and/or Copyright Clearance Center for denied permissions.

LIMITED LICENSE

The following terms and conditions apply only to specific license types:

15. **Translation**: This permission is granted for non-exclusive world **English** rights only unless your license was granted for translation rights. If you licensed translation rights you may only translate this content into the languages you requested. A professional translator must perform all translations and reproduce the content word for word preserving the integrity of the article. If this license is to re-use 1 or 2 figures then permission is granted for non-exclusive world rights in all languages.

16. **Posting licensed content on any Website**: The following terms and conditions apply as follows: Licensing material from an Elsevier journal: All content posted to the web site must maintain the copyright information line on the bottom of each image; A hyper-text must be included to the Homepage of the journal from which you are licensing athttp://www.sciencedirect.com/science/journal/xxxxx or the Elsevier homepage for books athttp://www.elsevier.com; Central Storage: This license does not include permission for a scanned version of the material to be stored in a central repository such as that provided by Heron/XanEdu.

Licensing material from an Elsevier book: A hyper-text link must be included to the Elsevier homepage at http://www.elsevier.com . All content posted to the web site must maintain the copyright information line on the bottom of each image.

Posting licensed content on Electronic reserve: In addition to the above the following clauses are applicable: The web site must be password-protected and made available only to bona fide students registered on a relevant course. This permission is granted for 1 year only. You may obtain a new license for future website posting.

For journal authors: the following clauses are applicable in addition to the above:

APPENDIX H: COPYRIGHT (Continued)

Permission granted is limited to the author accepted manuscript version* of your paper.

***Accepted Author Manuscript (AAM) Definition:** An accepted author manuscript (AAM) is the author's version of the manuscript of an article that has been accepted for publication and which may include any author-incorporated changes suggested through the processes of submission processing, peer review, and editor-author communications. AAMs do not include other publisher value-added contributions such as copy-editing, formatting, technical enhancements and (if relevant) pagination.

You are not allowed to download and post the published journal article (whether PDF or HTML, proof or final version), nor may you scan the printed edition to create an electronic version. A hyper-text must be included to the Homepage of the journal from which you are licensing athttp://www.sciencedirect.com/science/journal/xxxxx. As part of our normal production process, you will receive an e-mail notice when your article appears on Elsevier's online service ScienceDirect (www.sciencedirect.com). That e-mail will include the article's Digital Object Identifier (DOI). This number provides the electronic link to the published article and should be included in the posting of your personal version. We ask that you wait until you receive this e-mail and have the DOI to do any posting.

Posting to a repository: Authors may post their AAM immediately to their employer's institutional repository for internal use only and may make their manuscript publically available after the journal-specific embargo period has ended.

Please also refer to Elsevier's Article Posting Policy for further information.

18. **For book authors** the following clauses are applicable in addition to the above: Authors are permitted to place a brief summary of their work online only.. You are not allowed to download and post the published electronic version of your chapter, nor may you scan the printed edition to create an electronic version. **Posting to a repository:** Authors are permitted to post a summary of their chapter only in their institution's repository.

20. **Thesis/Dissertation**: If your license is for use in a thesis/dissertation your thesis may be submitted to your institution in either print or electronic form. Should your thesis be published commercially, please reapply for permission. These requirements include permission for the Library and Archives of Canada to supply single copies, on demand, of the complete thesis and include permission for UMI to supply single copies, on demand, of the complete thesis. Should your thesis be published commercially, please reapply for permission.

Elsevier Open Access Terms and Conditions

Elsevier publishes Open Access articles in both its Open Access journals and via its Open Access articles option in subscription journals.

Authors publishing in an Open Access journal or who choose to make their article Open Access in an Elsevier subscription journal select one of the following Creative Commons

APPENDIX H: COPYRIGHT (Continued)

user licenses, which define how a reader may reuse their work: Creative Commons Attribution License (CC BY), Creative Commons Attribution – Non Commercial - ShareAlike (CC BY NC SA) and Creative Commons Attribution – Non Commercial – No Derivatives (CC BY NC ND)

Terms & Conditions applicable to all Elsevier Open Access articles:

Any reuse of the article must not represent the author as endorsing the adaptation of the article nor should the article be modified in such a way as to damage the author's honour or reputation.

The author(s) must be appropriately credited.

If any part of the material to be used (for example, figures) has appeared in our publication with credit or acknowledgement to another source it is the responsibility of the user to ensure their reuse complies with the terms and conditions determined by the rights holder.

Additional Terms & Conditions applicable to each Creative Commons user license:

CC BY: You may distribute and copy the article, create extracts, abstracts, and other revised versions, adaptations or derivative works of or from an article (such as a translation), to include in a collective work (such as an anthology), to text or data mine the article, including for commercial purposes without permission from Elsevier

CC BY NC SA: For non-commercial purposes you may distribute and copy the article, create extracts, abstracts and other revised versions, adaptations or derivative works of or from an article (such as a translation), to include in a collective work (such as an anthology), to text and data mine the article and license new adaptations or creations under identical terms without permission from Elsevier

CC BY NC ND: For non-commercial purposes you may distribute and copy the article and include it in a collective work (such as an anthology), provided you do not alter or modify the article, without permission from Elsevier

Any commercial reuse of Open Access articles published with a CC BY NC SA or CC BY NC ND license requires permission from Elsevier and will be subject to a fee.

Commercial reuse includes:

- Promotional purposes (advertising or marketing)
- Commercial exploitation (e.g. a product for sale or loan)
- Systematic distribution (for a fee or free of charge)

Please refer to Elsevier's Open Access Policy for further information.

APPENDIX H: COPYRIGHT (Continued)

21. **Other Conditions**:

v1.7

If you would like to pay for this license now, please remit this license along with your payment made payable to "COPYRIGHT CLEARANCE CENTER" otherwise you will be invoiced within 48 hours of the license date. Payment should be in the form of a check or money order referencing your account number and this invoice number 501311350.
Once you receive your invoice for this order, you may pay your invoice by credit card. Please follow instructions provided at that time.

Make Payment To:
Copyright Clearance Center
Dept 001
P.O. Box 843006
Boston, MA 02284-3006

For suggestions or comments regarding this order, contact RightsLink Customer Support:customercare@copyright.com or +1-877-622-5543 (toll free in the US) or +1-978-646-2777.

Gratis licenses (referencing $0 in the Total field) are free. Please retain this printable license for your reference. No payment is required.

APPENDIX H: COPYRIGHT (Continued)

This is a License Agreement between Kalpana Ramakrishnan ("You") and Springer ("Springer") provided by Copyright Clearance Center ("CCC"). The license consists of your order details, the terms and conditions provided by Springer, and the payment terms and conditions.

All payments must be made in full to CCC. For payment instructions, please see information listed at the bottom of this form.

License Number	3434250488816
License date	Jul 22, 2014
Order Content Publisher	Springer
Order Content Publication	Cellular and Molecular Life Sciences
Order Content Title	Evolutionary functional analysis and molecular regulation of the ZEB transcription factors
Order Content Author	Alexander Gheldof
Order Content Date	Jan 1, 2012
Volume number	69
Issue number	15
Type of Use	Thesis/Dissertation
Portion	Figures
Author of this Springer article	No
Order reference number	None
Original figure numbers	1-5
Title of your thesis / dissertation	CEH-28 and ZAG-1 function in regulating differentiation of the C. elegans M4 pharyngeal neuron
Expected completion date	Jul 2014
Estimated size(pages)	212
Total	**0.00 USD**

APPENDIX H: COPYRIGHT (Continued)

Terms and Conditions

Introduction
The publisher for this copyrighted material is Springer Science + Business Media. By clicking "accept" in connection with completing this licensing transaction, you agree that the following terms and conditions apply to this transaction (along with the Billing and Payment terms and conditions established by Copyright Clearance Center, Inc. ("CCC"), at the time that you opened your Rightslink account and that are available at any time at http://myaccount.copyright.com).

Limited License
With reference to your request to reprint in your thesis material on which Springer Science and Business Media control the copyright, permission is granted, free of charge, for the use indicated in your enquiry.

Licenses are for one-time use only with a maximum distribution equal to the number that you identified in the licensing process.

This License includes use in an electronic form, provided its password protected or on the university's intranet or repository, including UMI (according to the definition at the Sherpa website: http://www.sherpa.ac.uk/romeo/). For any other electronic use, please contact Springer at (permissions.dordrecht@springer.com or permissions.heidelberg@springer.com).

The material can only be used for the purpose of defending your thesis limited to university-use only. If the thesis is going to be published, permission needs to be re-obtained (selecting "book/textbook" as the type of use).

Although Springer holds copyright to the material and is entitled to negotiate on rights, this license is only valid, subject to a courtesy information to the author (address is given with the article/chapter) and provided it concerns original material which does not carry references to other sources (if material in question appears with credit to another source, authorization from that source is required as well).

Permission free of charge on this occasion does not prejudice any rights we might have to charge for reproduction of our copyrighted material in the future.

Altering/Modifying Material: Not Permitted
You may not alter or modify the material in any manner. Abbreviations, additions, deletions and/or any other alterations shall be made only with prior written authorization of the author(s) and/or Springer Science + Business Media. (Please contact Springer at (permissions.dordrecht@springer.com or permissions.heidelberg@springer.com)

Reservation of Rights
Springer Science + Business Media reserves all rights not specifically granted in the combination of (i) the license details provided by you and accepted in the course of this licensing transaction, (ii) these terms and conditions and (iii) CCC's Billing and Payment terms and conditions.

APPENDIX H: COPYRIGHT (Continued)

Copyright Notice:Disclaimer
You must include the following copyright and permission notice in connection with any reproduction of the licensed material: "Springer and the original publisher /journal title, volume, year of publication, page, chapter/article title, name(s) of author(s), figure number(s), original copyright notice) is given to the publication in which the material was originally published, by adding; with kind permission from Springer Science and Business Media"

Warranties: None

Example 1: Springer Science + Business Media makes no representations or warranties with respect to the licensed material.

Example 2: Springer Science + Business Media makes no representations or warranties with respect to the licensed material and adopts on its own behalf the limitations and disclaimers established by CCC on its behalf in its Billing and Payment terms and conditions for this licensing transaction.

Indemnity
You hereby indemnify and agree to hold harmless Springer Science + Business Media and CCC, and their respective officers, directors, employees and agents, from and against any and all claims arising out of your use of the licensed material other than as specifically authorized pursuant to this license.

No Transfer of License
This license is personal to you and may not be sublicensed, assigned, or transferred by you to any other person without Springer Science + Business Media's written permission.

No Amendment Except in Writing
This license may not be amended except in a writing signed by both parties (or, in the case of Springer Science + Business Media, by CCC on Springer Science + Business Media's behalf).

Objection to Contrary Terms
Springer Science + Business Media hereby objects to any terms contained in any purchase order, acknowledgment, check endorsement or other writing prepared by you, which terms are inconsistent with these terms and conditions or CCC's Billing and Payment terms and conditions. These terms and conditions, together with CCC's Billing and Payment terms and conditions (which are incorporated herein), comprise the entire agreement between you and Springer Science + Business Media (and CCC) concerning this licensing transaction. In the event of any conflict between your obligations established by these terms and conditions and those established by CCC's Billing and Payment terms and conditions, these terms and conditions shall control.

Jurisdiction
All disputes that may arise in connection with this present License, or the breach thereof, shall be settled exclusively by arbitration, to be held in The Netherlands, in accordance with Dutch law, and to be conducted under the Rules of the 'Netherlands Arbitrage Instituut' (Netherlands Institute of Arbitration).***OR:***

APPENDIX H: COPYRIGHT (Continued)

All disputes that may arise in connection with this present License, or the breach thereof, shall be settled exclusively by arbitration, to be held in the Federal Republic of Germany, in accordance with German law.

Other terms and conditions:

v1.3

If you would like to pay for this license now, please remit this license along with your payment made payable to "COPYRIGHT CLEARANCE CENTER" otherwise you will be invoiced within 48 hours of the license date. Payment should be in the form of a check or money order referencing your account number and this invoice number None501358175. Once you receive your invoice for this order, you may pay your invoice by credit card. Please follow instructions provided at that time.

Make Payment To:
Copyright Clearance Center
Dept 001
P.O. Box 843006
Boston, MA 02284-3006

For suggestions or comments regarding this order, contact RightsLink Customer Support:customercare@copyright.com or +1-877-622-5543 (toll free in the US) or +1-978-646-2777.

Gratis licenses (referencing $0 in the Total field) are free. Please retain this printable license for your reference. No payment is required.

CITED LITERATURE

Aigner, K., L. Descovich, M. Mikula, A. Sultan, B. Dampier, S. Bonne, F. van Roy, W. Mikulits, M. Schreiber, T. Brabletz, W. Sommergruber, N. Schweifer, A. Wernitznig, H. Beug, R. Foisner, and A. Eger. 2007. "The transcription factor ZEB1 (deltaEF1) represses Plakophilin 3 during human cancer progression." *FEBS Lett* 581 (8):1617-24. doi: 10.1016/j.febslet.2007.03.026.

Albert, P. S., and D. L. Riddle. 1988. "Mutants of Caenorhabditis elegans that form dauer-like larvae." *Dev Biol* 126 (2):270-93.

Albertson, D. G., and J. N. Thomson. 1976. "The pharynx of Caenorhabditis elegans." *Philos Trans R Soc Lond B Biol Sci* 275 (938):299-325.

Alfonso, A., K. Grundahl, J. S. Duerr, H. P. Han, and J. B. Rand. 1993. "The Caenorhabditis elegans unc-17 gene: a putative vesicular acetylcholine transporter." *Science* 261 (5121):617-9.

Ardiel, E. L., and C. H. Rankin. 2010. "An elegant mind: learning and memory in Caenorhabditis elegans." *Learn Mem* 17 (4):191-201. doi: 10.1101/lm.960510.

Ashrafi, K. 2007. "Obesity and the regulation of fat metabolism." *WormBook*:1-20. doi: 10.1895/wormbook.1.130.1.

Ausubel, Frederick M. 1990. *Current protocols in molecular biology*. New York: Greene Pub. Associates and Wiley-Interscience : J. Wiley.

Avery, L., C. I. Bargmann, and H. R. Horvitz. 1993. "The Caenorhabditis elegans unc-31 gene affects multiple nervous system-controlled functions." *Genetics* 134 (2):455-64.

Avery, L., and H. R. Horvitz. 1987. "A cell that dies during wild-type C. elegans development can function as a neuron in a ced-3 mutant." *Cell* 51 (6):1071-8.

Avery, L., and H. R. Horvitz. 1989. "Pharyngeal pumping continues after laser killing of the pharyngeal nervous system of C. elegans." *Neuron* 3 (4):473-85.

Avery, L., and J. H. Thomas. 1997a. "Feeding and Defecation." In *C. elegans II*, edited by D. L. Riddle, T. Blumenthal, B. J. Meyer and J. R. Priess. Cold Spring Harbor (NY).

Avery, L., and J. H. Thomas. 1997b. "Feeding and Defecation." In *C. elegans II*, edited by D. L. Riddle, T. Blumenthal, B. J. Meyer and J. R. Priess, 679716. Cold Spring Harbor, NY: Cold Spring Harbor Laboratory Press.

Avery, L., and Y. J. You. 2012. "C. elegans feeding." *WormBook*:1-23. doi: 10.1895/wormbook.1.150.1.

Ballas, N., E. Battaglioli, F. Atouf, M. E. Andres, J. Chenoweth, M. E. Anderson, C. Burger, M. Moniwa, J. R. Davie, W. J. Bowers, H. J. Federoff, D. W. Rose, M. G. Rosenfeld, P. Brehm, and G. Mandel. 2001. "Regulation of neuronal traits by a novel transcriptional complex." *Neuron* 31 (3):353-65.

Bannister, A. J., and T. Kouzarides. 1996. "The CBP co-activator is a histone acetyltransferase." *Nature* 384 (6610):641-3. doi: 10.1038/384641a0.

Bartus, R. T., R. L. Dean, 3rd, B. Beer, and A. S. Lippa. 1982. "The cholinergic hypothesis of geriatric memory dysfunction." *Science* 217 (4558):408-14.

Berger, M. F., A. A. Philippakis, A. M. Qureshi, F. S. He, P. W. Estep, 3rd, and M. L. Bulyk. 2006. "Compact, universal DNA microarrays to comprehensively determine transcription-factor binding site specificities." *Nat Biotechnol* 24 (11):1429-35. doi: 10.1038/nbt1246.

Bianchi, L., and M. Driscoll. 2006. "Culture of embryonic C. elegans cells for electrophysiological and pharmacological analyses." *WormBook*:1-15. doi: 10.1895/wormbook.1.122.1.

Boulin, T., J. F. Etchberger, and O. Hobert. 2006. "Reporter gene fusions." *WormBook*:1-23. doi: 10.1895/wormbook.1.106.1.

Brenner, S. 1974. "The genetics of Caenorhabditis elegans." *Genetics* 77 (1):71-94.

CITED LITERATURE (continued)

Briscoe, J., and J. Ericson. 2001. "Specification of neuronal fates in the ventral neural tube." *Curr Opin Neurobiol* 11 (1):43-9.

Briscoe, J., A. Pierani, T. M. Jessell, and J. Ericson. 2000. "A homeodomain protein code specifies progenitor cell identity and neuronal fate in the ventral neural tube." *Cell* 101 (4):435-45.

Briscoe, J., L. Sussel, P. Serup, D. Hartigan-O'Connor, T. M. Jessell, J. L. Rubenstein, and J. Ericson. 1999. "Homeobox gene Nkx2.2 and specification of neuronal identity by graded Sonic hedgehog signalling." *Nature* 398 (6728):622-7. doi: 10.1038/19315.

Broihier, H. T., L. A. Moore, M. Van Doren, S. Newman, and R. Lehmann. 1998. "zfh-1 is required for germ cell migration and gonadal mesoderm development in Drosophila." *Development* 125 (4):655-66.

Burdine, R. D., C. S. Branda, and M. J. Stern. 1998. "EGL-17(FGF) expression coordinates the attraction of the migrating sex myoblasts with vulval induction in C. elegans." *Development* 125 (6):1083-93.

Burdine, R. D., E. B. Chen, S. F. Kwok, and M. J. Stern. 1997. "egl-17 encodes an invertebrate fibroblast growth factor family member required specifically for sex myoblast migration in Caenorhabditis elegans." *Proc Natl Acad Sci U S A* 94 (6):2433-7.

Burgoyne, R. D., and A. Morgan. 2003. "Secretory granule exocytosis." *Physiol Rev* 83 (2):581-632. doi: 10.1152/physrev.00031.2002.

Cacheux, V., F. Dastot-Le Moal, H. Kaariainen, N. Bondurand, R. Rintala, B. Boissier, M. Wilson, D. Mowat, and M. Goossens. 2001. "Loss-of-function mutations in SIP1 Smad interacting protein 1 result in a syndromic Hirschsprung disease." *Hum Mol Genet* 10 (14):1503-10.

Calixto, A., D. Chelur, I. Topalidou, X. Chen, and M. Chalfie. 2010. "Enhanced neuronal RNAi in C. elegans using SID-1." *Nat Methods* 7 (7):554-9. doi: 10.1038/nmeth.1463.

Cassada, R. C., and R. L. Russell. 1975. "The dauerlarva, a post-embryonic developmental variant of the nematode Caenorhabditis elegans." *Dev Biol* 46 (2):326-42.

Christensen, M., A. Estevez, X. Yin, R. Fox, R. Morrison, M. McDonnell, C. Gleason, D. M. Miller, 3rd, and K. Strange. 2002. "A primary culture system for functional analysis of C. elegans neurons and muscle cells." *Neuron* 33 (4):503-14.

Chua, H. L., P. Bhat-Nakshatri, S. E. Clare, A. Morimiya, S. Badve, and H. Nakshatri. 2007. "NF-kappaB represses E-cadherin expression and enhances epithelial to mesenchymal transition of mammary epithelial cells: potential involvement of ZEB-1 and ZEB-2." *Oncogene* 26 (5):711-24. doi: 10.1038/sj.onc.1209808.

Clark, S. G., and C. Chiu. 2003. "C. elegans ZAG-1, a Zn-finger-homeodomain protein, regulates axonal development and neuronal differentiation." *Development* 130 (16):3781-94.

Colon-Ramos, D. A., M. A. Margeta, and K. Shen. 2007. "Glia promote local synaptogenesis through UNC-6 (netrin) signaling in C. elegans." *Science* 318 (5847):103-6. doi: 10.1126/science.1143762.

Comijn, J., G. Berx, P. Vermassen, K. Verschueren, L. van Grunsven, E. Bruyneel, M. Mareel, D. Huylebroeck, and F. van Roy. 2001. "The two-handed E box binding zinc finger protein SIP1 downregulates E-cadherin and induces invasion." *Mol Cell* 7 (6):1267-78.

Conti-Fine, B. M., M. Milani, and H. J. Kaminski. 2006. "Myasthenia gravis: past, present, and future." *J Clin Invest* 116 (11):2843-54. doi: 10.1172/JCI29894.

Costantino, M. E., R. P. Stearman, G. E. Smith, and D. S. Darling. 2002. "Cell-specific phosphorylation of Zfhep transcription factor." *Biochem Biophys Res Commun* 296 (2):368-73.

Crump, J. G., M. Zhen, Y. Jin, and C. I. Bargmann. 2001. "The SAD-1 kinase regulates presynaptic vesicle clustering and axon termination." *Neuron* 29 (1):115-29.

CITED LITERATURE (continued)

Cui, M., and M. Han. 2003. "Cis regulatory requirements for vulval cell-specific expression of the Caenorhabditis elegans fibroblast growth factor gene egl-17." *Dev Biol* 257 (1):104-16.

Dalla Torre di Sanguinetto, S. A., J. S. Dasen, and S. Arber. 2008. "Transcriptional mechanisms controlling motor neuron diversity and connectivity." *Curr Opin Neurobiol* 18 (1):36-43. doi: 10.1016/j.conb.2008.04.002.

Dastot-Le Moal, F., M. Wilson, D. Mowat, N. Collot, F. Niel, and M. Goossens. 2007. "ZFHX1B mutations in patients with Mowat-Wilson syndrome." *Hum Mutat* 28 (4):313-21. doi: 10.1002/humu.20452.

De Marco Garcia, N. V., and T. M. Jessell. 2008. "Early motor neuron pool identity and muscle nerve trajectory defined by postmitotic restrictions in Nkx6.1 activity." *Neuron* 57 (2):217-31. doi: 10.1016/j.neuron.2007.11.033.

Dennler, S., M. J. Goumans, and P. ten Dijke. 2002. "Transforming growth factor beta signal transduction." *J Leukoc Biol* 71 (5):731-40.

Derynck, R., and R. J. Akhurst. 2007. "Differentiation plasticity regulated by TGF-beta family proteins in development and disease." *Nat Cell Biol* 9 (9):1000-4. doi: 10.1038/ncb434.

Dillner, N. B., and M. M. Sanders. 2004. "Transcriptional activation by the zinc-finger homeodomain protein delta EF1 in estrogen signaling cascades." *DNA Cell Biol* 23 (1):25-34. doi: 10.1089/104454904322745907.

Eger, A., K. Aigner, S. Sonderegger, B. Dampier, S. Oehler, M. Schreiber, G. Berx, A. Cano, H. Beug, and R. Foisner. 2005. "DeltaEF1 is a transcriptional repressor of E-cadherin and regulates epithelial plasticity in breast cancer cells." *Oncogene* 24 (14):2375-85. doi: 10.1038/sj.onc.1208429.

El Bejjani, R., and M. Hammarlund. 2012. "Neural regeneration in Caenorhabditis elegans." *Annu Rev Genet* 46:499-513. doi: 10.1146/annurev-genet-110711-155550.

Engel, M. E., M. A. McDonnell, B. K. Law, and H. L. Moses. 1999. "Interdependent SMAD and JNK signaling in transforming growth factor-beta-mediated transcription." *J Biol Chem* 274 (52):37413-20.

Estevez, M., L. Attisano, J. L. Wrana, P. S. Albert, J. Massague, and D. L. Riddle. 1993. "The daf-4 gene encodes a bone morphogenetic protein receptor controlling C. elegans dauer larva development." *Nature* 365 (6447):644-9. doi: 10.1038/365644a0.

Fernandez, A. P., J. Gibbons, and P. G. Okkema. 2004. "C. elegans peb-1 mutants exhibit pleiotropic defects in molting, feeding, and morphology." *Dev Biol* 276 (2):352-66. doi: 10.1016/j.ydbio.2004.08.040.

Fetissov, S. O., A. S. Jacoby, P. R. Brumovsky, J. Shine, T. P. Iismaa, and T. Hokfelt. 2003. "Altered hippocampal expression of neuropeptides in seizure-prone GALR1 knockout mice." *Epilepsia* 44 (8):1022-33.

Finney, M., and G. Ruvkun. 1990. "The unc-86 gene product couples cell lineage and cell identity in C. elegans." *Cell* 63 (5):895-905.

Fontemaggi, G., A. Gurtner, S. Strano, Y. Higashi, A. Sacchi, G. Piaggio, and G. Blandino. 2001. "The transcriptional repressor ZEB regulates p73 expression at the crossroad between proliferation and differentiation." *Mol Cell Biol* 21 (24):8461-70. doi: 10.1128/MCB.21.24.8461-8470.2001.

Fortini, M. E., Z. C. Lai, and G. M. Rubin. 1991. "The Drosophila zfh-1 and zfh-2 genes encode novel proteins containing both zinc-finger and homeodomain motifs." *Mech Dev* 34 (2-3):113-22.

Funahashi, J., R. Sekido, K. Murai, Y. Kamachi, and H. Kondoh. 1993. "Delta-crystallin enhancer binding protein delta EF1 is a zinc finger-homeodomain protein implicated in postgastrulation embryogenesis." *Development* 119 (2):433-46.

Gaudet, J., and S. E. Mango. 2002. "Regulation of organogenesis by the Caenorhabditis elegans FoxA protein PHA-4." *Science* 295 (5556):821-5. doi: 10.1126/science.1065175.

CITED LITERATURE (continued)

Genetta, T., D. Ruezinsky, and T. Kadesch. 1994. "Displacement of an E-box-binding repressor by basic helix-loop-helix proteins: implications for B-cell specificity of the immunoglobulin heavy-chain enhancer." *Mol Cell Biol* 14 (9):6153-63.

Gerstein, M. B., Z. J. Lu, E. L. Van Nostrand, C. Cheng, B. I. Arshinoff, T. Liu, K. Y. Yip, R. Robilotto, A. Rechtsteiner, K. Ikegami, P. Alves, A. Chateigner, M. Perry, M. Morris, R. K. Auerbach, X. Feng, J. Leng, A. Vielle, W. Niu, K. Rhrissorrakrai, A. Agarwal, R. P. Alexander, G. Barber, C. M. Brdlik, J. Brennan, J. J. Brouillet, A. Carr, M. S. Cheung, H. Clawson, S. Contrino, L. O. Dannenberg, A. F. Dernburg, A. Desai, L. Dick, A. C. Dose, J. Du, T. Egelhofer, S. Ercan, G. Euskirchen, B. Ewing, E. A. Feingold, R. Gassmann, P. J. Good, P. Green, F. Gullier, M. Gutwein, M. S. Guyer, L. Habegger, T. Han, J. G. Henikoff, S. R. Henz, A. Hinrichs, H. Holster, T. Hyman, A. L. Iniguez, J. Janette, M. Jensen, M. Kato, W. J. Kent, E. Kephart, V. Khivansara, E. Khurana, J. K. Kim, P. Kolasinska-Zwierz, E. C. Lai, I. Latorre, A. Leahey, S. Lewis, P. Lloyd, L. Lochovsky, R. F. Lowdon, Y. Lubling, R. Lyne, M. MacCoss, S. D. Mackowiak, M. Mangone, S. McKay, D. Mecenas, G. Merrihew, D. M. Miller, 3rd, A. Muroyama, J. I. Murray, S. L. Ooi, H. Pham, T. Phippen, E. A. Preston, N. Rajewsky, G. Ratsch, H. Rosenbaum, J. Rozowsky, K. Rutherford, P. Ruzanov, M. Sarov, R. Sasidharan, A. Sboner, P. Scheid, E. Segal, H. Shin, C. Shou, F. J. Slack, C. Slightam, R. Smith, W. C. Spencer, E. O. Stinson, S. Taing, T. Takasaki, D. Vafeados, K. Voronina, G. Wang, N. L. Washington, C. M. Whittle, B. Wu, K. K. Yan, G. Zeller, Z. Zha, M. Zhong, X. Zhou, J. Ahringer, S. Strome, K. C. Gunsalus, G. Micklem, X. S. Liu, V. Reinke, S. K. Kim, L. W. Hillier, S. Henikoff, F. Piano, M. Snyder, L. Stein, J. D. Lieb, and R. H. Waterston. 2010. "Integrative analysis of the Caenorhabditis elegans genome by the modENCODE project." *Science* 330 (6012):1775-87. doi: 10.1126/science.1196914.

Ghai, V., and J. Gaudet. 2008. "The CSL transcription factor LAG-1 directly represses hlh-6 expression in C. elegans." *Dev Biol* 322 (2):334-44. doi: 10.1016/j.ydbio.2008.07.018.

Gheldof, A., P. Hulpiau, F. van Roy, B. De Craene, and G. Berx. 2012. "Evolutionary functional analysis and molecular regulation of the ZEB transcription factors." *Cell Mol Life Sci* 69 (15):2527-41. doi: 10.1007/s00018-012-0935-3.

Golden, J. W., and D. L. Riddle. 1984. "The Caenorhabditis elegans dauer larva: developmental effects of pheromone, food, and temperature." *Dev Biol* 102 (2):368-78.

Gumienny, T. L., and C. Savage-Dunn. 2013. "TGF-beta signaling in C. elegans." *WormBook*:1-34. doi: 10.1895/wormbook.1.22.2.

Hall, D. H., and E. M. Hedgecock. 1991. "Kinesin-related gene unc-104 is required for axonal transport of synaptic vesicles in C. elegans." *Cell* 65 (5):837-47.

Hallam, S. J., A. Goncharov, J. McEwen, R. Baran, and Y. Jin. 2002. "SYD-1, a presynaptic protein with PDZ, C2 and rhoGAP-like domains, specifies axon identity in C. elegans." *Nat Neurosci* 5 (11):1137-46. doi: 10.1038/nn959.

Harfe, B. D., and A. Fire. 1998. "Muscle and nerve-specific regulation of a novel NK-2 class homeodomain factor in Caenorhabditis elegans." *Development* 125 (3):421-9.

Harvey, R. P. 1996. "NK-2 homeobox genes and heart development." *Dev Biol* 178 (2):203-16.

Higashi, Y., H. Moribe, T. Takagi, R. Sekido, K. Kawakami, H. Kikutani, and H. Kondoh. 1997. "Impairment of T cell development in deltaEF1 mutant mice." *J Exp Med* 185 (8):1467-79.

Hirose, T., B. D. Galvin, and H. R. Horvitz. 2010. "Six and Eya promote apoptosis through direct transcriptional activation of the proapoptotic BH3-only gene egl-1 in Caenorhabditis elegans." *Proc Natl Acad Sci U S A* 107 (35):15479-84. doi: 10.1073/pnas.1010023107.

Hobert, O. 2011. "Regulation of terminal differentiation programs in the nervous system." *Annu Rev Cell Dev Biol* 27:681-96. doi: 10.1146/annurev-cellbio-092910-154226.

CITED LITERATURE (continued)

Hobson, R. J., J. Geng, A. D. Gray, and R. W. Komuniecki. 2003. "SER-7b, a constitutively active Galphas coupled 5-HT7-like receptor expressed in the Caenorhabditis elegans M4 pharyngeal motorneuron." *J Neurochem* 87 (1):22-9.

Hobson, R. J., V. M. Hapiak, H. Xiao, K. L. Buehrer, P. R. Komuniecki, and R. W. Komuniecki. 2006. "SER-7, a Caenorhabditis elegans 5-HT7-like receptor, is essential for the 5-HT stimulation of pharyngeal pumping and egg laying." *Genetics* 172 (1):159-69. doi: 10.1534/genetics.105.044495.

Hocevar, B. A., T. L. Brown, and P. H. Howe. 1999. "TGF-beta induces fibronectin synthesis through a c-Jun N-terminal kinase-dependent, Smad4-independent pathway." *EMBO J* 18 (5):1345-56. doi: 10.1093/emboj/18.5.1345.

Horvitz, H. R., M. Chalfie, C. Trent, J. E. Sulston, and P. D. Evans. 1982. "Serotonin and octopamine in the nematode Caenorhabditis elegans." *Science* 216 (4549):1012-4.

Hu, F., C. Wang, J. Du, W. Sun, J. Yan, D. Mi, J. Zhang, Y. Qiao, T. Zhu, and S. Yang. 2010. "DeltaEF1 promotes breast cancer cell proliferation through down-regulating p21 expression." *Biochim Biophys Acta* 1802 (2):301-12. doi: 10.1016/j.bbadis.2009.12.002.

Hu, F., C. Wang, S. Guo, W. Sun, D. Mi, Y. Gao, J. Zhang, T. Zhu, and S. Yang. 2011. "deltaEF1 promotes osteolytic metastasis of MDA-MB-231 breast cancer cells by regulating MMP-1 expression." *Biochim Biophys Acta* 1809 (3):200-10. doi: 10.1016/j.bbagrm.2011.01.003.

Hu, P. J. 2007. "Dauer." *WormBook*:1-19. doi: 10.1895/wormbook.1.144.1.

Huber, P., T. Crum, L. M. Clary, T. Ronan, A. V. Packard, and P. G. Okkema. 2013. "Function of the C. elegans T-box factor TBX-2 depends on SUMOylation." *Cell Mol Life Sci* 70 (21):4157-68. doi: 10.1007/s00018-013-1336-y.

Ikeda, K., and K. Kawakami. 1995. "DNA binding through distinct domains of zinc-finger-homeodomain protein AREB6 has different effects on gene transcription." *Eur J Biochem* 233 (1):73-82.

Jacob, J., A. Hacker, and S. Guthrie. 2001. "Mechanisms and molecules in motor neuron specification and axon pathfinding." *Bioessays* 23 (7):582-95. doi: 10.1002/bies.1084.

Jacob, T. C., and J. M. Kaplan. 2003. "The EGL-21 carboxypeptidase E facilitates acetylcholine release at Caenorhabditis elegans neuromuscular junctions." *J Neurosci* 23 (6):2122-30.

Jethanandani, P., and R. H. Kramer. 2005. "Alpha7 integrin expression is negatively regulated by deltaEF1 during skeletal myogenesis." *J Biol Chem* 280 (43):36037-46. doi: 10.1074/jbc.M508698200.

Jia, K., P. S. Albert, and D. L. Riddle. 2002. "DAF-9, a cytochrome P450 regulating C. elegans larval development and adult longevity." *Development* 129 (1):221-31.

Kaletta, T., and M. O. Hengartner. 2006. "Finding function in novel targets: C. elegans as a model organism." *Nat Rev Drug Discov* 5 (5):387-98. doi: 10.1038/nrd2031.

Kamath, R. S., and J. Ahringer. 2003. "Genome-wide RNAi screening in Caenorhabditis elegans." *Methods* 30 (4):313-21.

Kent, W. J., C. W. Sugnet, T. S. Furey, K. M. Roskin, T. H. Pringle, A. M. Zahler, and D. Haussler. 2002. "The human genome browser at UCSC." *Genome Res* 12 (6):996-1006. doi: 10.1101/gr.229102. Article published online before print in May 2002.

Kim, K., and C. Li. 2004. "Expression and regulation of an FMRFamide-related neuropeptide gene family in Caenorhabditis elegans." *J Comp Neurol* 475 (4):540-50. doi: 10.1002/cne.20189.

Klassen, M. P., and K. Shen. 2007. "Wnt signaling positions neuromuscular connectivity by inhibiting synapse formation in C. elegans." *Cell* 130 (4):704-16. doi: 10.1016/j.cell.2007.06.046.

Krafchak, C. M., H. Pawar, S. E. Moroi, A. Sugar, P. R. Lichter, D. A. Mackey, S. Mian, T. Nairus, V. Elner, M. T. Schteingart, C. A. Downs, T. G. Kijek, J. M. Johnson, E. H. Trager, F. W. Rozsa, M. N. Mandal, M. P. Epstein, D. Vollrath, R. Ayyagari, M. Boehnke,

CITED LITERATURE (continued)

and J. E. Richards. 2005. "Mutations in TCF8 cause posterior polymorphous corneal dystrophy and ectopic expression of COL4A3 by corneal endothelial cells." *Am J Hum Genet* 77 (5):694-708. doi: 10.1086/497348.

Krieger, D. T. 1983. "Brain peptides: what, where, and why?" *Science* 222 (4627):975-85.

Krieglstein, K., and K. Unsicker. 1995. "Bovine chromaffin cells release a transforming growth factor-beta-like molecule contained within chromaffin granules." *J Neurochem* 65 (3):1423-6.

Krimpenfort, P., A. Ijpenberg, J. Y. Song, M. van der Valk, M. Nawijn, J. Zevenhoven, and A. Berns. 2007. "p15Ink4b is a critical tumour suppressor in the absence of p16Ink4a." *Nature* 448 (7156):943-6. doi: 10.1038/nature06084.

Krishna, S., L. L. Maduzia, and R. W. Padgett. 1999. "Specificity of TGFbeta signaling is conferred by distinct type I receptors and their associated SMAD proteins in Caenorhabditis elegans." *Development* 126 (2):251-60.

Kunitomo, H., H. Uesugi, Y. Kohara, and Y. Iino. 2005. "Identification of ciliated sensory neuron-expressed genes in Caenorhabditis elegans using targeted pull-down of poly(A) tails." *Genome Biol* 6 (2):R17. doi: 10.1186/gb-2005-6-2-r17.

Lacmann, A., D. Hess, G. Gohla, E. Roussa, and K. Krieglstein. 2007. "Activity-dependent release of transforming growth factor-beta in a neuronal network in vitro." *Neuroscience* 150 (3):647-57. doi: 10.1016/j.neuroscience.2007.09.046.

Lai, Z. C., M. E. Fortini, and G. M. Rubin. 1991. "The embryonic expression patterns of zfh-1 and zfh-2, two Drosophila genes encoding novel zinc-finger homeodomain proteins." *Mech Dev* 34 (2-3):123-34.

Lakso, M., S. Vartiainen, A. M. Moilanen, J. Sirvio, J. H. Thomas, R. Nass, R. D. Blakely, and G. Wong. 2003. "Dopaminergic neuronal loss and motor deficits in Caenorhabditis elegans overexpressing human alpha-synuclein." *J Neurochem* 86 (1):165-72.

Layden, M. J., J. P. Odden, A. Schmid, A. Garces, S. Thor, and C. Q. Doe. 2006. "Zfh1, a somatic motor neuron transcription factor, regulates axon exit from the CNS." *Dev Biol* 291 (2):253-63. doi: 10.1016/j.ydbio.2005.12.009.

Lazarova, D. L., M. Bordonaro, and A. C. Sartorelli. 2001. "Transcriptional regulation of the vitamin D(3) receptor gene by ZEB." *Cell Growth Differ* 12 (6):319-26.

Lee, J. M., S. Dedhar, R. Kalluri, and E. W. Thompson. 2006. "The epithelial-mesenchymal transition: new insights in signaling, development, and disease." *J Cell Biol* 172 (7):973-81. doi: 10.1083/jcb.200601018.

Lee, J. S., D. S. Min, C. Park, C. S. Park, and N. J. Cho. 2001. "Phytosphingosine and C2-phytoceramide induce cell death and inhibit carbachol-stimulated phospholipase D activation in Chinese hamster ovary cells expressing the Caenorhabditis elegans muscarinic acetylcholine receptor." *FEBS Lett* 499 (1-2):82-6.

Lerner, J. T., R. Sankar, and A. M. Mazarati. 2008. "Galanin and epilepsy." *Cell Mol Life Sci* 65 (12):1864-71. doi: 10.1007/s00018-008-8161-8.

Lewis, J. A., and J. T. Fleming. 1995. "Basic Culture Methods." In *Methods in Cell Biology-Caenorhabditis elegans: Modern Biological Analysis of an Organism*, 4-30. San Diego, CA: Academic Press.

Lewis, J. A., C. H. Wu, H. Berg, and J. H. Levine. 1980. "The genetics of levamisole resistance in the nematode Caenorhabditis elegans." *Genetics* 95 (4):905-28.

Li, C. 2005. "The ever-expanding neuropeptide gene families in the nematode Caenorhabditis elegans." *Parasitology* 131 Suppl:S109-27. doi: 10.1017/S0031182005009376.

Li, C., K. Kim, and L. S. Nelson. 1999. "FMRFamide-related neuropeptide gene family in Caenorhabditis elegans." *Brain Res* 848 (1-2):26-34.

Li, C., L. S. Nelson, K. Kim, A. Nathoo, and A. C. Hart. 1999. "Neuropeptide gene families in the nematode Caenorhabditis elegans." *Ann N Y Acad Sci* 897:239-52.

CITED LITERATURE (continued)

Link, C. D. 1995. "Expression of human beta-amyloid peptide in transgenic Caenorhabditis elegans." *Proc Natl Acad Sci U S A* 92 (20):9368-72.

Liu, Y., S. El-Naggar, D. S. Darling, Y. Higashi, and D. C. Dean. 2008. "Zeb1 links epithelial-mesenchymal transition and cellular senescence." *Development* 135 (3):579-88. doi: 10.1242/dev.007047.

Livak, K. J., and T. D. Schmittgen. 2001. "Analysis of relative gene expression data using real-time quantitative PCR and the 2(-Delta Delta C(T)) Method." *Methods* 25 (4):402-8. doi: 10.1006/meth.2001.1262.

Long, J., D. Zuo, and M. Park. 2005. "Pc2-mediated sumoylation of Smad-interacting protein 1 attenuates transcriptional repression of E-cadherin." *J Biol Chem* 280 (42):35477-89. doi: 10.1074/jbc.M504477200.

Luo, S., G. A. Kleemann, J. M. Ashraf, W. M. Shaw, and C. T. Murphy. 2010. "TGF-beta and insulin signaling regulate reproductive aging via oocyte and germline quality maintenance." *Cell* 143 (2):299-312. doi: 10.1016/j.cell.2010.09.013.

Malnic, B., J. Hirono, T. Sato, and L. B. Buck. 1999. "Combinatorial receptor codes for odors." *Cell* 96 (5):713-23.

Mani, S. A., W. Guo, M. J. Liao, E. N. Eaton, A. Ayyanan, A. Y. Zhou, M. Brooks, F. Reinhard, C. C. Zhang, M. Shipitsin, L. L. Campbell, K. Polyak, C. Brisken, J. Yang, and R. A. Weinberg. 2008. "The epithelial-mesenchymal transition generates cells with properties of stem cells." *Cell* 133 (4):704-15. doi: 10.1016/j.cell.2008.03.027.

Marques, G. 2005. "Morphogens and synaptogenesis in Drosophila." *J Neurobiol* 64 (4):417-34.

Massague, J. 1998. "TGF-beta signal transduction." *Annu Rev Biochem* 67:753-91. doi: 10.1146/annurev.biochem.67.1.753.

McIntire, S. L., E. Jorgensen, J. Kaplan, and H. R. Horvitz. 1993. "The GABAergic nervous system of Caenorhabditis elegans." *Nature* 364 (6435):337-41. doi: 10.1038/364337a0.

McKay, J. P., D. M. Raizen, A. Gottschalk, W. R. Schafer, and L. Avery. 2004. "eat-2 and eat-18 are required for nicotinic neurotransmission in the Caenorhabditis elegans pharynx." *Genetics* 166 (1):161-9.

McKinsey, G. L., S. Lindtner, B. Trzcinski, A. Visel, L. A. Pennacchio, D. Huylebroeck, Y. Higashi, and J. L. Rubenstein. 2013. "Dlx1&2-dependent expression of Zfhx1b (Sip1, Zeb2) regulates the fate switch between cortical and striatal interneurons." *Neuron* 77 (1):83-98. doi: 10.1016/j.neuron.2012.11.035.

Mello, C., and A. Fire. 1995. "DNA Transformation." In *Caenorhabditis elegans: Modern Biological Analysis of an Organism*, edited by H. F. Epstein and D. C. Shakes, 451-482. San Diego, CA: Academic Press.

Merritt, C., and G. Seydoux. 2010. "Transgenic solutions for the germline." *WormBook*:1-21. doi: 10.1895/wormbook.1.148.1.

Milton, A. C., A. V. Packard, L. Clary, and P. G. Okkema. 2013. "The NF-Y complex negatively regulates Caenorhabditis elegans tbx-2 expression." *Dev Biol* 382 (1):38-47. doi: 10.1016/j.ydbio.2013.08.001.

Min, D. S., N. J. Cho, S. H. Yoon, Y. H. Lee, S. J. Hahn, K. H. Lee, M. S. Kim, and Y. H. Jo. 2000. "Phospholipase C, protein kinase C, Ca(2+)/calmodulin-dependent protein kinase II, and tyrosine phosphorylation are involved in carbachol-induced phospholipase D activation in Chinese hamster ovary cells expressing muscarinic acetylcholine receptor of Caenorhabditis elegans." *J Neurochem* 75 (1):274-81.

Minoo, P., G. Su, H. Drum, P. Bringas, and S. Kimura. 1999. "Defects in tracheoesophageal and lung morphogenesis in Nkx2.1(-/-) mouse embryos." *Dev Biol* 209 (1):60-71. doi: 10.1006/dbio.1999.9234.

Morita, K., K. L. Chow, and N. Ueno. 1999. "Regulation of body length and male tail ray pattern formation of Caenorhabditis elegans by a member of TGF-beta family." *Development* 126 (6):1337-47.

CITED LITERATURE (continued)

Mowat, D. R., G. D. Croaker, D. T. Cass, B. A. Kerr, J. Chaitow, L. C. Ades, N. L. Chia, and M. J. Wilson. 1998. "Hirschsprung disease, microcephaly, mental retardation, and characteristic facial features: delineation of a new syndrome and identification of a locus at chromosome 2q22-q23." *J Med Genet* 35 (8):617-23.

Mu, Y., S. K. Gudey, and M. Landstrom. 2012. "Non-Smad signaling pathways." *Cell Tissue Res* 347 (1):11-20. doi: 10.1007/s00441-011-1201-y.

Nelson, L. S., M. L. Rosoff, and C. Li. 1998. "Disruption of a neuropeptide gene, flp-1, causes multiple behavioral defects in Caenorhabditis elegans." *Science* 281 (5383):1686-90.

Niacaris, T., and L. Avery. 2003. "Serotonin regulates repolarization of the C. elegans pharyngeal muscle." *J Exp Biol* 206 (Pt 2):223-31.

Nonet, M. L. 1999. "Visualization of synaptic specializations in live C. elegans with synaptic vesicle protein-GFP fusions." *J Neurosci Methods* 89 (1):33-40.

Ogryzko, V. V., R. L. Schiltz, V. Russanova, B. H. Howard, and Y. Nakatani. 1996. "The transcriptional coactivators p300 and CBP are histone acetyltransferases." *Cell* 87 (5):953-9.

Okkema, P. G., and A. Fire. 1994. "The Caenorhabditis elegans NK-2 class homeoprotein CEH-22 is involved in combinatorial activation of gene expression in pharyngeal muscle." *Development* 120 (8):2175-86.

Okkema, P. G., E. Ha, C. Haun, W. Chen, and A. Fire. 1997. "The Caenorhabditis elegans NK-2 homeobox gene ceh-22 activates pharyngeal muscle gene expression in combination with pha-1 and is required for normal pharyngeal development." *Development* 124 (20):3965-73.

Padua, D., and J. Massague. 2009. "Roles of TGFbeta in metastasis." *Cell Res* 19 (1):89-102. doi: 10.1038/cr.2008.316.

Papaioannou, S., D. Marsden, C. J. Franks, R. J. Walker, and L. Holden-Dye. 2005. "Role of a FMRFamide-like family of neuropeptides in the pharyngeal nervous system of Caenorhabditis elegans." *J Neurobiol* 65 (3):304-19. doi: 10.1002/neu.20201.

Patterson, G. I., and R. W. Padgett. 2000. "TGF beta-related pathways. Roles in Caenorhabditis elegans development." *Trends Genet* 16 (1):27-33.

Pauli, F., Y. Liu, Y. A. Kim, P. J. Chen, and S. K. Kim. 2006. "Chromosomal clustering and GATA transcriptional regulation of intestine-expressed genes in C. elegans." *Development* 133 (2):287-95. doi: 10.1242/dev.02185.

Pierce, S. B., M. Costa, R. Wisotzkey, S. Devadhar, S. A. Homburger, A. R. Buchman, K. C. Ferguson, J. Heller, D. M. Platt, A. A. Pasquinelli, L. X. Liu, S. K. Doberstein, and G. Ruvkun. 2001. "Regulation of DAF-2 receptor signaling by human insulin and ins-1, a member of the unusually large and diverse C. elegans insulin gene family." *Genes Dev* 15 (6):672-86. doi: 10.1101/gad.867301.

Pipaon, C., P. J. Real, and J. L. Fernandez-Luna. 2005. "Defective binding of transcriptional repressor ZEB via DNA methylation contributes to increased constitutive levels of p73 in Fanconi anemia cells." *FEBS Lett* 579 (21):4610-4. doi: 10.1016/j.febslet.2005.07.026.

Pocock, R., and O. Hobert. 2010. "Hypoxia activates a latent circuit for processing gustatory information in C. elegans." *Nat Neurosci* 13 (5):610-4. doi: 10.1038/nn.2537.

Poon, V. Y., M. P. Klassen, and K. Shen. 2008. "UNC-6/netrin and its receptor UNC-5 locally exclude presynaptic components from dendrites." *Nature* 455 (7213):669-73. doi: 10.1038/nature07291.

Postigo, A. A. 2003. "Opposing functions of ZEB proteins in the regulation of the TGFbeta/BMP signaling pathway." *EMBO J* 22 (10):2443-52. doi: 10.1093/emboj/cdg225.

Postigo, A. A., and D. C. Dean. 1999. "ZEB represses transcription through interaction with the corepressor CtBP." *Proc Natl Acad Sci U S A* 96 (12):6683-8.

CITED LITERATURE (continued)

Postigo, A. A., J. L. Depp, J. J. Taylor, and K. L. Kroll. 2003. "Regulation of Smad signaling through a differential recruitment of coactivators and corepressors by ZEB proteins." *EMBO J* 22 (10):2453-62. doi: 10.1093/emboj/cdg226.

Pradhan, L., C. Genis, P. Scone, E. O. Weinberg, H. Kasahara, and H. J. Nam. 2012. "Crystal structure of the human NKX2.5 homeodomain in complex with DNA target." *Biochemistry* 51 (32):6312-9. doi: 10.1021/bi300849c.

Raharjo, W. H., V. Ghai, A. Dineen, M. Bastiani, and J. Gaudet. 2011. "Cell architecture: surrounding muscle cells shape gland cell morphology in the Caenorhabditis elegans pharynx." *Genetics* 189 (3):885-97. doi: 10.1534/genetics.111.132449.

Raizen, D. M., R. Y. Lee, and L. Avery. 1995. "Interacting genes required for pharyngeal excitation by motor neuron MC in Caenorhabditis elegans." *Genetics* 141 (4):1365-82.

Ramakrishnan, K., P. Ray, and P. G. Okkema. 2014. "CEH-28 activates dbl-1 expression and TGF-beta signaling in the C. elegans M4 neuron." *Dev Biol* 390 (2):149-59. doi: 10.1016/j.ydbio.2014.03.015.

Ray, P., R. Schnabel, and P. G. Okkema. 2008. "Behavioral and synaptic defects in C. elegans lacking the NK-2 homeobox gene ceh-28." *Dev Neurobiol* 68 (4):421-33. doi: 10.1002/dneu.20599.

Refai, O., P. Rohs, P. E. Mains, and J. Gaudet. 2013. "Extension of the Caenorhabditis elegans Pharyngeal M1 neuron axon is regulated by multiple mechanisms." *G3 (Bethesda)* 3 (11):2015-29. doi: 10.1534/g3.113.008466.

Reinke, V., M. Krause, and P. Okkema. 2013. "Transcriptional regulation of gene expression in C. elegans." *WormBook*:1-34. doi: 10.1895/wormbook.1.45.2.

Riazuddin, S. A., N. A. Zaghloul, A. Al-Saif, L. Davey, B. H. Diplas, D. N. Meadows, A. O. Eghrari, M. A. Minear, Y. J. Li, G. K. Klintworth, N. Afshari, S. G. Gregory, J. D. Gottsch, and N. Katsanis. 2010. "Missense mutations in TCF8 cause late-onset Fuchs corneal dystrophy and interact with FCD4 on chromosome 9p." *Am J Hum Genet* 86 (1):45-53. doi: 10.1016/j.ajhg.2009.12.001.

Ringstad, N., and H. R. Horvitz. 2008. "FMRFamide neuropeptides and acetylcholine synergistically inhibit egg-laying by C. elegans." *Nat Neurosci* 11 (10):1168-76. doi: 10.1038/nn.2186.

Roberts, A. F., T. L. Gumienny, R. J. Gleason, H. Wang, and R. W. Padgett. 2010. "Regulation of genes affecting body size and innate immunity by the DBL-1/BMP-like pathway in Caenorhabditis elegans." *BMC Dev Biol* 10:61. doi: 10.1186/1471-213X-10-61.

Roy Chowdhuri, S., T. Crum, A. Woollard, S. Aslam, and P. G. Okkema. 2006. "The T-box factor TBX-2 and the SUMO conjugating enzyme UBC-9 are required for ABa-derived pharyngeal muscle in C. elegans." *Dev Biol* 295 (2):664-77. doi: 10.1016/j.ydbio.2006.04.001.

Sanchez-Tillo, E., L. Siles, O. de Barrios, M. Cuatrecasas, E. C. Vaquero, A. Castells, and A. Postigo. 2011. "Expanding roles of ZEB factors in tumorigenesis and tumor progression." *Am J Cancer Res* 1 (7):897-912.

Sander, M., S. Paydar, J. Ericson, J. Briscoe, E. Berber, M. German, T. M. Jessell, and J. L. Rubenstein. 2000. "Ventral neural patterning by Nkx homeobox genes: Nkx6.1 controls somatic motor neuron and ventral interneuron fates." *Genes Dev* 14 (17):2134-9.

Sarov, M., J. I. Murray, K. Schanze, A. Pozniakovski, W. Niu, K. Angermann, S. Hasse, M. Rupprecht, E. Vinis, M. Tinney, E. Preston, A. Zinke, S. Enst, T. Teichgraber, J. Janette, K. Reis, S. Janosch, S. Schloissnig, R. K. Ejsmont, C. Slightam, X. Xu, S. K. Kim, V. Reinke, A. F. Stewart, M. Snyder, R. H. Waterston, and A. A. Hyman. 2012. "A genome-scale resource for in vivo tag-based protein function exploration in C. elegans." *Cell* 150 (4):855-66. doi: 10.1016/j.cell.2012.08.001.

Savage, C., P. Das, A. L. Finelli, S. R. Townsend, C. Y. Sun, S. E. Baird, and R. W. Padgett. 1996. "Caenorhabditis elegans genes sma-2, sma-3, and sma-4 define a conserved

CITED LITERATURE (continued)

family of transforming growth factor beta pathway components." *Proc Natl Acad Sci U S A* 93 (2):790-4.

Sawin, E. R., R. Ranganathan, and H. R. Horvitz. 2000. "C. elegans locomotory rate is modulated by the environment through a dopaminergic pathway and by experience through a serotonergic pathway." *Neuron* 26 (3):619-31.

Schaefer, A. M., G. D. Hadwiger, and M. L. Nonet. 2000. "rpm-1, a conserved neuronal gene that regulates targeting and synaptogenesis in C. elegans." *Neuron* 26 (2):345-56.

Schafer, W. R. 2005. "Deciphering the neural and molecular mechanisms of C. elegans behavior." *Curr Biol* 15 (17):R723-9. doi: 10.1016/j.cub.2005.08.020.

Schafer, W. R. 2006. "Neurophysiological methods in C. elegans: an introduction." *WormBook*:1-4. doi: 10.1895/wormbook.1.113.1.

Segalat, L., D. A. Elkes, and J. M. Kaplan. 1995. "Modulation of serotonin-controlled behaviors by Go in Caenorhabditis elegans." *Science* 267 (5204):1648-51.

Seydoux, G., and A. Fire. 1994. "Soma-germline asymmetry in the distributions of embryonic RNAs in Caenorhabditis elegans." *Development* 120 (10):2823-34.

Shen, K., and C. I. Bargmann. 2003. "The immunoglobulin superfamily protein SYG-1 determines the location of specific synapses in C. elegans." *Cell* 112 (5):619-30.

Shi, Y., J. Sawada, G. Sui, B. Affar el, J. R. Whetstine, F. Lan, H. Ogawa, M. P. Luke, Y. Nakatani, and Y. Shi. 2003. "Coordinated histone modifications mediated by a CtBP co-repressor complex." *Nature* 422 (6933):735-8. doi: 10.1038/nature01550.

Shirakihara, T., M. Saitoh, and K. Miyazono. 2007. "Differential regulation of epithelial and mesenchymal markers by deltaEF1 proteins in epithelial mesenchymal transition induced by TGF-beta." *Mol Biol Cell* 18 (9):3533-44. doi: 10.1091/mbc.E07-03-0249.

Shirasaki, R., and S. L. Pfaff. 2002. "Transcriptional codes and the control of neuronal identity." *Annu Rev Neurosci* 25:251-81. doi: 10.1146/annurev.neuro.25.112701.142916.

Sieber, C., J. Kopf, C. Hiepen, and P. Knaus. 2009. "Recent advances in BMP receptor signaling." *Cytokine Growth Factor Rev* 20 (5-6):343-55. doi: 10.1016/j.cytogfr.2009.10.007.

Sieburth, D., J. M. Madison, and J. M. Kaplan. 2007. "PKC-1 regulates secretion of neuropeptides." *Nat Neurosci* 10 (1):49-57. doi: 10.1038/nn1810.

Singh, A., and J. Settleman. 2010. "EMT, cancer stem cells and drug resistance: an emerging axis of evil in the war on cancer." *Oncogene* 29 (34):4741-51. doi: 10.1038/onc.2010.215.

Smit, R. B., R. Schnabel, and J. Gaudet. 2008. "The HLH-6 transcription factor regulates C. elegans pharyngeal gland development and function." *PLoS Genet* 4 (10):e1000222. doi: 10.1371/journal.pgen.1000222.

Smith, C. J., T. O'Brien, M. Chatzigeorgiou, W. C. Spencer, E. Feingold-Link, S. J. Husson, S. Hori, S. Mitani, A. Gottschalk, W. R. Schafer, and D. M. Miller, 3rd. 2013. "Sensory neuron fates are distinguished by a transcriptional switch that regulates dendrite branch stabilization." *Neuron* 79 (2):266-80. doi: 10.1016/j.neuron.2013.05.009.

Song, B. M., and L. Avery. 2012. "Serotonin activates overall feeding by activating two separate neural pathways in Caenorhabditis elegans." *J Neurosci* 32 (6):1920-31. doi: 10.1523/JNEUROSCI.2064-11.2012.

Specht, H., H. Peterziel, M. Bajohrs, H. H. Gerdes, K. Krieglstein, and K. Unsicker. 2003. "Transforming growth factor beta2 is released from PC12 cells via the regulated pathway of secretion." *Mol Cell Neurosci* 22 (1):75-86.

Speese, S., M. Petrie, K. Schuske, M. Ailion, K. Ann, K. Iwasaki, E. M. Jorgensen, and T. F. Martin. 2007. "UNC-31 (CAPS) is required for dense-core vesicle but not synaptic vesicle exocytosis in Caenorhabditis elegans." *J Neurosci* 27 (23):6150-62. doi: 10.1523/JNEUROSCI.1466-07.2007.

CITED LITERATURE (continued)

Steger, K. A., and L. Avery. 2004. "The GAR-3 muscarinic receptor cooperates with calcium signals to regulate muscle contraction in the Caenorhabditis elegans pharynx." *Genetics* 167 (2):633-43. doi: 10.1534/genetics.103.020230.

Strange, K., M. Christensen, and R. Morrison. 2007. "Primary culture of Caenorhabditis elegans developing embryo cells for electrophysiological, cell biological and molecular studies." *Nat Protoc* 2 (4):1003-12. doi: 10.1038/nprot.2007.143.

Sulston, J., M. Dew, and S. Brenner. 1975. "Dopaminergic neurons in the nematode Caenorhabditis elegans." *J Comp Neurol* 163 (2):215-26. doi: 10.1002/cne.901630207.

Sulston, J. E., and H. R. Horvitz. 1977. "Post-embryonic cell lineages of the nematode, Caenorhabditis elegans." *Dev Biol* 56 (1):110-56.

Sulston, J. E., E. Schierenberg, J. G. White, and J. N. Thomson. 1983. "The embryonic cell lineage of the nematode Caenorhabditis elegans." *Dev Biol* 100 (1):64-119.

Suzuki, Y., M. D. Yandell, P. J. Roy, S. Krishna, C. Savage-Dunn, R. M. Ross, R. W. Padgett, and W. B. Wood. 1999. "A BMP homolog acts as a dose-dependent regulator of body size and male tail patterning in Caenorhabditis elegans." *Development* 126 (2):241-50.

Takagi, T., H. Moribe, H. Kondoh, and Y. Higashi. 1998. "DeltaEF1, a zinc finger and homeodomain transcription factor, is required for skeleton patterning in multiple lineages." *Development* 125 (1):21-31.

Takayama, J., S. Faumont, H. Kunitomo, S. R. Lockery, and Y. Iino. 2010. "Single-cell transcriptional analysis of taste sensory neuron pair in Caenorhabditis elegans." *Nucleic Acids Res* 38 (1):131-42. doi: 10.1093/nar/gkp868.

Thacker, C., and A. M. Rose. 2000. "A look at the Caenorhabditis elegans Kex2/Subtilisin-like proprotein convertase family." *Bioessays* 22 (6):545-53. doi: 10.1002/(SICI)1521-1878(200006)22:6<545::AID-BIES7>3.0.CO;2-F.

Thiery, J. P. 2003. "Epithelial-mesenchymal transitions in development and pathologies." *Curr Opin Cell Biol* 15 (6):740-6.

Thor, S., and J. B. Thomas. 2002. "Motor neuron specification in worms, flies and mice: conserved and 'lost' mechanisms." *Curr Opin Genet Dev* 12 (5):558-64.

Van de Putte, T., M. Maruhashi, A. Francis, L. Nelles, H. Kondoh, D. Huylebroeck, and Y. Higashi. 2003. "Mice lacking ZFHX1B, the gene that codes for Smad-interacting protein-1, reveal a role for multiple neural crest cell defects in the etiology of Hirschsprung disease-mental retardation syndrome." *Am J Hum Genet* 72 (2):465-70. doi: 10.1086/346092.

Vandewalle, C., J. Comijn, B. De Craene, P. Vermassen, E. Bruyneel, H. Andersen, E. Tulchinsky, F. Van Roy, and G. Berx. 2005. "SIP1/ZEB2 induces EMT by repressing genes of different epithelial cell-cell junctions." *Nucleic Acids Res* 33 (20):6566-78. doi: 10.1093/nar/gki965.

Vandewalle, C., F. Van Roy, and G. Berx. 2009. "The role of the ZEB family of transcription factors in development and disease." *Cell Mol Life Sci* 66 (5):773-87. doi: 10.1007/s00018-008-8465-8.

Verschueren, K., J. E. Remacle, C. Collart, H. Kraft, B. S. Baker, P. Tylzanowski, L. Nelles, G. Wuytens, M. T. Su, R. Bodmer, J. C. Smith, and D. Huylebroeck. 1999. "SIP1, a novel zinc finger/homeodomain repressor, interacts with Smad proteins and binds to 5'-CACCT sequences in candidate target genes." *J Biol Chem* 274 (29):20489-98.

Vogler, G., and J. Urban. 2008. "The transcription factor Zfh1 is involved in the regulation of neuropeptide expression and growth of larval neuromuscular junctions in Drosophila melanogaster." *Dev Biol* 319 (1):78-85. doi: 10.1016/j.ydbio.2008.04.008.

Von Stetina, S. E., J. D. Watson, R. M. Fox, K. L. Olszewski, W. C. Spencer, P. J. Roy, and D. M. Miller, 3rd. 2007. "Cell-specific microarray profiling experiments reveal a comprehensive picture of gene expression in the C. elegans nervous system." *Genome Biol* 8 (7):R135. doi: 10.1186/gb-2007-8-7-r135.

CITED LITERATURE (continued)

Wacker, I., V. Schwarz, E. M. Hedgecock, and H. Hutter. 2003. "zag-1, a Zn-finger homeodomain transcription factor controlling neuronal differentiation and axon outgrowth in C. elegans." *Development* 130 (16):3795-805.

Waggoner, L. E., G. T. Zhou, R. W. Schafer, and W. R. Schafer. 1998. "Control of alternative behavioral states by serotonin in Caenorhabditis elegans." *Neuron* 21 (1):203-14.

Wakamatsu, N., Y. Yamada, K. Yamada, T. Ono, N. Nomura, H. Taniguchi, H. Kitoh, N. Mutoh, T. Yamanaka, K. Mushiake, K. Kato, S. Sonta, and M. Nagaya. 2001. "Mutations in SIP1, encoding Smad interacting protein-1, cause a form of Hirschsprung disease." *Nat Genet* 27 (4):369-70. doi: 10.1038/86860.

Walker, F. O. 2007. "Huntington's disease." *Lancet* 369 (9557):218-28. doi: 10.1016/S0140-6736(07)60111-1.

Watanabe, Y., K. Kawakami, Y. Hirayama, and K. Nagano. 1993. "Transcription factors positively and negatively regulating the Na,K-ATPase alpha 1 subunit gene." *J Biochem* 114 (6):849-55.

Weaver, M., J. M. Yingling, N. R. Dunn, S. Bellusci, and B. L. Hogan. 1999. "Bmp signaling regulates proximal-distal differentiation of endoderm in mouse lung development." *Development* 126 (18):4005-15.

Weinshenker, D., G. Garriga, and J. H. Thomas. 1995. "Genetic and pharmacological analysis of neurotransmitters controlling egg laying in C. elegans." *J Neurosci* 15 (10):6975-85.

Wess, J., A. Duttaroy, W. Zhang, J. Gomeza, Y. Cui, T. Miyakawa, F. P. Bymaster, L. McKinzie, C. C. Felder, K. G. Lamping, F. M. Faraci, C. Deng, and M. Yamada. 2003. "M1-M5 muscarinic receptor knockout mice as novel tools to study the physiological roles of the muscarinic cholinergic system." *Receptors Channels* 9 (4):279-90.

White, J. G., E. Southgate, J. N. Thomson, and S. Brenner. 1983. "Factors that determine connectivity in the nervous system of Caenorhabditis elegans." *Cold Spring Harb Symp Quant Biol* 48 Pt 2:633-40.

White, J. G., E. Southgate, J. N. Thomson, and S. Brenner. 1986a. "The structure of the nervous system of the nematode Caenorhabditis elegans." *Philos Trans R Soc Lond B Biol Sci* 314 (1165):1-340.

White, J. G., E. Southgate, J. N. Thomson, and S. Brenner. 1986b. "The Structure of the Nervous System of the Nematode Caenorhabditis elegans." *Philosophical Transactions of the Royal Society of London. B, Biological Sciences* 314 (1165 %U http://rstb.royalsocietypublishing.org/content/314/1165/1.abstract):1-340.

Wijesekera, L. C., and P. N. Leigh. 2009. "Amyotrophic lateral sclerosis." *Orphanet J Rare Dis* 4:3. doi: 10.1186/1750-1172-4-3.

Wilson, M., D. Mowat, F. Dastot-Le Moal, V. Cacheux, H. Kaariainen, D. Cass, D. Donnai, J. Clayton-Smith, S. Townshend, C. Curry, M. Gattas, S. Braddock, B. Kerr, S. Aftimos, H. Zehnwirth, C. Barrey, and M. Goossens. 2003. "Further delineation of the phenotype associated with heterozygous mutations in ZFHX1B." *Am J Med Genet A* 119A (3):257-65. doi: 10.1002/ajmg.a.20053.

Wu, G., A. Feder, G. Wegener, C. Bailey, S. Saxena, D. Charney, and A. A. Mathe. 2011. "Central functions of neuropeptide Y in mood and anxiety disorders." *Expert Opin Ther Targets* 15 (11):1317-31. doi: 10.1517/14728222.2011.628314.

Wu, M. Y., and C. S. Hill. 2009. "Tgf-beta superfamily signaling in embryonic development and homeostasis." *Dev Cell* 16 (3):329-43. doi: 10.1016/j.devcel.2009.02.012.

Yaguchi, J., L. M. Angerer, K. Inaba, and S. Yaguchi. 2012. "Zinc finger homeobox is required for the differentiation of serotonergic neurons in the sea urchin embryo." *Dev Biol* 363 (1):74-83. doi: 10.1016/j.ydbio.2011.12.024.

Yanik, M. F., H. Cinar, H. N. Cinar, A. D. Chisholm, Y. Jin, and A. Ben-Yakar. 2004. "Neurosurgery: functional regeneration after laser axotomy." *Nature* 432 (7019):822. doi: 10.1038/432822a.

CITED LITERATURE (continued)

Yoshida, S., K. Morita, M. Mochii, and N. Ueno. 2001. "Hypodermal expression of Caenorhabditis elegans TGF-beta type I receptor SMA-6 is essential for the growth and maintenance of body length." *Dev Biol* 240 (1):32-45. doi: 10.1006/dbio.2001.0443.

You, A., J. K. Tong, C. M. Grozinger, and S. L. Schreiber. 2001. "CoREST is an integral component of the CoREST- human histone deacetylase complex." *Proc Natl Acad Sci U S A* 98 (4):1454-8. doi: 10.1073/pnas.98.4.1454.

Zhang, Q., D. W. Piston, and R. H. Goodman. 2002. "Regulation of corepressor function by nuclear NADH." *Science* 295 (5561):1895-7. doi: 10.1126/science.1069300.

Zhang, S., D. Banerjee, and J. R. Kuhn. 2011. "Isolation and culture of larval cells from C. elegans." *PLoS One* 6 (4):e19505. doi: 10.1371/journal.pone.0019505.

Zhang, S., and J. R. Kuhn. 2013. "Cell isolation and culture." *WormBook*:1-39. doi: 10.1895/wormbook.1.157.1.

Zhang, X., and Y. Zhang. 2012. "DBL-1, a TGF-beta, is essential for Caenorhabditis elegans aversive olfactory learning." *Proc Natl Acad Sci U S A* 109 (42):17081-6. doi: 10.1073/pnas.1205982109.

Zhang, Y. E. 2009. "Non-Smad pathways in TGF-beta signaling." *Cell Res* 19 (1):128-39. doi: 10.1038/cr.2008.328.

Zhen, M., X. Huang, B. Bamber, and Y. Jin. 2000. "Regulation of presynaptic terminal organization by C. elegans RPM-1, a putative guanine nucleotide exchanger with a RING-H2 finger domain." *Neuron* 26 (2):331-43.

Zhu, N. L., C. Li, J. Xiao, and P. Minoo. 2004. "NKX2.1 regulates transcription of the gene for human bone morphogenetic protein-4 in lung epithelial cells." *Gene* 327 (1):25-36. doi: 10.1016/j.gene.2003.11.013.

Zugasti, O., and J. J. Ewbank. 2009. "Neuroimmune regulation of antimicrobial peptide expression by a noncanonical TGF-beta signaling pathway in Caenorhabditis elegans epidermis." *Nat Immunol* 10 (3):249-56. doi: 10.1038/ni.1700.

Zweier, C., B. Albrecht, B. Mitulla, R. Behrens, M. Beese, G. Gillessen-Kaesbach, H. D. Rott, and A. Rauch. 2002. ""Mowat-Wilson" syndrome with and without Hirschsprung disease is a distinct, recognizable multiple congenital anomalies-mental retardation syndrome caused by mutations in the zinc finger homeo box 1B gene." *Am J Med Genet* 108 (3):177-81.

CITED LITERATURE (continued)

VITA

NAME Kalpana Ramakrishnan

EDUCATION PhD., Department of Biological Sciences, University of Illinois at Chicago, 2014

M.S., Biology, Illinois Institute of Technology, Chicago, Illinois, 2011

B.Tech.,Biotechnology, SASTRA University., India , 2007

TEACHING Teaching Assistant, Genetics Laboratory , Department of Biological Sciences, University of Illinois at Chicago, Fall 2008-Fall 2011

Teaching Assistant, Developmental Biology Lectures, Department of Biological Sciences, University of Illinois at Chicago, Fall 2012

HONORS Research Achievement Award, 2014

UIC Chancellor's Student Service Award for significant service in the UIC campus 2011-2013

UIC Liberal Arts and Sciences Alumni Association Graduate Merit Award recognizing academic excellence and service to UIC and the community , November 2011

UIC Women in Science and Engineering, Peer Mentor of the Year Award, April 2011

Student Presenter Award, UIC Graduate College, 2011

PROFESSIONAL MEMEBERSHIP Association for Women in Science, (AWIS), Chicago Chapter

Women in Bio, Chicago Chapter

ABSTRACTS CEH-28 activates *dbl-1* expression and signaling in the M4 pharyngeal neuron – 19th International *C. elegans* Meeting at University of California Los Angeles (UCLA), *June 2013*

CEH-28 regulates M4 pharyngeal neuron by activating *dbl-1* expression 18th International *C. elegans* Meeting at University of California Los Angeles (UCLA), *June 2011*

CEH-28 regulates *dbl-1* expression and neuroendocrine function of the M4 neuron - *C. elegans* Neuronal Development and Synaptic function at University of Wisconsin Madison, *June 2010*

CITED LITERATURE (continued)

PUBLICATIONS CEH-28 activates *dbl-1* expression and TGF-β signaling in the *C. elegans* M4 pharyngeal neuron" **Ramakrishnan K**, Ray P and Okkema PG. *Journal of Developmental Biology*. (2014)

Regulation of *C. elegans* neuronal differentiation by the ZEB-family factor ZAG-1 and the NK-2 homeodomain factor CEH-28 (in review)